AL/CF-TR-1995-0110

ARMSTRONG LABORATORY

# FORCE-REFLECTING ANTHROPOMORPHIC HAND MASTERS

Christopher J. Hasser

CREW SYSTEMS DIRECTORATE
BIODYNAMICS AND BIOCOMMUNICATIONS DIVISION
WRIGHT-PATTERSON AFB OH 45433-7901

JULY 1995



INTERIM REPORT FOR THE PERIOD JUNE 1991 TO JULY 1995





AIR FORCE MATERIEL COMMAND
WRIGHT-PATTERSON AIR FORCE BASE, OHIO 45433-6573

NOTICE

When US Government drawings, specifications, or other data are used for any purpose other than a definitely related Government procurement operation, the Government thereby incurs no responsibility nor any obligation whatsoever, and the fact that the Government may have formulated, furnished, or in any way supplied the said drawings, specifications, or other data, is not to be regarded by implication or otherwise, as in any manner, licensing the holder or any other person or corporation, or conveying any rights or permission to manufacture, use or sell any patented invention that may in any way be related thereto.

Please do not request copies of this report from the Armstrong Laboratory. Additional copies may be purchased from:

National Technical Information Service
5285 Port Royal Road
Springfield VA 22161

Federal Government agencies and their contractors registered with Defense Technical Information Center should direct requests for copies of this report to:

Defense Technical Information Center
Cameron Station
Alexandria VA 22314

TECHNICAL REVIEW AND APPROVAL

AL/CF-TR-1995-0110

This report has been reviewed by the Office of Public Affairs (PA) and is releasable to the National Technical Information Service (NTIS). At NTIS, it will be available to the general public, including foreign nations.

This technical report has been reviewed and is approved for publication.

FOR THE COMMANDER

Thomas J Moore

THOMAS J. MOORE, Chief
Biodynamics and Biocommunications Division
Crew Systems Directorate
Armstrong Laboratory

# DISCLAIMER NOTICE

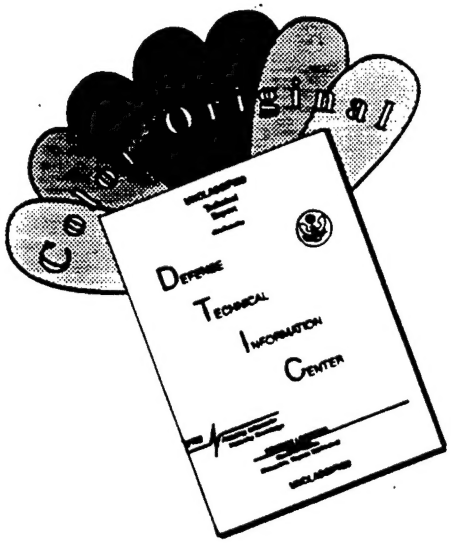


THIS DOCUMENT IS BEST QUALITY AVAILABLE. THE COPY FURNISHED TO DTIC CONTAINED A SIGNIFICANT NUMBER OF COLOR PAGES WHICH DO NOT REPRODUCE LEGIBLY ON BLACK AND WHITE MICROFICHE.

# REPORT DOCUMENTATION PAGE

Form Approved
OMB No. 0704-0188



| 1. AGENCY USE ONLY (Leave blank) | 2. REPORT DATE | 3. REPORT TYPE AND DATES COVERED |
|---|---|---|
| | July 1995 | Interim - June 1991 to July 1995 |

**4. TITLE AND SUBTITLE**
Force-Reflecting Anthropomorphic Hand Masters

**5. FUNDING NUMBERS**
PE - 62202F
PR - 7231
TA - 38
WU - 08

**6. AUTHOR(S)**
Christopher J. Hasser

**7. PERFORMING ORGANIZATION NAME(S) AND ADDRESS(ES)**
Armstrong Laboratory, Crew Systems Directorate
Biodynamics and Biocommunications Division
Human Systems Center
Air Force Materiel Command
Wright-Patterson AFB OH 45433-7901

**8. PERFORMING ORGANIZATION REPORT NUMBER**
AL/CF-TR-1995-0110

**9. SPONSORING/MONITORING AGENCY NAME(S) AND ADDRESS(ES)**

**10. SPONSORING/MONITORING AGENCY REPORT NUMBER**

**11. SUPPLEMENTARY NOTES**

**12a. DISTRIBUTION/AVAILABILITY STATEMENT**
Approved for public release; distribution is unlimited.

**12b. DISTRIBUTION CODE**

**13. ABSTRACT** *(Maximum 200 words)*

A fully "present" telerobotic or virtual reality (VR) hand interface would require perfect position, force, and tactile feedback to all of the operator's finger segments. A functional interface must meet a task-dependent subset of these requirements. Most interfaces have developed in the form of an exoskeleton that is worn on the hand.

The state of the art in anthropomorphic force-reflecting hand exoskeletons is characterized by a small number of independent efforts in government, academic, and commercial laboratories. Efforts are in widely varying stages of development, and have been slowed by the serious design limitations of this application, and by a dearth of suitable actuators.

This report applies existing data on human sensing and biodynamic capabilities to generate hand master design criteria. Current efforts are reviewed for an assessment of the state of the art. Specific actuator technologies are evaluated for their potential, particularly emerging technologies in magnetostrictive and piezoelectric actuation. The report offers recommendations concerning design compromises and areas of future development.

Appendices present calculations of maximum human finger joint torques, measurements of maximum human finger joint speeds, coverage of hand mechanics and anthropometry, photographs of hand masters, and a data sheet for each known force-reflecting hand master.

| 14. SUBJECT TERMS | | | 15. NUMBER OF PAGES |
|---|---|---|---|
| man-machine interface | force reflection | haptic feedback | 135 |
| force-reflecting | hand exoskeleton | teleoperation | 16. PRICE CODE |
| haptic | anthropomorphic | virtual reality | |

| 17. SECURITY CLASSIFICATION OF REPORT | 18. SECURITY CLASSIFICATION OF THIS PAGE | 19. SECURITY CLASSIFICATION OF ABSTRACT | 20. LIMITATION OF ABSTRACT |
|---|---|---|---|
| UNCLASSIFIED | UNCLASSIFIED | UNCLASSIFIED | UNLIMITED |

This page intentionally left blank.

# PREFACE

The Human Sensory Feedback (HSF) for Telepresence Project at the Armstrong Laboratory (AL/CFBA) was founded in 1986 in what was then the Harry G. Armstrong Aerospace Medical Research Laboratory. The mission of the HSF team is to study the human interface with telerobotic and virtual systems, sponsor the development of human interface technology, and transition the fruits of this labor to users who have practical requirements. Current work concentrates on force-reflecting arm masters, force-reflecting hand masters, and tactile feedback.

The author wrote this technical report to document the knowledge base accumulated by the HSF group on force-reflecting dexterous hand masters. This report defines salient issues, surveys the state of the art, and offers insights aimed at improving the state of the art. It is also intended to serve as a reference resource to current researchers and an introduction to newcomers in the field. The author has made every attempt to "compare apples to apples," so that information from widely varied sources can contribute to a solid and broad understanding of the issues.

## Acknowledgements

Numerous people deserve thanks for providing information, providing photographs, and reviewing drafts of this report. This author apologizes for errors that have slipped through despite their help, and for any names that have been omitted from this acknowledgement. The author would like to thank the following people for their assistance: Kai-Nan An, John Bares, Steve Begej, Grigore Burdea, Darwin Caldwell, Kelly Cole, Warren Darling, Brian Eberman, Dave Giurintano, Allen and Josephine Grahn, Joe Hale, Bruno Jau, Ron Julian, Larry Li, Marty Luka, Beth Marcus, Thomas Massie, Charles Nixon, Louis Rosenberg, Fraser Smith, Merry Spahr, Mandayam Srinivasan, Jeanie Stewart, Hong Tan, Joe Teter, Bill Townsend, and Paul Whalen.

# TABLE OF CONTENTS

# LIST OF FIGURES

# LIST OF TABLES

This page intentionally left blank.

# INTRODUCTION

## Background

Many circumstances require that work be done in environments that are inaccessible or too dangerous for humans to enter. These environments may be under water, in space, or contaminated by nuclear, biological, or chemical agents. Completion of the work requires humans to extend their reach into the forbidden environment. Simple, dedicated tasks, such as opening and closing valves, may be accomplished with remotely operated servos or similar automation. More complex but still structured tasks such as painting automobiles can be performed by an autonomous robot. A huge array of unstructured tasks is left unserviced by automation. For example, a valve assembly designed for indefinite service life might become stuck or broken in an area of a nuclear plant that has become contaminated. These tasks may often be accomplished with telerobotic manipulators whose joints are directly controlled by human operators, or by semi-autonomous robots that are supervised intermittently by a human. In addition, systems capable of full autonomy may benefit from telerobotic backup capability in the event of failures or situations that the autonomous algorithm is not robust enough to deal with.

Telerobotic manipulation systems normally have a robotic slave arm connected to some sort of end effector, ranging in complexity from parallel-jaw grippers to anthropomorphic (human-like) hands. Dexterous, multi-finger robot hands offer much more capability than simple parallel-jaw grippers. Hands can form more stable grasps with less force, reach into smaller areas using fingers, manipulate objects in addition to simply grasping, and use tools designed for human use. A hand may also be able to reform an unsatisfactory grasp without putting an object down; the only remedy available with a parallel-jaw gripper would be to simply clamp harder (which may break the grasped object or not work anyway). These attributes build upon the flexibility inherent in teleoperation. Barring significant advances in autonomous robot control, teleoperation is currently the only way to control sophisticated robot hands (refer to Salisbury for a discussion [101]). Adding actuators to the equipment worn by the operator to control the robot hand allows the operator to feel the forces experienced by the robot hand. This force feedback allows operators to use the minimum necessary grasp force and to feel the slave's interactions with the environment. This reduces the danger of damage to the slave or environment, and shortens task completion times [75, 89].

A dexterous hand master is a device that measures the finger positions of a human operator for input to a dexterous robotic slave hand or a virtual environment. In the virtual application, the hand master may control either a virtual slave hand, or some other virtual device or process. A hand master normally consists of an exoskeletal structure worn on the hand of the operator, or a non-exoskeletal device into which the operator inserts his or her fingers. The hand master may have actuators to "reflect" forces and tactile stimuli acting on the fingers of the slave hand to those of the operator's hand (see Figure 1). These sensory feedback mechanisms have the potential to greatly enhance the manipulation capabilities of teleoperated hands (it might be argued that manipulation is nearly impossible without these senses). Some proof-of-concept hand masters have attached to as few as one or two fingers. Working hand masters for telerobotic manipulation normally interface with three or four fingers. Functional hand masters are frequently mounted on a seven degree-of-freedom (dof) exoskeletal arm master, or on a non-exoskeletal platform with fewer

degrees of freedom (at least six dofs are needed for normal operation). Seven dof arms offer the advantage of redundancy (being able to reach a certain point and orientation in space in more than one way), and have the potential to be used in whole-arm manipulation, where the arms themselves are used as opposing "fingers" to grasp and manipulate large objects. Since unstructured tasks requiring telerobotic dexterity often require the capability offered by a seven dof platform, most hand masters for telerobotics have been intended for use with seven dof exoskeletal arm masters [5, 56, 57, 84, 85].

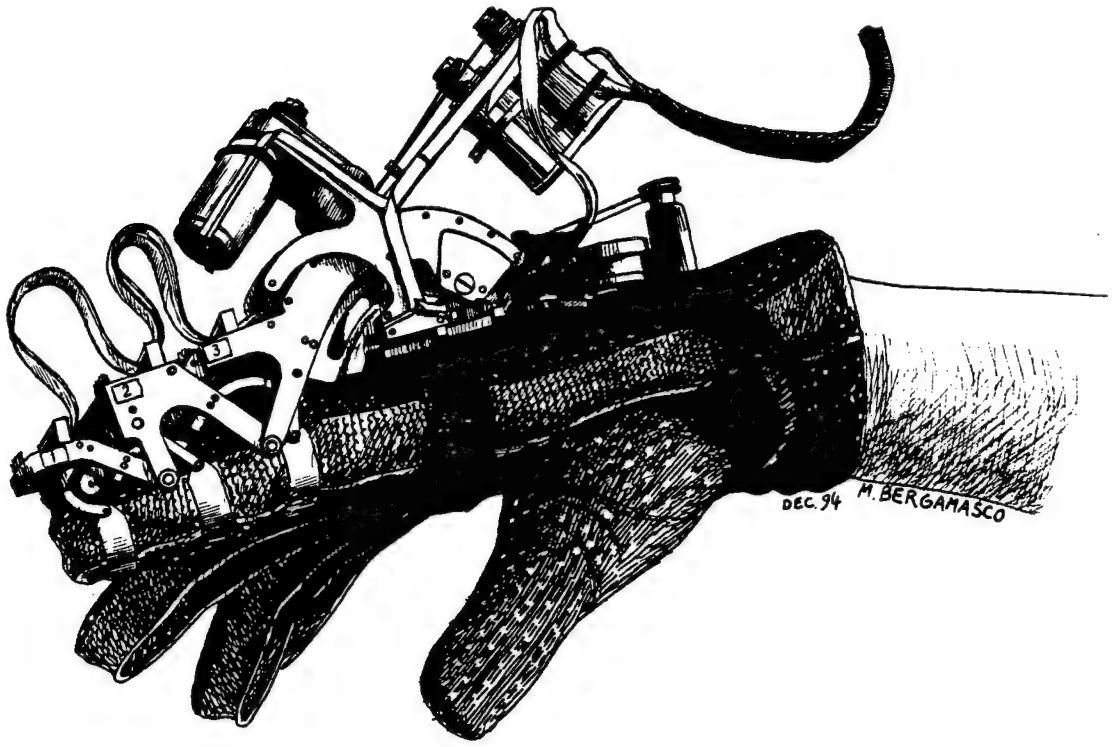


Figure 1: A Force-Reflecting Exoskeletal Hand Master (Courtesy M. Bergamasco)

Though a "complete" sensory feedback hand master would be able to display both manipulation forces and tactile stimuli to the user, this report focuses almost exclusively on the former. The physiological manipulation studies of Johansson and others, as well as the force-reflecting hand master design and operating experience of Jau et al., suggests tactile feedback is necessary and that force reflection alone cannot provide sufficient sensory feedback [58, 121]. In trials with one of the most advanced force-reflecting hand master-slave systems yet fielded, Jau found that the lack of tactile feedback significantly hampered tool maniulation [58]. In addition to giving information about surface details, curvature, and texture, the tactile sense produces a perception of contact location that can be crucial in manipulation. Only a few force-reflecting projects have included complex tactile feedback [32, 63, 84, 85]. The tactile feedback problem equals or exceeds the depth of the force feedback problem, and full coverage of it could easily double the size of this report (see Kaczmarek and Shimoga for excellent reviews [61, 109, 110]). The addition of tactile feedback to a force-reflecting hand master adds mass and complexity to a class of systems that already exists

near the boundary of feasibility. The fact that both research areas can be cost and labor intensive also helps to explain why few efforts have attempted to add tactile feedback to force-reflecting hand exoskeletons. The first dual tactile/force systems that actually work and are followed up by published experiments with some generalizability will involve simplification of at least one of the systems. Kontarinis, Howe, et al. have added complex tactile feedback to a simple (planar) high-fidelity finger master-slave system. Work ongoing in the Armstrong Laboratory will add a simple one-actuator tactile device to the PHANToM™ haptic interface (which reflects forces in three dimensions rather than two). Follow-on work will add shape-memory alloy (SMA) driven tactile arrays similar to those of Kontarinis and Howe.

A significant similarity exists between human interface devices for telerobotics and for the emerging field of virtual reality. In fact, more often than not, these devices are identical. This includes arm masters, hand masters, head-mounted displays, tactile and audio feedback devices, etc. Simulated "hands-on" molecular docking applications at UNC Chapel Hill and at the Air Force's Wright Laboratory are examples of virtual reality systems using master controllers originally designed for telerobotics. Dexterous hand masters will also find use in virtual reality, as well as telerobotics. In fact, at least one hand master was designed for human-computer interface [50]. Far into the future, as autonomous robot hands take over tasks previously serviced by teleoperation, virtual reality applications will flourish.

## Definitions

Dexterous hand masters can have several different forms. Oomichi defined four different types of hand masters [86]:

**"Fitted along fingers"** The exoskeletal structure fits closely along the dorsal aspect (back) of the fingers, with straps, rings, or thimbles securing it to the fingers.

**"Similar shape"** The operator's hand nests inside a large version of the slave hand with fingertip attachments.

**"Faced" type** The exoskeleton faces the palm of the operator's hand. The exoskeleton "hand" mirrors the operator's hand, with the two connected together at the fingertips. The majority of the exoskeleton remains outside of the operator's finger workspace.

**Combination of "similar shape" and "faced"** No closely fitted finger attachments, with exoskeletal elements on both palmar and dorsal side of hand.

Zarudiansky defined a different type of device, in which the user inserts the hand into a box, and cables are attached from the walls of the box to the fingertips [123]. The device as illustrated by Zarudiansky could represent forces in only a limited number of directions. Another hand master concept uses air bladders placed on the palmar aspect of the fingers, similar to Oomichi's "fitted along fingers" type, but with a less rigid structure and mounted on the opposite side of the fingers [60].

Parallels exist between dexterous robotic hands and dexterous hand masters. Oomichi's "similar shape" hand master exemplifies these parallels, and applies to hand masters that are very much

like the robotic hands that they control, with respect to shape, kinematics, and other parameters. One difference between robot hands and hand masters is that the structure of a robot hand can exist within the robot fingers–it may soon even be possible to direct-drive robot fingers at the joints [38]. Direct-driving human fingers with mechanical actuators is obviously impossible; at least some transmission will be required. This limitation is an indication of the serious mass and volume restrictions placed on hand master designers; the structure of the hand already exists, so the mass and volume of the hand master must be placed around the hand without interfering with it. This makes the design of hand masters arguably more difficult than the design of robot hands, a task which has captured the efforts of some of the best mechanical designers for many years.

The following definitions clarify the terminology in this report. Some have been adapted from Mishkin and Jau [77].

**Manipulation:** Acting upon an object with one or more hands in more ways than just simple grasping. Accepted examples usually include turning or repositioning an object in one hand, and pulling the trigger of a power tool that is being grasped. In order to have manipulation capability by itself, a single end effector must have at least three digits, each with at least a two-dof base knuckle joint.

**Dexterity:** The combination of mechanical manipulative capability and sensorized (force, position, and tactile) "smartness" that actually allows manipulative tasks to be performed.

**Multi-DOF End Effector:** End effectors that possess more than one dof, but do not have manipulative capabilities unless otherwise stated.

**Dexterous Hand:** A hand with at least three manipulative fingers and incorporating sufficient sensors to possess dexterity.

**Anthropomorphic Hand:** A hand with a thumb, two to four fingers, a palm and wrist in a human-shaped configuration, which is capable of dexterous manipulations, and for which the thumb can rotate outward to form a flat, open-faced hand for pushing or two hand operation. Additional features may include fingernails, soft surfaces on inner hand surfaces, and compliance in the joints.

Terms denoting different finger bones and joints appear frequently throughout this report:

**Carpal Bones:** The cluster of bones at the base of the palm.

**Metacarpal Bones:** The bones in the palm of the hand; one connects to the base of each finger at the metacarpal-phalangeal (MCP) joint.

**Phalanges:** Bones for the individual finger segments. The singular form is "phalanx."

**Metacarpal-Phalangeal (MCP) Joint:** The "base" knuckle joint, at the root of the finger. Each MCP joint has two degrees of freedom: flexion/extension (bending) and abduction/adduction (sideways movement).

**Proximal Interphalangeal (PIP) Joint:** The middle knuckle.

**Distal Interphalangeal (DIP) Joint:** The last knuckle, closest to the fingertip.

# History

One of the earliest applications of teleoperation was for the handling of "hot" radioactive materials. A Remote Control Group was founded at Argonne National Laboratory (ANL) in 1947 [34]. Systems progressed from master-slave devices with purely mechanical linkages between master and slave, to electrical devices with primitive switch interfaces, and finally to master-slave electromechanically servoed devices. For decades, however, the end effectors of these teleoperators were simple, usually parallel-jaw grippers. An early ANL manipulator patented by Ray Goertz is an historic example of an early device equipped with a parallel-jaw gripper [35]. Ralph Mosher at General Electric described the GE Handyman, a two-arm telerobot system, in 1960 and 1964 [79, 78]. The Handyman had 10 degrees of freedom per arm, three of which functioned in the hand. The hands each had two digits, with one pincer-dof to bring the digits together, and one flexion/extension dof in each digit. The slave arm and hand were controlled by kinematically identical arm and hand masters. Mosher's outline of general requirements for a force-reflecting teleoperator is still germane 30 years later.

In 1966, Jones and Thousand patented one of the earlier documented designs of a force-reflecting hand master [60]. The design incorporates air bladders, with one worn on the palmar aspect of each finger. In 1967, Johnson and Corliss published a photograph of the Central Research Laboratories (CRL) electropneumatic hand, made by CRL in Red Wing Minnesota (Johnson and Corliss, p. 102) [59]. The photograph shows a primitive one to three dof gripper with two fingers controlled by a human hand wearing a leather work glove fitted with a low profile exoskeleton on the index finger. The exoskeleton appears to have two pneumatic cylinders lying flat on its links. In 1981, Zarudiansky patented a design with the hand suspended in a box; he proposed cables pulling from various sides of the box to reflect forces to the operator [123]. Zarudiansky also produced illustrations of possible joint angle sensors, including a hemispherical track with a center of curvature at the axis of rotation of the finger joint. No references were found to document construction of his concepts.

Recent implementation of hand masters began with devices having only position control of the slave, with no force feedback. Two finger position measurement devices exist that are literal gloves. The DataGlove, marketed by VPL Research, was delivered to NASA Ames in 1986 and was patented in 1992 (Figure 5) [40]. It uses fiber optic sensors to detect finger joint angles. The VPL DataGlove has enjoyed wide popularity in the virtual reality market. Unfortunately, the relationship between sensor measurements and human joint angles is not linear, and the device requires extensive calibration effort to drive a robot hand [44]. Burdea et al. used the VPL DataGlove as part of a force-feedback hand master, but have since developed their own position sensing apparatus [21, 36]. Rovetta et al. have used the VPL DataGlove to control a robot hand, and plan to develop force feedback [99].

The second device, the Virtex CyberGlove, is a soft glove like the VPL DataGlove, but it uses strain sensors [65]. An entertainment device, the Nintendo PowerGlove, uses similar technology. The CyberGlove can include up to 20 sensors, covering all finger flexions plus two wrist bends. The CyberGlove seems to be better suited to teleoperation applications than the VPL DataGlove, with a more stable output and no fingertips on the glove to complicate sizing [73]. The CyberGlove also has less trouble with sensor coupling, giving measurements for each joint that are relatively less

polluted by movements of nearby joints. NASA Johnson is considering the use of a CyberGlove to teleoperate a Stanford/JPL Hand [67].

An early position-control hand master appeared at Sarcos Research Corp. and the University of Utah by 1986. The Arthur D. Little Dexterous Hand Master (DHM), currently licensed by EXOS, Inc. was the next (after the VPL DataGlove) anthropomorphic master to be commercially available (Figure 7). Arthur D. Little sold a left-right pair to the Armstrong Aerospace Medical Research Laboratory in 1988. Similar work occurred in Japan in the mid to late-eighties, with at least one researcher (Maeda at MEL) constructing a position-control hand master as part of a full arm master-slave system [69].

Devices also exist that add tactile feedback to a position sensing system, but do not include force feedback. Advanced Robotics Research Ltd. (ARRL) and Airmuscle developed the Teletact Glove in England. It has air bladders under each phalanx for tactile feedback. While this form of tactile feedback cannot give information on object texture or fine details, the sense of contact location may be useful in manipulation. The Teletact Glove uses force-sensing resistors to measure joint angle. The Teletact II is instead integrated with a VPL DataGlove for joint angle measurement.

Efforts to develop anthropomorphic force-reflecting hand controllers did not begin in earnest until the mid-eighties. The TOPS system, developed by the Center for Engineering Design at the University of Utah and Sarcos Research Corp. for the U. S. Navy, was probably the first formidable example to emerge (Figures 10 and 11) [52]. Two hand master prototypes were built. Both were hydraulically powered and used antagonistic cable tendon pairs to transmit forces to the finger joints. The first-stage prototype has nine actuated degrees of freedom in both the master and slave hands; with the antagonistic tendon design, 18 actuators were needed. All finger actuators are linear. Custom miniature hydraulic cylinders and servo valves were developed for the project [52].

The TOPS system also includes an arm master and slave with anthropomorphic wrist, elbow, and shoulder, resulting in a full arm and hand teleoperation system. The hand master has a four dof thumb and two fingers. The fingers each have two flexion/extension dofs, and the hand master has a single dof to spread the fingers apart. Four dofs on the thumb combine with the five allocated to the fingers for a total of nine dofs. The master and slave systems were designed to be kinematically identical. The hand master was designed to have axes of rotation coincidental with those of the operator's hand and finger joints. The extremely complex TOPS system was successfully tested in an underwater tank, performing tasks such as threading steel cables through large eye hooks. The TOPS system is not in active use today, though Sarcos markets a commercial spinoff with a semi-dexterous (non-anthropomorphic) end effector (Figures 12 and 13) [53, 54].

The second comprehensive arm and hand master-slave system to emerge in the United States was developed by Bruno Jau at the Jet Propulsion Laboratory (NASA JPL) in the late eighties and early nineties [56, 57]. The hand master is a 16 dof exoskeleton, part of an overall master-slave arm and hand system with 23 dof (16 for the hand plus seven for the arm) and seven extra compliance-control dofs on the slave arm. The master and slave are kinematically identical. The hand has three fingers and an anthropomorphic thumb mounted at the side of the palm. All actuators are backdriveable DC servo motors. Actuators for the hand master are mounted on the forearm, near the elbow. Transmission between actuator package and hand master is by flex cable. Four-bar mechanisms and pulleys backdrive the human finger joints. The driven pulleys are located above the finger joints and four-bar mechanisms link the pulleys with finger linkages. An off-the-shelf

glove secures the hand master to the operator's hand. Metal parts of the hand master are stitched to the glove. The hand master is adjustable for size. A base plate on the back of the hand transmits force to the operator to reflect slave wrist forces. The system has a number of interesting features, including position and strain-gauge force sensors embedded at every joint of the master glove (16 position and 16 force sensors). Jau claims a 0.83 N (3 oz) force-reflection threshold. Fiber optic cables carry communications between system components.

At the same time JPL and Sarcos were developing systems in the United States, parallel development progressed in Japan. Iwata developed a hand master on a miniature Stewart-type platform (6 dof parallel stage) with a single dof for each of the first two fingers and the thumb [50]. The device was intended mainly for interaction with computer environments, as evidenced by the limited degrees of freedom in the digits and the limited range of motion of the parallel stage. A much more comprehensive system equal in magnitude of effort to the JPL and Sarcos systems was developed by Mitsubishi Heavy Industries (MHI) in collaboration with the Electrotechnical Laboratory (Figures 14 and 15) [83, 84, 85, 86]. MHI developed a complete two-arm bilateral force-reflecting system. The system has demonstrated various tasks typical of nuclear plant maintenance , such as the disassembly of a large valve. An earlier, one-arm version of the system enabled an operator to turn a nut on a bolt without being able to see the workpieces.

The MHI project was initiated in 1983. The master and slave arms both have 7 dof. The left hand has 14 dof, while the right hand has 13 dof [86]. The hands have four fingers, with 3 dof each (one abduction/adduction and two flexion/extension dofs per finger). The 13th dof in the slave is provided by a bending joint at the palm. The 14th dof in the left hand is provided by a rotating "swing joint", with an offset at the base of the thumb. The slave fingers also have a number of tactile sensors. These tactile sensors provide feedback to actuated pads that push on the operator's fingers to provide a tactile sense of the contact state on the fingers.

The master and slave fingers have position-sensing potentiometers about 5 mm in diameter. The slave has two-axis force sensors with a 0.1 N threshold located in each finger. The master has force sensors in the center of each link in the finger sections. The master hand has thimble-like attachments on the fingertips, similar to the TOPS system by Sarcos. The thimbles appear to cover the distal interphalangeal (DIP) joints, which are not free to move. The design is a combination of "similar shape" and "faced," as defined by Oomichi [86]. The hand passes through a band that surrounds the palm and the back of the hand. Other than this band and the finger thimbles, the rest of the back of the operator's hand is left unencumbered.

At least four more efforts exist in the United States, at varying levels of maturity. The most mature is the Sensing and Force Reflecting Exoskeleton (SAFiRE) developed by EXOS, Inc. [72, 71, 26]. EXOS began developing the SAFiRE under a Phase I Small Business Innovation Research (SBIR) contract with NASA Marshall that concluded in August 1991. The SAFiRE uses DC servo motors mounted on the back of the hand or the forearm with gearheads and cable tendon transmissions to the joints. A two-dof index finger prototype has been demonstrated, and a thumb is under development. EXOS recently completed a Phase II SBIR project on the SAFiRE, and delivered a prototype to NASA Marshall. In June of 1994, EXOS completed another Phase I SBIR project, to construct a Hand Exoskeleton Haptic Display (HEHD), essentially a Phase I SAFiRE modified to include slip feedback.

Burdea at Rutgers has developed at least two generations of prototype hand masters actuated by pneumatic cylinders (Figure 16) [21, 23, 36]. The pneumatic cylinders are placed in the palm, with only one actuator per finger, connected between the fingertip and a base in the palm. The system is lightweight and relatively inexpensive, but cannot reflect lateral (abduction or adduction) finger forces, or forces between the fingers.

Begej Corporation is continuing to develop a two-finger-and-thumb hand master for NASA JSC, also under a Phase II SBIR contract. A six-month Phase I contract was completed in September 1990. Tactile sensing and pneumatic feedback technology make the Begej effort unique; the hand master has thimble-like fingertips with 3 mm diameter pneumatically actuated rubber diaphragms for multi-element tactile feedback. The Begej device also uses DC servo motors similar to those on the SAFiRE, but the motors are co-located on the back of the hand master fingers, with the associated gear reduction and transmission to joint rotation. The final device is intended to have PIP joints and two-dof MCP joints in the fingers, and comparable dofs in the thumb.

Researchers at Vanderbilt University developed a force-augmentation hand exoskeleton for persons wearing bulky gloves such as those found in space suits [108]. The exoskeleton has three fingers and no thumb. It uses a four-bar linkage model of the finger joint mechanism, driven by a DC servo motor mounted on the forearm. The motor transmits torque through a gearhead to a solid drive bar with universal joints at either end, down to a ball-screw assembly mounted on the back of the hand, to convert rotational motion to linear motion. Steel cables connect the ball-screw assembly to cams at the joints.

In July 1993, Technical Research Associates (TRA) began a Phase II SBIR contract sponsored by the Air Force (Armstrong Laboratory) to develop magnetostrictive actuators for force-reflecting hand exoskeletons (Figures 18 and 19). The Phase II followed a successful Phase I project which produced prototype linear motors and joint brakes. In Phase II, TRA is attempting to integrate refined actuators into a force-reflecting hand exoskeleton.

## Existing Force-Reflecting Hand Master Systems

When this report was begun, only a handful of force-reflecting hand exoskeletons existed; however, in recent years a second handful of efforts have begun. The players continue to be a mix of academic laboratories and government-sponsored companies. Only one in-house government effort exists, at NASA's Jet Propulsion Laboratory. At least two efforts exist in Europe, and at least one in Japan. Table 1 summarizes the known efforts. More information appears in Appendix F, "Hand Master Data Sheets."

Of the efforts listed, only two (at Rutgers and JPL) are known to have published significant work involving fully-functional hand masters used in manipulation; the Rutgers Master with a virtual slave, and the Jau/JPL master with a slave robot hand [58, 92]. Sarcos also achieved operational capability with the system it developed for the Naval Ocean Systems Center (NOSC), but no publications describing that work have been found.

Table 1: Summary of Existing Force-Feedback Hand Masters

| # | Organization | Device Name | No. of Fingers | No. of Joints | Actuation | Transmission |
|---|---|---|---|---|---|---|
| 1 | ARTS/PERCRO Lab | Hand Force Feedback System | 4 | 16, 4* | electric | |
| 2 | Begej Corp. | Master Glove Controller | 1 | 2 | electric | lead screw/cam |
| 3 | Cybernet | PER-Fingers | 5 | 5, 6* | electric | |
| 4 | Dartmouth | | 2 | 5, 2† | electric | sheathed cable tendon |
| 5 | EXOS | SAFiRE | | | electric | cable (sheaths & pulleys) |
| 6 | Lab. Rob. de Paris | LRP Hand Master | 5 | 14 | electric | cable tendons |
| 7 | Mitsubishi Heavy Industries | | 4 | 14 | | |
| 8 | JPL | Jau/JPL | 4 | 16 | electric | torque cables |
| 9 | Rutgers | PMDFF, RMII | | | pneumatic | pneumatic |
| 10 | Sarcos | TOPS | 3 | 9 | hydraulic | hydraulic |
| 11 | U. of Tsukuba | – | 3 | 3 | electric | |
| 12 | Virtex | CyberForce? | | | electric | sheathed plastic cables |

| Sponsor | Contact Person | e-mail | Status†† | References | # |
|---|---|---|---|---|---|
| | Massimo Bergamasco | bergamasco@sssup1.sssup.it | A | [5, 4] | 1 |
| NASA Johnson | Stefan Begej, L. Li | li@ctsd2.jsc.nasa.gov | D | [3] | 2 |
| NASA | Heidi Jacobus | heidi@cybernet.com | A | | 3 |
| VA | Sunil K. Singh | sunil@northstar.dartmouth.edu | D | [13] | 4 |
| NASA Marshall | Beth Marcus | bam@media-lab.media.mit.edu | A | [26, 33, 71, 72, 26] | 5 |
| | M. Bouzit | bouzit@robot.uvsq.fr | A | [18] | 6 |
| MITI | Takeo Oomichi | | | [83, 84, 85, 86] | 7 |
| NASA JPL | Bruno Jau | | D | [55, 57, 56] | 8 |
| | Grigore Burdea | burdea@telerobo.rutgers.edu | A | [19, 20, 23, 21, 36] | 9 |
| U.S. Navy | | f.smith@sarcos.com | D | [52, 53, 54] | 10 |
| – | Hiroo Iwata | – | A | [50] | 11 |
| | Jim Kramer | info@virtex.com | A | [64] | 12 |

* Second number for degrees of freedom with position-sensing only (no force feedback)

† Number of additional joints that receive force-reflection but are not independently controlled

†† A=active, D=dormant

# APPLICATIONS, JUSTIFICATIONS, AND CHALLENGES

The special features of force-reflecting anthropomorphic hand masters make a wide range of applications possible. The name itself implies two significant features: the ability to apply forces to the operator's fingers, and the ability to operate several multi-jointed slave fingers independently. Neither of these added capabilities comes cheaply, so each must be justified by the intended application. Most publications dealing with force-reflecting anthropomorphic hand masters accept the utility of force reflection and anthropomorphism, focusing on the new developments being presented. The luxury of space in this technical report creates an opportunity to justify these basic assumptions.

While an anthropomorphic hand is necessarily multi-fingered, many multi-fingered robot hand designs are non-anthropomorphic. For brevity, this report outlines the benefits of anthropomorphic hands, without separately discussing multi-finger hands. The assumption here is that the kinematic similarity between the operator's hand and an anthropomorphic hand it controls make anthropomorphism the obvious choice for teleoperation. The more different the slave hand is from the operator's, the harder it will be to teleoperate with natural hand movements; however, non-anthropomorphic hands will still have many of the benefits cited for anthropomorphic hands.

Once system designers have decided to include force reflection and anthropomorphism in a hand master, significant challenges must be overcome before a useful system can be produced. The fourth subsection in this section briefly describes those challenges.

## Applications

Uses for a force-reflecting anthropomorphic hand interface fall into at least three categories. The first, and the most obvious, is direct teleoperation of an anthropomorphic robot hand. The second category of uses would take advantage of the high-fidelity force and position interface to teach the complex function of the human hand to intelligent manipulators, or to better understand human grasping. The third application would be to synthetic (virtual) environment interfaces, for which the list of uses is limited only by the imagination.

A fourth possible category would be in hand rehabilitation, where the ability to cycle the rehabilitating fingers through a given trajectory or with a given force might prove useful [13, 58]. As with upper-body man-amplification systems that have been developed, there would be no "slave," just the human limb wearing an exoskeleton. A force-feedback glove could potentially fill the dual role of a physical therapy device during rehabilitation sessions and a force-augmentation device to amplify the strength of the fingers while performing daily tasks. Force augmentation may also be useful if the operator's hand has an encumbrance such as a space suit glove, as with the Vanderbilt device [108].

Any task requiring the fine manipulation capabilities of the human hand could use a force-reflecting hand master for teleoperator control of a slave hand. Candidate applications include extra vehicular activity (EVA) substitution in space, telerobotic assembly in inaccessible environments (e.g. underwater or in ultra clean rooms), and telesurgery. Operations with delicate or small objects or with unpredictable requirements are especially good candidates.

Uses for dexterous, and most likely anthropomorphic, hands will be found for virtual and telepresent surgery and other medical procedures. While great success can be found with special purpose devices such as laparoscopic camera manipulators [120], or with teleoperation of zero and one dof surgical tools such as scalpels and forceps [88], the surgeon's or diagnostician's hand is an irreplaceable tool for many tasks. The hand and fingers are well-suited to grasping semi-solid organs, probing, palpating, and manipulating other body parts. Preparing a teleoperated surgical suite for a generalized battery of procedures using only exchangeable end effectors with no dexterous hands may well be an unrealistic task.

For any task that may be teleoperated with a dexterous hand, training using a hand master interfaced to a virtual reality environment may prove useful. EXOS, Inc. developed a graphic simulator to demonstrate the uses of the SAFiRE hand exoskeleton for astronaut training in microgravity glovebox operations [26]. Force-reflecting hand masters may eventually find their way into commercial and entertainment applications (requiring of course, great reductions in cost). An architect's client could walk through a simulated structure turning doorknobs, running faucets, and operating appliances. Consumer products could be rapidly prototyped in virtual environments using CAD data and consumer-tested with no fabrication costs or delays.

Individual applications can justify the use of a force-reflecting hand master; however, an alternate way to consider the possibilities would be to view the enhanced hand interface as a means of broadening the communications bandwidth between the human and the remote (synthetic) environment. Primitive systems without sensory feedback choke the operator's ability to perceive the environment and act on it. Successive improvements will continue to increase efficiency, add capabilities, and reduce the risk of damaging the remote manipulator or its environment. Information system interfaces have advanced from punch cards and paper printouts towards the dream of human intelligence augmentation. Parallel advances in the physical human-machine interface will catalyze applications unimaginable with today's current state of technology.

## Anthropomorphic Justification

Mishkin and Jau concluded that dexterous manipulation would be required to replace astronaut extravehicular activity (EVA) [77]; however, the complexity and cost of anthropomorphic robot hands have generally prevented their use in the field. Parallel-jaw grippers have been used since the inception of telerobotics, due to their simplicity. Many tasks can be successfully adapted to the use of parallel-jaw grippers; however, parallel-jaw end effectors are severely limited. They cannot handle small objects, must rely on high frictional forces to hold most objects, and cannot manipulate objects in the hand. Dexterous slave hands provide a larger variety of grasps, and grasps with more stability, than parallel-jaw grippers. They are also better able to handle tools and objects designed for human use. Sophisticated robot hands can even manipulate objects within their grasp.

If multi-fingered (dexterous) hands are so capable, why are they not more popular? Design complexity, cost, and limitations in component technologies (such as actuators) have been significant reasons. Specialized, interchangeable-tool end effectors have offered an alternate solution with more capability than parallel-jaw grippers. Since interchangeable-tool end effectors have been more

technically realizable in the short term, some engineers designing systems for EVA have found this solution attractive.

Interchangeable-tool end effectors offer the advantages of simpler, proven designs, easier implementation, positive locking (no chance of dropping tools), and are much more amenable to autonomous control (no need to autonomously control a complicated multi-finger hand for a simple tool task). The bottom line is that many tasks require simple limited-degree of freedom tools (often with one degree of freedom or none at all). Many manual tasks require only tool use and no dexterity; once a tool is firmly grasped in a hand, manipulation capabilities are rarely used (motion occurs at the wrist). If a mission can be accomplished with only three or four of these tools, then designing the exchangeable tool set may well be simpler and less costly than designing a multi-dof anthropomorphic hand. However, the variety or complexity of the tasks can increase to make an exchangeable tool approach costly and impractical. Furthermore, specialized-tool end effectors are committed to tasks as the designers originally perceived them. Designers' perceptions may be wrong, or different needs may arise as the mission evolves or new missions are added. People forced to find creative solutions to unstructured problems often discover new uses for tools, or use objects not even intended to be tools. Specialized end effectors, by restricting the operator to modes envisioned by the original engineers, could severely hamper contingency operations and eliminate the benefits of telerobotic access.

For an unpredictable or broad range of tasks, anthropomorphic robot hands have strong appeal. Task-specific tools limit the capability of a system. Tool exchange and locking mechanisms will increase task completion time and design expense. Relatively large end effectors must be stored within the workspace of the manipulator. Exchangeable end effectors also inflict a weight penalty. In many instances, manual tools capable of accomplishing the tasks may already exist at the site; the redundant weight of the exchangeable tools and the additional weight of the tool-locking mechanisms must be added to the system weight. Anthropomorphic hands may involve more development effort, but will eliminate the development time required to produce special tools and equipment for use with less capable end effectors. Teleoperation of tasks that the operator would normally perform directly with his or her hand may be difficult with an exchangeable tool system. Operations requiring complex manipulation of the environment require multi-finger dexterity. Anthropomorphic hands have many advantages for both tool handling and direct manipulation [77]:

- Can rotate thumb outwards (abduction) to form open-faced, flat hand useful for two-handed operation
- Easier to pick up objects
- Can use off-the-shelf tools
- Form stable cradle grasps without relying on high clamping forces
- May be able to reform unsatisfactory grasp without putting grasped object down
- Access smaller spaces with fingertips or fingernails
- Grasp object from different directions, without detailed prior knowledge of object shape and orientation
- Force control and compliance on small manipulators (fingers) permits very delicate tasks not possible with clumsy end effectors
- Very versatile: can use fingernails, fingers, palm, arm, or two hands

- Increased grasp capability with compliant grasping can greatly ease assembly tasks
- With sufficient degrees of freedom, can manipulate grasped objects

All of these attributes can give an anthropomorphic system an ergonomic transparency and speed of operation not attainable with other approaches. Salisbury offers four reasons for adding multi-degree-of-freedom hands to teleoperators that agree substantially with those given by Mishkin and Jau [101]:

- A wider variety of more stable grasping patterns
- Increased bandwidth of motion for small motions
- Increased resolution of motion and force exertion
- A greater number and quality of channels available for haptic sensing of the environment
- New modes of manipulation (e.g. controlled slipping, partially constrained grasps, and ballistic motions)

It has been said that an experienced carpenter, surgeon, etc. experiences the task through the tool, with the tool being merely an extension of his or her body. Conversely, the novice experiences the tool in his or her hand. This bit of conventional wisdom does not mention that sometimes the hand is the tool, not just a tool holder. Handless tool-exchange end effectors must perform without the most versatile tool of all—an anthropomorphic hand. This can be seen readily when one human body interacts with another in the caregiver-patient role. The hands and fingers are ideally suited for opening a patient's airway with a jaw thrust, probing between ribs to insert a chest tube, applying pressure to a wound, probing for landmarks or debris, etc. Some excellent surgical tools can be developed for teleoperated surgery with limited degrees of freedom, and entire procedures are probably possible using instruments with only one or two degrees of freedom, but any comprehensive management of patients in a teleoperated system will require at least one dexterous hand.

While anthropomorphic dexterous hands offer the gold standard for a flexible teleoperation system, non-anthropomorphic multi-finger hands have been able to achieve significant capability with fewer degrees of freedom. A multi-dof end effector such as that present on the commercially available Sarcos Dexterous Teleoperation System (DTS) can provide flexibility in grasping objects and tools, and performing tasks like turning nuts on bolts, etc. [53]. The DTS end effector has three "digits," and three degrees of freedom, including a thumb with two dofs at the base. The thumb rotates 90 degrees out to the side, and also rotates towards the first and second fingers to form a pinch grasp (90 degree range of motion). The second finger abducts and adducts laterally up to 45 degrees. All three digits are stiff and machined out of aluminum. The first finger is rigidly affixed to the hand. The end effector is capable of performing five standard grasps: wrap, cradle, power, pinch, and lateral.

While the end effector of the DTS master-slave system cannot be used to reposition objects within its grasp, the designers have achieved a capability for stable grasps and utility far exceeding that of a parallel-jaw gripper. Nevertheless, anthropomorphic hands and hand masters are unparalleled in their flexibility and capability. They have the potential to make the connection between

operator and environment more transparent, reducing task completion times and making new tasks possible.

## Force Reflection Justification

Since hand master systems are so uncommon, and systems with working force reflection even rarer, studies comparing dexterous telemanipulation with force reflection to that without force reflection are difficult to find; however, numerous studies support the value of force feedback in non-dexterous arm telemanipulation tasks. Before considering the use of force reflection in an application, at least three disadvantages must be reckoned with:

- Cost and complexity
- Weight and volume
- Can contribute to instability with time delay

These disadvantages are not without remedy. Cost and complexity, as well as weight and volume, of systems should be reduced as the technology advances, though force feedback systems will never be as simple as those without force feedback. The issue of time delay affects only a portion of teleoperation applications. Approaches which use predictive displays may provide some help in coping with time delays. Some control solutions exist which aim to gracefully degrade performance with increasing delay in order to guarantee stability.

Given that the addition of force reflection has a large initial cost, numerous operating advantages in many areas reduce subsequent costs:

- Reduces requirement for position accuracy between master and slave
- Reduces training time
- Reduces dependence on visual feedback for some tasks
- Reduces task completion time
- Reduces grasp forces
- Reduces errors

Force reflection diminishes the need for accuracy between master and slave positions. Being able to feel the environment quickly allows the human operator to adapt to a certain level of inaccuracy. In normal manipulation tasks, people rely more on the senses of touch and force than on position. Training time will likely be reduced due to the intuitive nature of force reflection, and the operator not having to learn to cope with absent or cross-modal sensory information (e.g. visual display of force information). The addition of force feedback will reduce the operator's dependence on visual feedback [75], allowing haptic exploration or groping when vision fails to give sufficient understanding or becomes obscured. Force feedback may also contribute to grasp stability, as the operator will be able to quickly and intuitively adjust grasp forces in response to force changes in

the slave environment that are not perceptible through vision, and would be potentially difficult to feed back using cross-modal feedback from tactile vibrators.

Hannaford et al. showed that the addition of force feedback to their tasks reduced completion time by 30%, sum of squared forces by 86%, and errors by 63%. In those experiments, a person operating a PUMA 560 robot with the JPL six-axis force-reflecting arm controller (with a cylindrical grip terminus) performed tasks on a remote task board [39]. The modular task board contained Velcro™ attachment, peg-in-hole matrix, electrical connector, and bayonet connector subtasks. Task completion time, sum of squared forces, and number of errors were measured. Completion time for one task was 92 sec with position control, 63 sec with force feedback, and 14 sec when executed directly by a bare-handed operator. Marked reductions in sums of squared forces were noted with the progression from position control (3500 $lb^2$-s) to force feedback (500 $lb^2$-s)) to bare-handed execution (200 $lb^2$-s). The number of errors per repetition dropped from 3.0 to 1.1 when force feedback augmented position control (no errors were observed for bare-handed operation).

Patrick et al. compared simple position control to control with either force feedback or simplified feedback via a piezoelectric vibrator [89]. Subjects used an Argonne E-2 arm teleoperator system, tapping as rapidly as possible between two points. The width of the targets and their separation determined the index of difficulty in this Fitts' Law task. Task completion time with the addition of tactile contact (vibration) feedback compared favorably to completion time with force feedback. Both were significantly better than no feedback at all. A key weakness of tactile feedback alone is that the master cannot physically force the operator to stop a motion when the virtual or remote slave encounters an immovable object. The operator may feel his hand and hand master inside the bounds of a remote or virtual object while receiving sensory information based upon the slave's contact with the outside of the object; position registration between master and slave is lost. As task difficulty increases, the gap between force and tactile completion times widens. This shows advantages of force over tactile feedback, but suggests that the additional complexity of force feedback must be justified by higher task difficulty. An alternate justification might be an environment where damage is likely or consequences of damage are severe.

Richard et al. used a Rutgers Portable Dextrous Master with Force Feedback to manipulate three virtual objects in a computer simulation: a ball, a spring, and a soda can [93]. The authors showed that for the tasks studied, the presence of virtual force feedback reduced learning time by 50% and increased dexterity (as measured by reduction in plastic deformation of the soda can) by 50%. In another study with 64 subjects, Richard et al. showed that after training, force feedback to the hand decreased plastic deformation of a hard virtual ball by 65% from trials with no force feedback (other than cues from a graphics simulation of the ball and slave hand) [94]. Auditory feedback of forces only reduced plastic deformation by 55% in the hard ball case. For the soft ball, auditory feedback actually worked better, reducing forces by 40% versus a 21% reduction with force feedback. The authors suggested (and this author agrees) that this result may have occurred because the subjects' haptic senses were much more susceptible to the reduction in dynamic range than was their auditory sense. The relative effect of friction in the force-reflecting system would also be greater with the reduced forces of the soft ball manipulation.

# Challenges

The design of a dexterous force-reflecting hand master presents daunting challenges. Just as in the design of dexterous robot hands, many actuated degrees of freedom must be arranged with serious mass, volume, and geometric restrictions. Transmission factors such as friction and backdriveability must be dealt with. Power densities required from the actuators are not readily attainable with available technology, and may be impossible without significant innovations. Furthermore, the sensitivity of the human hand and the demanding requirements of dexterous manipulation call for a high-fidelity interface. High bandwidth and high dynamic range (ratio of largest force attainable to smallest force reliably reproducible), as well as low friction, will be necessary.

Beyond the mechanical challenges lie significant ergonomic obstacles as well. The human hand has at least 20 degrees of freedom, including three flexion/extension (bending) motions and one abduction/adduction (lateral) motion per digit. Following the motions of the thumb and reflecting forces to it has proven particularly onerous to most investigators, and any future efforts should give early consideration to the special problems of the thumb. Tracking complex motions with a light, stiff exoskeleton that can be comfortably worn, yet apply significant forces to the fingers, is a study in contradictions and engineering compromises. Many outstanding mechanical designers have fallen short in their understanding of the ergonomic and anatomical challenges of the application. It is this understanding and a triumph over the obstacles that will separate successful devices from those that are simply expensive pieces of hardware strapped onto the hand. In a valid, but far from complete, list Burdea cites four problem areas in the implementation of force-reflecting hand masters [20]:

- Inadequacy of current actuators
- Increased system complexity (mechanical design, computer hardware, and control software)
- Coupling of forces between degrees of freedom
- Physical fatigue of human operator (heavy, awkward hardware)

The quality of actuation systems has been recognized as the critical shortcoming in dexterous telemanipulation where force feedback is required [6, 20]. All of the challenges make dexterous force-reflecting hand masters a high-cost endeavor, but many applications promise high returns. Furthermore, advancing technology, avoiding overdesign, and selective degradation for low-end applications will aid in the utilization of hand master devices.

# SYSTEM COMPONENTS

## Actuators

The force-reflecting hand exoskeleton application places harsh demands on actuators. The necessary power must be available to supply relatively high forces at the appropriate speed. High frequency response, stiffness, power-to-volume ratio, and power-to-mass ratio must be attained. As co-located actuators become more prominent, torque-to-mass ratio will gain importance [43]. Since a large percentage of funding in this area has come from NASA, methods with large weight penalties have not been favored (e.g. hydraulics and pneumatics with heavy power plants and reservoirs). Electromagnetic motor drives have so far been the most widely used; however, some significant results have been achieved with hydraulics and pneumatics [21, 51]. One large hydraulic system was developed for the U.S. Navy for use underwater, so the weight penalty was not as great an issue [51]. Developmental actuator technologies such as those using piezoelectric or magnetostrictive materials may soon prove useful, and more speculative approaches such as polymer muscles and functional neuromuscular stimulation may provide some long-term options.

Hollerbach et al. have conducted a comparative analysis of actuator technologies for robotics [43]. The authors discuss nearly all of the actuators considered here, with relatively greater emphasis on traditional actuators and less on novel technologies such as piezoelectric and magnetostrictive actuators.

### Present

**Electromagnetic motors** have been the most popular choice for hand exoskeleton applications, despite their disadvantages [3, 57, 71]. Heavy components, low power densities at small scales, and heat dissipation problems reduce the appeal of these motors. The static force capability of electromagnetic motors also does not compare favorably to that of pneumatics or hydraulics.

An example helps to illustrate the limitations of electromagnetic motors. The MicroMo 1331 012S is a miniature DC motor that has been used by at least one designer in hand exoskeleton applications. It has a diameter of 1.30 cm and a length of 3.12 cm, for a volume of 4.14 $cm^3$. It has a mass of 20 grams (0.71 oz). The motor can supply up to 2 W continuous power or 2.7 W peak power. Table 2 contains performance specifications for the motor. The power-to-mass ratio of this small motor compares favorably to larger designs that have achieved ratios of around 100 W/kg, but the torque-to-mass ratio is only one quarter of that possible with a larger motor such as the 6 kg, 618 W Aerotech 1410-01 [43].

When used with a 43:1 gearhead, the total volume of the actuator package would increase to 7.2 $cm^3$, reducing the continuous and peak power densities to 0.29 $W/cm^3$ and 0.38 $W/cm^3$, respectively. (The mass would increase to 55 grams). These power densities are at the low end of the acceptable range for co-located (at the finger) force feedback actuators, neglecting the added power necessary to support the mass of the motors themselves and the short transmission required to transfer forces to the structure of the exoskeleton. This configuration would provide 30 N-cm continuous and 45 N-cm peak torque. This peak torque is less than 10% of the maximum that

Table 2: Performance Specifications for the MicroMo 1331 012S Motor [48]

| | Power-to-volume ($W/cm^3$) | Power-to-mass (W/kg) | Stall torque (N-m) | Torque-to-mass (N-m/kg) |
|---|---|---|---|---|
| continuous | 0.48 | 99 | 0.0025 | 0.12 |
| peak | 0.65 | 134 | 0.0089 | 0.44 |

Table 3: Performance Specifications for the MicroMo 1331 012S Motor with Gearhead [48]

| | Power-to-volume ($W/cm^3$) | Power-to-mass (W/kg) | Stall torque (N-m) | Torque-to-mass (N-m/kg) |
|---|---|---|---|---|
| continuous | 0.29 | 36 | 0.30 | 5.5 |
| peak | 0.38 | 49 | 0.45 | 8.2 |

can be produced by a human (derived later in this report). Table 3 contains revised performance figures for the motor with the 35 gram (1.23 oz) gearhead.

Another designer uses a geared DC motor attached to a split screw that rotates inside a threaded tube, creating linear motion. This actuator, called MINNAC, was used for a multi-finger robot hand [98]. The MINNAC design can be scaled to any size DC motor. A force of 58 N (13 lb) and a speed of 1.25 cm/s (0.5 in/s) have been cited. Liberally estimating power at maximum force and maximum speed gives a power of 0.73 W, not enough for hand master applications. The speed alone is cause for concern, as 1.25 cm/s is not nearly fast enough to track human finger motion; though the speed would be less of a concern if similarly slow actuators were used on the slave. The lack of backdriveability of this particular approach also makes it inappropriate. While inductive motors and gearheads may sometimes be useful in hand exoskeletons, the marginal power density and relatively low peak torque reduce the attractiveness of the approach.

**Hydraulic** systems provide a force capability, power output, stiffness, and bandwidth that can be difficult to match with other technologies, at the expense of high mass, fluid leaks, design difficulty, and expensive parts. An added disadvantage is that a relatively large hydraulic power plant must be placed off of the hand, and tubing routed across joints to reach the actuators. Remote placement of the hydraulic power plant can increase the power density on the hand, but the power plant still reduces system portability. Furthermore, performance figures such as torque-to-mass ratio are highly nonlinear functions of mass; small reductions in size can significantly reduce torque-to-mass ratio [43]. Hardware overhead necessary for any actuator also reduces the clear performance lead of hydraulics as actuator size is reduced. The Sarcos TOPS system, designed for the U.S. Navy, did incorporate a number of degrees of freedom into the fingers using hydraulic actuation [51]. The author was not able to find performance figures for this hand master in the published literature.

**Pneumatic** components are typically lighter than hydraulics, and pneumatic power plants and distribution systems are not as difficult to manage. Despite these advantages, the relatively low bandwidth, low actuation stiffness, and low power capability make pneumatics less attractive. Remotely located pneumatic cylinders also require at least two antagonistic actuators for each degree of freedom so they can operate in a pull-pull fashion. Despite these disadvantages, for applications where low bandwidth and stiffness can be tolerated, inexpensive pneumatic systems may be suitable.

Possible pneumatic actuation methods include traditional rotary vane and linear cylinder devices. More unusual approaches such as bellows have been mentioned, and one patent by Jones and Thousand envisions air bladders placed on the palmar side of the fingers that would inflate and stiffen to reflect forces [60]. No information on realization of the idea is available, though frequency response might be expected to be a problem. McKibben muscles (braided mesh-enclosed elastic tubes that contract when pressurized) have been used since the 1950's; the Rubbertuator [27, 43] and ROMAC actuators are two such contemporary devices [43]. Rotary vane actuators have not been seriously considered, but pneumatic cylinders have been used in at least one family of prototype hand masters by Burdea at Rutgers [23, 21, 36]. At least one arm master uses pneumatic actuation, and may have pneumatic actuation in an attached hand master (the source is unclear) [83].

The Rutgers Portable Dextrous Force Feedback Master (PDMFF) has three pneumatic cylinders, with one placed between the palm and the tip of the thumb and the other two between the palm and the tips of the first two fingers. This arrangement allows for single dof force reflection between the digits and the palm. It does not allow for reflection of abduction/adduction (lateral) forces, and the ability to represent thumb-index finger pinches is unclear. The placement of the cylinders on the palm also reduces the working volume of the fingers, although steps have been taken to reduce the size of the cylinders. The original PDMFF uses a VPL DataGlove for position measurement. Early PDMFF designs could achieve maximum piston forces of 2.2-4.4 N (0.5-1.0 lb) at pressures of 60-90 psi. Rise time to a step input is between 50 and 100 ms, and feedback signal bandwidth is noted to be between 10 and 20 Hz [22]. Shimoga cites 20-30 Hz as the minimum bandwidth with which the feedback forces should be presented for meaningful perception [109, 110].

Shimoga interprets Burdea's bandwidth figure as a sampling rate, and states that a sampling rate of 200-300 Hz is necessary to produce the required 20-30 Hz force reflection bandwidth (based upon the practical "ten times" sampling rule, not Nyquist's "two times" sampling theory). Shimoga concludes that Burdea's sampling rate is much too low to be adequate [109, 110]. Inspection of Figure 4 in Burdea [22] (or Figure 7 in [23]), showing a step response with at least 20 force samples plotted in the first 100 ms, and personal communication with Burdea support the conclusion that the sampling rate was actually around 200 Hz, and that the 10-20 Hz figure refers to the frequency content of the force signal [17, 21, 22]. At 35 psi, the pneumatic cylinder/servovalve combination tracked a square wave from minimum to maximum force (zero displacement) at a rate of 11 Hz with unity gain [17].

A Second-Generation Rutgers Master (SGRM or RMII) has recently been developed [36]. It adds position sensing to the pistons, eliminating the need for a sensing glove. A fourth piston has also been added to reflect forces to the ring finger. The RM II uses a new pressure controller with pressure feedback. This system can track a square wave from minimum to maximum force (zero displacement) with a pressure of 35 psi at a rate of 14 Hz with unity gain [17]. Air cylinders of

Pyrex glass and moving pistons of lexan or graphite reduce frictional forces to less than one gram. More recent information puts the frictional forces at five grams (0.05 N), and the maximum force at 16.4 N, indicating an enviable dynamic range of 330:1 [17]. This advantage is tempered by the fact that the pneumatic cylinders do not have the bandwidth or stiffness of other actuators; however, one advantage of the device is its light weight of about 70 grams [36].

**Dissipative joint brakes** may serve as useful force reflection devices in applications where actuators are not feasible. Such controlled-impedance hand master joints would stiffen when the slave finger encounters environmental forces, and lock when the slave encounters an immovable obstacle. The slave position would be controlled by the master position. This approach has the advantage of not having to provide motive power, and would be especially suited to reflecting grasping forces by using the brakes to oppose the grip of the operator. This would eliminate one serious disadvantage of position-control hand masters by preventing the master from going "inside" the boundaries of the object being grasped.

Joint brake systems could not reflect forces in situations where the environment does work on the slave (e.g. moving objects, rebounding compliant objects, and objects being lowered or falling through gravity). Simplicity, high torque, high bandwidth, low weight, and low cost would be the relative advantages of this approach. A joint brake could also be made with low friction in the off state and, therefore, easy backdriveability. The idea of using joint brakes in hand master applications has been examined by Townsend et al. A single-joint prototype achieved a maximum joint torque of 450 N-cm, but has not been implemented in any existing systems [118]. Dissipative-only feedback may result in a diminished sense of presence and perhaps increased task completion time for some tasks. Nonetheless, a subset of tasks may be adequately serviced by such a system.

One interesting possibility would be to combine passive brakes with an actuator. The output of a single actuator per finger could be modulated by brakes (one per joint). A single cable routed along the back of the finger could pull the finger joints to extension, though this system could not handle the rare situation where an environmental force pushes the fingers towards flexion (e.g. the back of the finger colliding with an obstacle). Adding the capability to drive flexion would require another cable per finger. It appears that this idea has not been tested.

## Developmental

Mechanical rectification of the tiny oscillatory motions made by piezoelectric crystals offers a promising alternative to inductive motor technology. Power densities for this technology have reached the range which would make it suitable for force-reflecting hand masters. An analogous technology using magnetostrictive materials may also compete for this application. Both of these technologies may provide high forces at low speeds in a small-volume package suitable for co-location at a hand master joint. Some designs may be configured to apply no force or full braking force when unactivated, either allowing complete backdriveability or obviating the need for motor brakes. Both piezoelectric and magnetostrictive actuators may be used for either motors or dissipative joint brakes. Since both approaches involve micro-stepping designs which cause incremental position changes, careful work must be done to develop methods which enable direct force or torque control. Such methods may use compliant components or intentional slipping within the motor. Preliminary experiments with a prototype magnetostrictive motor indicate that force control is feasible [7].

**Piezoelectric** motors translate the vibration of piezoelectric materials to linear or rotary motion using frictional forces to produce usable torques or forces at low speeds, without the need for gear reduction. The dependence of the motive forces on friction demands close contact between surfaces and leads to wear, so piezoelectric actuators can require precise machining. These actuators are typically driven by a power signal at about 30-130 kHz, gated on and off at a lower frequency (1-2 kHz). Varying the duty cycle of this gated signal determines the power applied to the actuator. Gating frequencies in the audible kilohertz range (less than 20 kHz) can cause annoying and potentially hazardous noise in some designs; this drawback must be addressed for successful application of the technology.

Two general types of piezoelectric motors rely on either wave motion or discrete vibrations. Wave types generally rely on standing or traveling waves creating differential motion between two plates through frictional coupling of the forces. Discrete vibration designs rely on a more straightforward expansion of a piezoelectric element in frictional contact with a drive bar or rod that it pushes forward a tiny distance with each vibration. The piezoelectric elements provide both the motive force and the frictional force, usually by being placed at an angle to the drive bar.

In a variation on the discrete vibration approach, it is also possible to combine an expanding piezoelectric element with piezoelectric clamps to create an "inchworm" linear motor like the one built by Newton et al. [81]. In a comparable, but innovative prototype, Miesner uses piezoelectric clamps and magnetostrictive extender rods in an electrically resonant LC circuit to achieve motion with minimal control circuitry [76]. The two extender rods measure 15 cm (6 in) long and 1.3 cm (0.5 in) in diameter. This arrangement works because the magnetostrictive rod and its electromagnetic driver coil act as an inductive circuit element, and the piezoelectric clamps act as capacitive elements. The prototype motor achieved a no-load speed of 2.5 cm/s (1 in/s) and a stall force of 115 N (26 lb). Miesner is collaborating with Teter at the Naval Surface Warfare Center (NSWC).

Investigators at AEG in Frankfurt, Germany have explained the general principle of traveling wave motors in clear terms, and described the successful demonstration of a disc-shaped motor as big as the palm of a man's hand [102]. Speeds approaching 60 rpm (6.28 rad/s) were claimed, with research indicating a service life up to 15,000 hours at low torque. No maximum torque figures have been published, but a torque goal of 200 N-cm has been mentioned.

Panasonic has developed a 4 cm diameter traveling wave ultrasonic motor with a mass of 70 grams [112]. Running at a nominal drive frequency of 70 kHz, it has an 800 rpm (84 rad/s) no-load speed and a stall torque of 0.8 kgf-cm (7.8 N-cm). At an operating speed of 330 rpm (35 rad/s) and an operating torque of 0.3 kgf-cm (2.9 N-cm), it can deliver 1 W of power. Stationary wave techniques can have higher conversion efficiency than the traveling wave approach chosen by Panasonic, but at the expense of a larger structure and fixed rotation direction. Panasonic chose the traveling wave technique because its rotation can be reversed, as well as its potential for miniaturization.

Tomikawa et al. considered both longitudinal and torsional modes of vibration, presenting three different motor designs [117]. The first has a low-speed torque of about 25 N-cm ("multi mode vibrator type"), with no-load speeds up to 80 rpm (8.4 rad/s). The other two designs each have a stall torque of about 10 N-cm, and 90-120 rpm (9.4-12.6 rad/s) no-load speeds. Size information was not available, but both of the latter designs are elongated cylinders, one with a diameter on the order of 2.5 cm.

Maeno et al. examined a ring-type traveling wave ultrasonic motor developed by Canon for autofocus cameras [70]. Nominal operating frequency for the motor is 30 kHz. The authors calculated the dynamic contact behavior of the rotor and stator using a supercomputer. Test data show measured torques up to 16 N-cm at 6 cm/sec, with no radius or stall torque given. Efficiency approached 40% in the upper half of the motor's torque range.

Schoenwald evaluated a linear piezoelectric motor manufactured by Micro-Pulse Systems [103]. To maintain adequate contact between the friction drive surfaces and the drive shaft, spring-loaded clips are used; the bulk of the entire assembly is a serious disadvantage for hand master use. The maximum power output is 0.3185 W, and occurs at approximately 16 cm/s. A generous estimate of power density (neglecting the spring-loaded housing) is 1-2 W/cm$^3$.

Ohnishi presented a friction drive linear motor for x-y stage micropositioning, with similarities to the design evaluated by Schoenwald [82]. Peak stall forces up to about 6.9 N were achieved at a drive frequency of 90 kHz, and a pulse-width modulation (PWM) duty cycle of 50%. Under the same conditions, the device achieved no-load velocities of about 2.8 cm/s. Since the design was for an x-y stage, miniaturization was not as critical as for a hand master application. The device measures 36 mm $\times$ 15 mm $\times$ 5 mm, without the springs used to load the actuator against the drive bar. Polyimide composite material is adhered to the surface of the vibrating parts, pushing the drive bar for wear prevention and friction force enhancement.

Uchino describes various ultrasonic actuator applications, as well as theory [119]. Uchino includes two ultrasonic motor designs, calling them "vibratory coupler," and "surface wave." The surface wave motor appears to have a traveling wave design; the author's prototype achieved a maximum torque of about 10 N-cm, consistent with other published figures. The vibratory coupler design may be similar to the stationary wave technique cited elsewhere, with only one direction of motion, but higher conversion efficiency. Uchino's vibratory coupler achieved a rotational torque up to about 127 N-cm, which is very high for this sort of device. The vibratory coupler design achieved speeds over 100 rpm (10.5 rad/s), but the speed at which 127 N-cm was obtained is unknown. Dimensions were not given for either motor. The vibratory coupler design actually approaches the speeds and torques needed for hand-master force reflection, but its single direction of motion and lack of information on its size make its utility doubtful.

Most piezoelectric motors developed in the past 10 years have had maximum torques on the order of 10 N-cm, with speeds in the range of centimeters per second. These motors produce torques roughly half that achieved by EXOS using DC servo motors; the torques are also less than 5% of the maximum human metacarpal-phalangeal (base knuckle) torques cited below. While piezoelectric motors have found success in applications such as x-y stage micropositioning and camera autofocusing, dexterous force feedback will require further progress in force control, manufacturability, wear tolerance, and miniaturization. The required progress is not likely to come from wave type motors, judging from work to date, but may very well come from discrete vibration piezoelectric motors. Recent work, including that by Grahn at Bonneville Scientific Inc. (BSI), makes that progress seem likely.

A rotary piezoelectric motor has been developed by Grahn and integrated into a robot finger joint [38]. The device consists of two clamping and two pushing piezoelectric elements that alternately clamp and push the joint either clockwise or counterclockwise. The stall torque of this BSI motor is 56.5 N-cm (5 in-lb) [37]. Grahn estimates a no-load motor speed of 12.6 rad/s (120 rpm),

nearly 75% of the 17 rad/s maximum human MCP joint speed. While power information is not directly available, linear interpolation yields an estimate of 28 N-cm (2.5 in-lb) at 6.3 rad/s (60 rpm), for a power estimate of (6.3 rad/s)(0.28 N-m) = 1.8 W. The motor weighs 6-8 grams, and has power-to-mass and torque-to-mass ratios of 225 W/kg and 70.6 N-m/kg, respectively. Since the prototype motor directly drives a robot finger joint, this weight does not include any torque transmission hardware that an exoskeleton would require.

BSI has also developed linear piezoelectric motors. Two prototypes exist, both with volumes of approximately 27 $cm^3$ (1.65 $in^3$) and masses of roughly 57 grams (2 oz). Prototype 1 has achieved a stall force of 250 N (57 lbs) and a no-load velocity of 12.7 cm/s. The motor has lifted a 71 N (16 lbs) bowling ball at a velocity of 10.2 cm/s (4 in/s), with a power output of (71 N)(0.102 m/s)=7.2 W in that task.

BSI Prototype 2 has achieved a stall force of 576 N (129 lbs) and a no-load speed of 18 cm/s (7 in/s). Linear interpolation indicates a potential power of (288 N)(0.09 m/s)=26 W. With 26 W of power, and the volume and mass figures given above, the prototype has power-to-volume and power-to-mass ratios of 0.97 $W/cm^3$ and 460 W/kg, respectively.

Motor performance can vary widely depending on drive frequency, drive waveform, relative timing of element actuation, and mechanical settings. Linear interpolation probably overestimates the power available from these motors. Actual performance, as indicated by the stall force, no-load speed, and power tests of Prototype 1, is still well over the minimum requirements. Since the crudely-packaged prototypes have significant excess capacity, reducing their size for location at the finger joint of a hand master should be possible.

**Magnetostrictive** motors have similarities to piezoelectric motors in that they must mechanically rectify small oscillatory motions of the driving element(s), and also have the potential to produce high forces at low speeds. Magnetostrictive materials change shape when subjected to magnetic fields. For example, a cylindrical rod of the material Terfenol-D wrapped with a coil of wire will elongate and narrow when current passes through the coil. The resulting strain is small, on the order of two parts per 1000, but is about an order of magnitude larger than that available from most piezoelectrics [11]. The pressure produced can also be double that available from piezoelectrics.

Early development of Terfenol-D occurred at the Naval Surface Warfare Center's Magnetism Group, and was first considered for use in sonar transducers. A patented motor design by Teter and Clark shows a Terfenol-D cylinder being squeezed through a tube by an electromagnetic field traveling down the longitudinal axis of the actuator (a peristaltic effect, somewhat like the esophagus propelling food toward the stomach) [116]. No prototype motor was constructed. Unfortunately this design uses the magnetostrictive material as the wear element and requires extremely tight tolerances so that the magnetostrictive material can be propelled through the tube without sticking or freely sliding.

A prototype motor built for the Armstrong Laboratory by Brimhall used three Terfenol-D rods, one to push or extend along the axis of motion, and the other two to clamp the drive bar [8]. One of the clamping actuators grips the drive bar, the pusher rod elongates as the drive bar slides freely through the second clamp, and then the second clamp grips the drive bar to hold the displacement just accomplished while the first clamp rebounds with the contraction of the pusher rod. The

process then repeats, like a mountaineer ascending a rope with two ratchets (jumars) acting as the clamp actuators and his or her muscles acting as the pusher rod. An early proof-of-concept motor achieved a velocity of 0.76 cm/s (0.3 in/s) at relatively low force, but significant improvements have been made in a second prototype that can move at a no-load speed of 13 cm/s and produce a stall force of 9.5 N, with a motor mass of only 16 grams (Figures 18 and 19). The Terfenol-D rods can theoretically have a power density of 190 W/cm$^3$. When the coil volume and the structure required to rectify the strains are taken into consideration, this estimate drops to 12 W/cm$^3$, neglecting inefficiencies. A structure twice as big as projected and 17% (1/6) efficient would still have a power density of 1 W/cm$^3$, which exceeds the required power density for force-feedback hand masters of 0.3-0.7 W/cm$^3$ derived later in this report.

The same project also produced a simple joint brake in which a Terfenol-D rod elongated against a hinge or ball joint surface to provide a resistive torque. A prototype built with a 26 mm (1.03 in) long by 5.1 mm (0.2 in) diameter rod showed that this type of actuator can easily generate torques useful for hand master applications, though improvements in backdriven friction and tolerances must be made to obtain the desired performance. The Terfenol-D rods require a preload stress which should be decoupled from the frictional clamping surface so that backdriven friction can be reduced.

Heat dissipation may be a problem, requiring potting compounds around the coils and possibly heat sinks. Current magnetostrictive motor prototypes operate at drive frequencies in the audible range, so noise can be just as much of a problem as with piezoelectric motors. Brimhall states it should be feasible to raise the driving frequency of one of his magnetostrictive motors over 20 kHz to eliminate the noise problem [7]. Magnetostrictive and piezoelectric technologies currently compete for dominance in the emerging rectified-vibration motor field, with the piezoelectric work approximately two years ahead and currently leading in performance (see Table 4).

## Long Term

**Shape Memory Alloy (SMA)** actuators have been considered for robotic applications [105], and for application to force-reflecting hand masters [20]. SMA wires and springs contract when heated, and expand again under prestress. SMA has an attractive power-to-mass ratio of almost 100 W/kg, in the range of human muscle performance. SMA actuators can contract much faster than they can relax, since contraction typically depends on Ohmic heating of the element with an electric current, and relaxation depends on the cooling rate of the wire, which is much slower. The chief disadvantage arising during contraction is a very low efficiency of 2-5% [30, 31]. Heat dissipation problems severely limit the relaxation rate of the wires. The stroke of SMA wire actuators has been variably reported at 2-10%, with typical strains of 6% [42]. Even lower strains must be used for increased fatigue life. To achieve the strains necessary for robotic applications, designers have relied on long wires, force reduction through leverage to increase stroke, and pulley designs where the wires double back on themselves (as in a block and tackle). SMA springs can achieve significantly better strokes than wires, at the cost of the compliance inherent in the spring.

Becker et al. used two opposing SMA springs to actuate a prosthetic finger [2]. With a current of 1 Amp passed through the springs, the finger moved at 0.07 rad/s (4 degrees per second), with faster speeds reported for higher currents (which ranged as high as 2 Amps in the study). The stiffness of the springs increased with increased current, ranging from 16 g/mm (1.6 N/cm or

Table 4: Comparison of Actuator Characteristics

| Actuator | Torque/mass | Power/mass | Power/volume | Stall torque (Stall force) | No-load speed | Mass |
|---|---|---|---|---|---|---|
| MicroMo 1331 w/o gearhead | 0.44 N-m/kg | 134 W/kg | 0.65 W/cm$^3$ | 0.0025 N-m | | 20 g |
| MicroMo 1331 w/43:1 gearhead | 8.2 N-m/kg | 49 W/kg | 0.38 W/cm$^3$ | 0.45 N-m | | 55 g |
| McGill/MIT EM Motor* [43] | 15 N-m/kg | 200 W/kg | | | | |
| Sarcos Dexterous Arm electrohydraulic rotary actuator* [43] | 120 N-m/kg | 600 W/kg | | | | |
| Utah/MIT Dexterous Hand electropneumatic servovalve [43] | 20 N-m/kg | 200 W/kg | | | | |
| BSI piezoelectric motor #1 | 44 N-m/kg† | 126 W/kg | 0.27 W/cm$^3$ | 250 N | 12.7 cm/s | 57 g |
| BSI piezoelectric motor #2 | 100 N-m/kg† | 460 W/kg | 0.97 W/cm$^3$ | 576 N | 18 cm/s | 57 g |
| BSI finger motor | 70.6 N-m/kg | 225 W/kg | | 0.565 N-m | 12.6 rad/s | 6-8 g |
| Burleigh Instruments inchworm piezoelectric motor [43] | 3 N-m/ kg | 0.1 W/kg | | | | |
| TRA magnetostrictive motor #2 | 5.9 N-m/kg† | | | 9.5 N | 13 cm/s | 16 g |
| Kiesewetter magnetostrictive motor [62] | 500 N-m/kg | 5 W/kg | | | 1 cm/s | |
| PVA-PAA polymeric actuator [24] | 17 N-m/kg | 6 W/kg | | | | |
| NiTi SMA (Hirose, cited in [43]) | 1 N-m/kg | 6 W/kg | | | | |
| Human biceps muscle [43] | 20 N-m/kg | 50 W/kg | | | | |

* performance will be reduced at finger sizes

† at a 1 cm lever arm

0.90 lb/in) for no current to 34 g/mm (3.3 N/cm or 1.9 lb/in) for 1.5 A. Becker et al. also estimate the power-to-mass ratio for a 1.0 mm diameter SMA wire as 4 W/g (4000 W/kg), 40 times the estimate given by Ikuta.

Hitachi used SMA actuators to construct a three-finger robot hand with four degree-of-freedom fingers and a two degree-of-freedom wrist [80]. The wrist uses four 0.35 mm SMA wires for each degree of freedom, achieving a rotation rate of 1.6 rad/s (90 degrees per second). Each of the 12 finger joints is powered by a number of 0.2 mm SMA wires in parallel. The block of 14 actuators is in the forearm, driving the wrist via pulleys and the fingers via sheathed cable tendons. The actuator block is 40 cm (15.75 in) long, 8 cm (3.15 in) wide, 5 cm (2 in) high, and weighs 1.5 kg (3.3 lbs). All finger actuators are preloaded by springs in the actuator package, and also have antagonistic springs at the finger joints. The wrist SMA wires double over pulleys for an actual wire length three times the length of the assembly, while the finger actuators are single-length.

Power-to-mass ratios from 100 W/kg to 4000 W/kg have been cited [2, 47]. Theoretically, the power-to-mass ratio of an SMA actuator can be infinitely increased by continuing to raise the rate at which energy is delivered to the wire, assuming a constant efficiency (although at some point acceleration forces will yield the wire). While a good design can achieve adequate stroke and force, the downfall of SMA actuators will likely be their inefficiency and response time. Waste heat will raise the temperature of surrounding structures, and inhibit the cooling of neighboring wires. Active cooling would have to be introduced to make relaxation times acceptable and to dissipate all of the waste heat, substantially reducing the power-to-mass ratio of the overall system. The large peak powers necessary to rapidly heat the SMA actuators would also require precise control to prevent overshoot and damage to the wires. An alternate option may be to alter the properties of

the SMA wires by exposing them to large electromagnetic fields, significantly reducing contraction and elongation times [46].

**Contractile polymer** gels exhibit abrupt volume changes in response to external variables such as acid-base (pH), other ionic, or electrical conditions. This method of converting chemical or electrical energy to mechanical energy is analogous to that of human muscle. Artificial muscles formed from bundles of polymer gel fibers have been considered for use as robotic actuators [9, 10, 106, 107]. Polymer muscles can shrink or swell up to 1000 times their original volume, producing forces up to 100 N per square centimeter of cross-sectional area at contraction rates on the order of a second [10]. Early polymer gels changed very slowly over minutes or hours, but it may be possible in the near future to create gels with strength and speed comparable to human muscle.

Caldwell studied Polyvinyl Alcohol - Polyacrylic Acid (PVA-PAA) gels, which use water to produce dilation and acetone to produce contraction. He used the polymer muscles both as actuators for a robotic gripper, and as a variable compliance tendon acting as a transmission device for a robotic finger. The variable compliance tendon application arises from the polymer's ability to change its elastic modulus from as high as 400 $N/mm^2$ when unswollen to less than 1 $N/mm^2$ when swollen by 50%. Caldwell compared polymer muscles to natural muscles; the performance figures are given in Table 5. He gives figures for 0.1 mm thick muscle sheets, and notes that response rate is related to the inverse square of polymer muscle thickness; thus, a 0.02 mm muscle would be expected to respond at a rate of 250%/s. This is nearly 23 times faster than the 11%/s possible with the thicker gels. Assuming force capability remains unchanged (through the use of parallel actuators), power-to-mass ratio would increase to 132 W/kg. This would be significantly better than the 49 W/kg available from a MicroMo 1331 DC motor with gearhead, but less than the 170 W/kg goal for actuators co-located on the finger joint. Of course, this power-to-mass ratio neglects the overhead of the fluid delivery system.

Even if strength and speed requirements can be exceeded, polymer gel muscles must be adequately controlled to be useful. Brock developed a dynamic model and control system of a polymer gel muscle [9]. The contractile polymer gel undergoes abrupt volume changes in response to an acid-base reaction, directly converting chemical to mechanical energy. A nonlinear sliding mode control system tracks desired joint trajectories of a single link controlled by two antagonist muscles. Both the model and controller were implemented and produced acceptable tracking performance at 2 Hz.

Table 5: Comparison of Artificial Muscles to Human Muscles

| | | Polymer | | |
|---|---|---|---|---|
| | **Human muscle** | Caldwell [25] | Brock [10] | **SMA** |
| Power/weight (W/kg) | 40-225 | 5.8 | | 100-4000 |
| Chemical-mechanical efficiency (%) | 45-70 | | | |
| Electrical-mechanical efficiency (%) | | | | 5 |
| Force ($N/cm^2$) | 15-40 | 30 | 100 | 50000 |
| Contractile rate (%/s) | 25-1800 | 11 | | > 15 |

Contractile polymers are still speculative, and have numerous disadvantages. They usually require a complicated chemical setup, with fluid circulation. Solvent diffusion and transport delays complicate control of the muscles, hindering rapid starts, stops, or reversals. Systems with fluid circulation will require extremely high flow rates for realistic robotic applications. They still lack the response times necessary for robotics, and control can be more difficult than with other actuators. As with natural muscles, polymer muscles only have a power stroke in one direction (you cannot push on a rope), so two actuators are required for every degree of freedom. Alternatively, a stronger single actuator might be used with a spring-return to enable forces in the actuator's direction of extension.

**Functional Neuromuscular Stimulation (FNS)** is a form of myoelectric muscle stimulation used in rehabilitation to cause specific muscle groups to perform a function (such as walking). This technique has been mentioned as a possibility for applying force feedback to a telerobot or virtual environment operator without the encumbrance of a motorized exoskeleton. Extensor muscles would be myoelectrically activated to oppose flexion motions, and vice versa. The idea is appealing, but is plagued by numerous challenges.

The most obvious obstacles are in applying the stimulus to the subject repeatably and reliably. Donning and doffing the apparatus would be difficult, with precise placement of electrodes required, and probably not well-suited to an operational environment. The relationship between stimulator pulse amplitude and the resulting muscle force is called the "recruitment curve," and is nonlinear. It varies between subjects, with fatigue and with electrode placement. This could result in tedious calibration being required for each operator, and make maintaining the system at a consistent level of performance very difficult.

Problems of appropriate force generation and control also appear. In the finger muscles at least, the extensors are weaker than the flexors, and might not be well suited to oppose them unless forces are far below maximum (though forces below maximum *are* desirable). Without a method for measuring the applied muscle forces, the force reflection system would have to operate open-loop. Likewise, since the force output from the user's limb is a sum of his or her desired force and the reflected force stimulating opposing muscle groups, determining the user's desired output force would be difficult.

The presence of these challenges does not necessarily eliminate the possibility of successfully applying FNS to force reflection. So far the idea has not been tested. One advantage might be high bandwidth. Any proposed investigation of FNS should strive to develop a controllable system compatible with the demands of use in realistic situations.

## Actuator Conclusions

The principal shortcoming of actuators for force-reflecting hand master applications has been low power densities and low power-to-mass ratios. While the desire to achieve the required power in an acceptably small package has dominated the discussion, other factors like bandwidth and dynamic range of forces also have a high priority. Table 4 presents a comparison of characteristics for some relevant actuators.

DC inductive motors are currently doing yeoman's work in hand master applications. DC motors do not have the power density required for direct placement on the back of finger joints, nor the force output for directly driving those joints; these systems will continue to rely on performance-sapping transmissions and gear reduction, with actuators located on the back of the hand or forearm.

Due to their particular features, pneumatic and hydraulic actuation will continue to fill niche needs within the hand master community. Pneumatics may continue to find use in less expensive, lower performance systems where weight on the hand is a large concern. Hydraulics may occasionally be used for high performance applications not vulnerable to weight or cost penalties. Where overall weight (including power plant) is an issue, DC motors are currently the only option. Advances in actuator technology must be made to improve performance over current hand masters. Actuators co-located at the finger joints would allow for modularity and significantly simplify control. Any new actuators must be force controllable. Developmental technologies such as piezoelectric and magnetostrictive actuators show great promise and may soon be proven in hand master applications. Long term technologies such as artificial muscles and myoelectric stimulation remain speculative.

## Transmissions

Since many hand master exoskeletons have had actuators mounted off the hand, intricate transmission systems have been the norm. These transmissions have included cables [26, 57, 84], hydraulics [51], pneumatics [21], ball or lead screw, etc. [108]. Cable transmissions may be either push-pull or torsional, using sheaths or pulleys as guides. A designer with experience on both the Utah-MIT Dexterous Hand (UMDH) and Navy TOPS system (both of which have complicated cable tendon transmissions) claims that tendon transmission design doubles or triples development time.

Nature uses forearm-mounted finger actuators (muscles) transmitting forces through tendons, but Nature also had millions of years of development time with which to perfect low-friction compact systems with advanced control methods. Cable transmissions raise questions of cable routing, cross-coupling of torques across joints, and friction. Fluid power transmissions require power converters at the joint and usually require bulky tubing which can interfere with free movement of the joints and force reflection to them. These problems make elimination of extensive transmissions desirable. If actuators with suitably high power density could be found, location of those actuators on the exoskeleton fingers themselves might be appealing, though modest transmissions would still be needed to transfer motion and forces to the exoskeletal structure.

One investigator tried to develop a novel cable transmission, with cable gear reduction (rather than toothed gears) at the joint, motivated partially by the philosophy that geared systems are not dynamically robust in force-servoed systems due to backlash, friction, and compliance. This approach has successfully produced a very stiff, backlash-free, arm-sized manipulator [118]. With gear reduction at the joint, the cable from the joint to a remotely located actuator moves at high-speed and carries low forces, eliminating many of the problems typically associated with cable drives. This approach did not prove practical for knuckle-size gears due to the fact that steel cables small enough to accept the small radii of curvature necessary in these mechanisms could not be manufactured [118].

Oomichi et al. designed an interesting "water cylinder" transmission for the slave hand of the Mitsubishi Heavy Industries dexterous hand/arm teleoperator [83]. Each DC motor located in the forearm of the slave robot arm is connected via a gear reduction stage to a drive pulley with a short pull-pull cable attached to an antagonistic pair of hydraulic cylinders. From these two cylinders, two fluid hoses transfer power down the arm. Near the robot fingers, two more hydraulic cylinders transfer power to another pull-pull cable that drives the finger joint. The device is treated as a wire tendon system, with the fluid transfer to avoid the friction in a sheathed cable guide. The system incorporating this transmission was used to disassemble a large valve from a nuclear power plant (turning nuts, lifting cables and valve covers, unsealing gaskets, etc.), but no specific performance figures were included in the literature.

## Hand Attachment - Human Factors

After actuator selection, successful hand interface design is perhaps the most difficult task in realizing a force-reflecting hand master. The difficulty of this interface and the severe design constraints it imposes raise the cost of force-reflecting hand masters beyond feasibility for many applications.

Oomichi avoided some of the difficulties in designing an exoskeleton for the back of the hand by attaching the MHI hand master to the operator's hand only at the fingertips [86]. Massie constructed the PHANToM™, a miniature three dof rigid manipulator, with a finger thimble on a gimbal (for free orientation movement) (Figure 20) [49]. More than one PHANToM™ can be used, one for each finger to create a "hand in a box" style hand master similar to that of Zarudianski [123], but more capable. A system like this could probably not accommodate more than three PHANToM™s, and it would not be at all portable, but may be superior for some desktop applications.

Given that a back-of-the-finger exoskeleton has been chosen for implementation, a successful design must have the following attributes:

- Comfortable to wear for extended periods of time
- Finger structure not wider than fingers
- Laterally stable (must not flop back and forth on fingers)
- Stable and comfortable palm attachment
- Adjustable for different hand sizes
- Joints that successfully track finger movements without constraining fingers
- Sufficiently rigid structure
- Low friction
- Low mass
- Relatively easy donning and doffing

The compliance of human skin and the fact that finger joints are not simple hinges makes the task of designing an exoskeleton joint difficult. The top surface of a finger segment not only rotates,

but translates distally (away from the base) when the joint just proximal to it (closer to the base) bends. This is due to the fact that the axis of rotation of the finger joint is inside the finger, and the top surface of the finger lies some radial distance away. The larger the radius (the bigger the knuckle), the greater the translation that will accompany a given angular movement of the joint. There would appear to be at least two options: 1. to devise an exoskeleton that tracks the dorsal surface of the finger, with a separate rotation and translation motion for each joint; and 2. to devise an exoskeleton joint with an axis of rotation coincident with the finger joint's axis of rotation. All known dorsal exoskeletal hand masters that have addressed this problem have done so with the latter approach, using hemispherical cams or linkages (such as four-bar) with coincident axes of rotation [52, 55].

The hand master must attach firmly to the hand for reliable position sensing and force feedback, as well as to avoid interfering with normal hand motions. Some position control masters wobble significantly on the back of the hand, especially if passive pivots not corresponding to joint motion are added. It is important for the hand master to move in all the necessary degrees of freedom, but in no more than those necessary. Finger joints do bend in a plane, but the plane may not be exactly parallel to the plane of rotation of the previous link. Bergamasco et al. describe this movement as "oblique flexion" [6]. In a rigidly fitted hand master this might require angular offsets to the exoskeleton joints. Adequately adjustable links with well-designed flexion/extension joints all rotating in the same plane for each finger will probably be sufficient for the fingers; the thumb will require a more complicated link arrangement.

## Adjustability

Hand masters must be adjustable for different sized hands. This includes different phalangeal link lengths, different finger circumferences, and different palm sizes. Without adjustments, the devices will be inadequate for use. Even research prototypes have a need to be adjustable so that they may be evaluated by more than one member of the research team (hopefully a non-adjustable device would fit at least one member of the team!). Brimhall and Goodwin have stated that proximal phalanx length variability accounts for most of the variability in total finger length, and that an exoskeleton with fixed distal and medial phalanx links and adjustable proximal links may be adequate for 90% of user hands [7].

## Grounding of Forces

For every force, there exists an equal and opposite reactive force. If the force-feedback device is grounded to earth ground, the user experiences the force as an environmental interaction, and only feels the feedback force. For example, a force-reflecting arm controller bolted to the floor will reflect forces back to the operator, and the reactive forces opposing the reflected forces (holding the arm master at equilibrium so it doesn't tip over) will be supplied by the floor. If the arm master is instead a backpack-type exoskeleton with its base mounted on a backpack frame attached to the operator via shoulder straps and a hip belt, the reactive forces must be supplied by the operator's body at the grounding points at the shoulders and hips. If the operator commands the slave to press down on a table that will generate a reflected force upward, then he or she will experience the reactive force as downward pressure on the shoulder straps and hip belt. Likewise, pushing

sideways against something in the slave environment will result in torsion about the torso at the hip belt and shoulder straps.

Forces reflected to fingers may be grounded at a number of locations, including the palm and back of the hand, the forearm, and earth ground. Tan et al. found that humans are less sensitive to pressure changes on the skin when contact area is decreased; they recommend minimizing contact area of grounding points and maximizing the perimeter of that area to improve the illusion of true grounding [115]. This idea has not been tested. A series of narrow bands or straps at the grounding point rather than one wide band might be one way to implement this suggestion. The PHANToM™ uses earth ground for completely authentic grounding of interactions with the environment and between fingertips (assuming the use of more than one PHANToM™) [49]. The choice of earth ground has a fidelity advantage, but an implicit loss of portability. It is also difficult for this sort of device to deal with the case where there actually **should** be a reactive force felt on the palm (as in full-hand grasping).

Jau has a rigid attachment point at the wrist of his hand master so that it can be integrated with a force-reflecting arm exoskeleton, and its reactive forces can be grounded proximally to the arm, which is grounded with a backpack to the person wearing the device [55]. The reactive forces from finger manipulation are not expected to be noticed by the operator at the backpack shoulder and hip harness, though wrist forces might be less negligible.

Burdea's Rutgers Master has pneumatic cylinders between the palm and fingertips [36]. The reactive forces from the fingertip force reflection appear at the palm. This is perfectly natural for whole-handed grasps where the reactive force of an actual object would be felt on the palm (precisely the type of situation a PHANToM™-like device does not portray with fidelity), but not useful for any other situation (many of which PHANToM™-like devices portray excellently). Clearly, the strengths of each approach are application-specific. Consideration should be given during design to the intended tasks and the way in which the force-reflecting system will transmit the reactive forces.

## Point of Reflected Force Application

Not only will the hand master design affect the transmission points of reactive forces, but it will also affect the point of transmission of the forces reflected to the hand. This obvious point is worth a brief note. In a hand master with only fingertip attachments, contact between an object or the environment and proximal finger segments will be felt as a force at the fingertips. Likewise, in an exoskeletal hand master with rings or straps around every phalange, pure fingertip forces will be impossible to represent; some force will always be distributed along the phalanges. Likewise, with a comprehensive system like the Jau/JPL device, reflected forces will undoubtedly be sometimes felt at other than intended points. Some forces will be impossible to represent, as with the Rutger's master, with fingertip-to-palm pneumatic cylinders that cannot produce abduction/adduction (lateral) forces between fingers. As with the reactive forces, the most important design influence should be the feedback necessary to perform the intended tasks. Bergamasco et al. also raise the above issues in a general introduction to force-reflecting hand master design considerations [6].

# SUCCESS CRITERIA

In the design of teleoperation masters, there is a tendency to strive for absolute fidelity. Theoretically, a master-slave system with perfect anthropomorphic fidelity could do everything a human can do. One might assume that usefulness is directly related to fidelity. As fidelity increases, usefulness may well increase, but this relationship is difficult to predict. For a given application, successive increases in fidelity will eventually approach a point of diminishing returns. In fact, strategically chosen reductions in fidelity or anthropomorphism may provide more cost-effective and attainable solutions to certain problems than the elusive "perfect" hand master. Designers should make design compromises to minimize cost and maximize functionality; however, since functionality may be quite task-dependent, it can be a difficult metric to use.

The difficulty in finding actuators and transmissions adequate to meet the force, power, and other demands of the application creates the largest stumbling block on the road to success. Selection of these components, as well as the other aspects of the system, depends on a good knowledge of the requirements for success, including an understanding of human hand capabilities and the relative successes of prototype systems previously constructed. One basic question is the configuration of the digits; how many digits should a hand master-slave system have, and how many degrees of freedom should each digit have?

## Configuration

### Fingers

Two human fingers can perform 40% of the hand tasks considered in a study by Mishkin and Jau, three fingers can accomplish 90%, and four can complete a full 99% of the tasks [77]. These data, represented graphically in Figure 2, suggest that three fingers will give the maximum benefit considering simply the percentage of tasks achievable. Adding the third finger more than doubles the tasks possible, but adding the fourth only increases capability by an additional 10%. While one may draw inferences from Figure 2 about the number of fingers appropriate for a master-slave hand system, the data in Figure 2 represent human hand capabilities and may not reliably indicate the number of fingers needed by a teleoperated hand system. Salisbury showed from kinematic considerations that three fingers are necessary for manipulation [100]. Of course, if a critical task lies above the 90th percentile, then the fourth finger becomes relatively more valuable. For example, Salisbury asserts that four fingers are necessary to enable regrasping in the hand [100]. The range of practical tasks that can be performed by a two-finger manipulator, but not by a parallel-jaw gripper, is likely very small; this makes the selection of a two-finger configuration unlikely.

Jacobsen et al. examined tasks ranging from delicate tasks, such as threading nuts onto bolts, to high-strength tasks, such as wielding a hammer [51]. The number of digits and degrees of freedom necessary to perform a wide range of grasps indicative of dexterity was determined. A thumb and two fingers were declared necessary. The thumb required four dofs, three for flexion/extension of the knuckles and one abduction/adduction degree of freedom to bring the thumb from a position on the side of the hand into manual opposition with the fingers. The two fingers each required

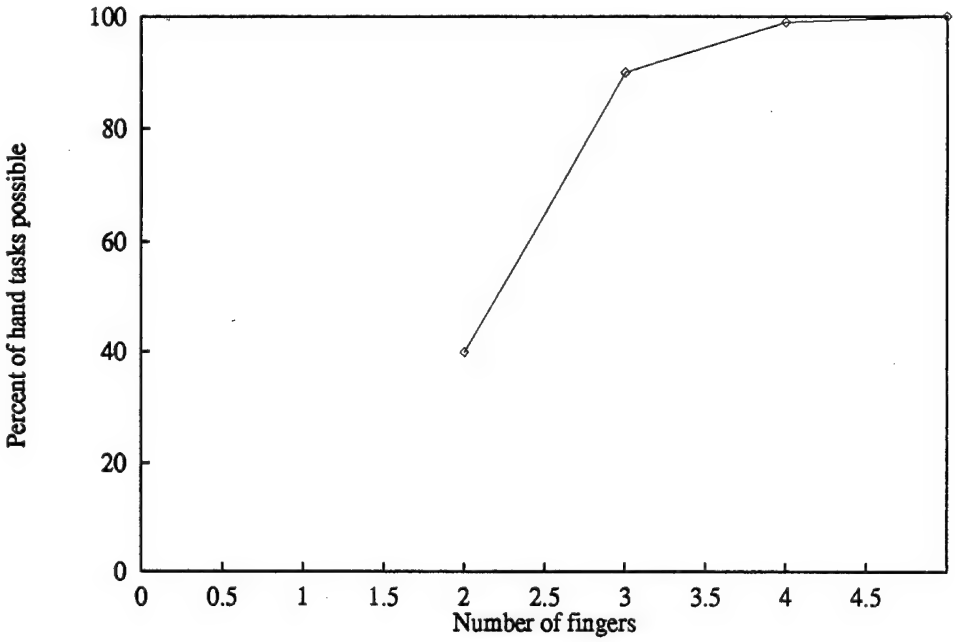


Figure 2: Percent of Hand Tasks Possible with Given Number of Human Fingers

two degrees of freedom for flexion/extension of the proximal and medial knuckles (the most distal knuckles being omitted). Instead of individual abduction/adduction degrees of freedom for lateral movements of the two fingers, a single degree of freedom was deemed sufficient to spread the fingers. Jacobsen et al. also recommended an anthropomorphic three dof wrist.

Burdea has asserted that three digits are optimal and can perform many robotic manipulation and assembly tasks [22]. One might conclude from the discussion above that a three-digit configuration is the most appropriate for a capable and economical hand master-slave; however, experience may be strengthening the argument for a fourth finger. Since Mishkin and Jau published their report, the Jau/JPL hand master system became operational [58]. Experiments with the system showed that most tools could not be held and operated using only three fingers. The four-finger configuration allows three fingers to hold an object or tool still while a fourth repositions itself or pulls a trigger (the Naval Ocean Systems Center, as well as NASA, has placed an emphasis on the need for trigger pull). Burdea has also added force-reflection to a fourth finger of the Rutgers Master.

The recommended number of fingers and number of degrees of freedom per digit varies, but salient points of agreement seem to be:

- The importance of an anthropomorphic thumb
- Marginal benefit of the distal finger knuckle
- Need for lateral degrees of freedom in at least the thumb and forefinger

One compromise that might be workable would be to have a fully force-reflecting thumb, but fingers with force reflection only on flexion/extension dofs. Non-force-reflecting abduction/adduction dofs would passively follow movements and measure position for transmission to the slave. Eliminating force reflection in these dofs would raise the possibility of losing position registration between the master and slave when the matching slave dof encounters an immovable object, but this approach would work for tasks like turning a nut on a bolt, which requires thumb abduction/adduction but only index finger flexion/extension.

One drawback of the three-finger solution is that it narrows the breadth of power grasps and reduces the stability of grasps. Attempting to use a hammer with only the thumb and first two fingers will reveal the important role that the little and ring fingers play in providing leverage and stabilizing power grasps. On the slave end, this problem can be solved by moving the second finger (third digit) out farther from the index finger, or by making it as wide as two or three fingers for a modified "mitten" look. The latter approach was chosen by TOPS designers at Sarcos [52].

A master controlling a modified configuration like this could be left unchanged (thumb, index, and middle fingers in exoskeleton), the third exoskeleton digit could be moved to the ring or little finger, or a third exoskeleton digit could be made to encompass the middle, ring, and little fingers. The second option would move the two-finger exoskeleton digits away from each other, buying more room for the exoskeleton structure. The third option would not be workable for more than one or two flexion/extension dofs, since the knuckles of adjacent fingers are not coaxial. Where space is a problem, designing the hand master for the thumb, index, and ring fingers might be an attractive option.

## Number of Hands

Jau et al. state that during operational trials of their teleoperated hand system it became apparent that a second hand would be needed to make tool operations useful [58]. They cite the usefulness of the second hand for repositioning tools in the first hand. Some other uses for a second hand would be holding workpieces steady, manipulating objects around obstacles (passing tools or workpieces from one hand to another), and manipulating large objects that require a dexterous grasp with two hands (e.g. circular valve handles). To justify the expense of two hands for a particular class of tasks, it would be useful to determine the percentage of tasks that could be done by a single dexterous arm and hand system, a two-arm system with one dexterous hand and one parallel-jaw gripper, and a two-arm system with two dexterous hands. Jau has done an analysis of hand usefulness for EVA tasks, considering 195 astronaut EVA tools. Only six could be handled by an industrial robot end effector, while 29 could be handled by a one-arm fingered hand system and 171 could be handled by a two-arm fingered hand system [58]. The fact that the addition of a second arm and fingered hand multiplies the system capability by nearly six times and that a two-hand system would likely be less than twice the price of a one-hand system argues strongly for the desirability of a two-hand system. The analysis would be a bit more informative if information were available on the relative amount of time each tool would be used in space, or on what percentage of missions could be completed, rather than simply the number of tools usable. Jau did not assess how many tools could be handled by a combination of one fingered hand and one industrial end effector (perhaps providing a marked improvement in performance over a single fingered hand without the cost penalty of having two fingered hands).

While two-handed systems may be required by some tasks, research plans should avoid calling for the construction of more than one master-slave hand system until the design is proven. Efforts that attempt to leap to full anthropomorphic redundancy without careful risk reduction at the lower levels (joint, finger, finger and thumb, hand, arm, etc.) are likely to fail, wasting resources on duplicating an immature design.

# Human Capabilities

An understanding of the capabilities of the human hand provides a basis for the development of hand master design criteria. Ideally, devices will have fidelity exceeding that of the human senses, in order to "fool" the operator into suspending his or her disbelief and becoming immersed in the remote or virtual environment. Whereas fidelity should exceed that of the human, power capability should be some fraction of the human's. It is useful to first determine what that human maximum is, and then use experience and experimental data to form an opinion of what that fraction should be.

## Force and Torque

Forces normal to each phalange (bone) of each finger in a cylindrical maximum-strength power grasp were recorded by An, et al., based upon data from an unknown number of subjects [1]. An's apparatus allowed strain gauge measurements to be taken at the mid-point of each phalange; a summary of these measurements appears in Table 6. Assuming representative phalangeal lengths and joint angles for a hand in a cylindrical grasp, joint torques corresponding to the above forces were calculated (Table 7). Appendix A contains details of this calculation, including tables of assumed phalangeal lengths and joint angles.

According to Sutter, et al., maximum force exerted at the tips of human index and middle fingers is about 50 N (11.24 lb), and maximum at the tip of the ring finger is about 40 N (9.0 lb) [113]. The data for 10 subjects of unknown gender were averaged to obtain these figures. The approach used to calculate joint torques from An's mid-phalangeal force data has been used to calculate joint torques from Sutter's fingertip force data (Table 8). Sutter measured maximum fingertip forces with the fingers fully extended, so all angles are zero in the torque calculation.

Table 6: Maximum Mid-Phalangeal Joint Forces Exerted by Human Fingers in a Cylindrical Power Grasp (Newtons) [1]

| | Proximal | Middle | Distal |
|---|---|---|---|
| Index | 42 | 22 | 62 |
| Middle | 24 | 40 | 68 |
| Ring | 15 | 28 | 44 |
| Little | 7 | 20 | 31 |

Table 7: Joint Torques Exerted by Human Fingers in Cylindrical Grasp [N-cm] (An, et al.)

| | MCP | PIP | DIP |
|---|---|---|---|
| Index | 270 | 228 | 77.5 |
| Middle | 322 | 289 | 85.0 |
| Ring | 203 | 180 | 55.0 |
| Little | 126 | 120 | 39.8 |

Table 8: Joint Torques Exerted by Human Fingers in Fingertip Force Test [N-cm] (Sutter, et al.)

| | MCP | PIP | DIP |
|---|---|---|---|
| Index | 463 | 213 | 62.5 |
| Middle | 500 | 225 | 62.5 |
| Ring | 370 | 170 | 50 |
| Little | N/A | N/A | N/A |

While these two sets of calculations yield torques for joints in different positions (cylindrically wrapped vs. fully extended at all three joints), Sutter observed that maximum joint torque is more or less independent of MCP joint angle for the angles in question. Some of Sutter's measurements were made with the PIP and DIP joints splinted, and some without; it is not clear which set of data is represented in his final results. Though Sutter and An's data were obtained under different circumstances, a cautious comparison may be useful.

Tables 7 and 8 show significant differences between some of the torques calculated from An's data and those calculated from Sutter's data. The MCP torque estimate derived from Sutter is highest, but An's data led to higher PIP and DIP torque estimates. An attempt to explain the disparity would be worthwhile, assuming that the differences are statistically significant. The following discussion will argue that joint torques derived from Sutter's data better represent the maximum MCP joint torques, and those derived from An's data more accurately represent maximum PIP and DIP torques. Composite results for maximum joint torques appear in Table 9. The next few paragraphs discuss the rationale for using An's data for the PIP and DIP calculations and Sutter's data for the MCP calculations. Readers inclined to take this reasoning on faith should skip ahead to the discussion of finger abduction and adduction on page 38.

**An's experiment did not fully challenge the MCP joints, but it challenged the PIP and DIP joints more than Sutter's.**

A potential explanation is that An's apparatus only measured forces normal to the surface of the cylinder. Non-normal forces at the distal and medial phalanges would add to the magnitude of the torque transmitted to (supported by) the MCP joint. Since any non-normal forces in An's experiment were not measured, they could not be represented in any estimations of joint torques, leading to a possible underestimation of MCP torque. Another possible explanation is that An's

Table 9: Maximum Torque Capabilities of Human Finger Joints [N-cm]

| | MCP | PIP | DIP |
|---|---|---|---|
| Index | 463 | 228 | 77.5 |
| Middle | 500 | 289 | 85.0 |
| Ring | 370 | 180 | 55.0 |
| Little | N/A | 120 | 39.8 |

cylinder experiment may not have equally challenged all of the finger joints; the PIP and DIP joints may have been at maximal effort while the MCP joints were not.

Translating the MCP joint torque into a projected fingertip force will show that the MCP joint torque derived from An's data is not sufficient to support the actual maximum fingertip force observed by Sutter. An's maximum phalangeal forces translate into an index finger MCP joint torque of 2.70 N-m. Incorporating Sutter's result that maximum joint torque is more or less independent of joint angle, this corresponds to an index fingertip force of about 29.2 Newtons (acting 9.25 cm from the base of a 10.5 cm finger), 60% of Sutter's measured maximum index fingertip force. This leads to the conclusion that the MCP joint torques derived from An's data were not the maximum attainable torques.

An's experiment challenged PIP and DIP joints more than Sutter's experiment. The following example supports this assertion. If tip force is inferred from the calculated index finger PIP torque, instead of the MCP torque, tip force would be:

$$228 \text{ N-cm}/4.25 \text{ cm} = 53 \text{ N}$$

That is, if one clamped the finger at the proximal phalange (preventing fingertip force from relying on MCP torque), splinted the DIP joint (also eliminating it from the equation), and measured maximum fingertip forces, the PIP joint could produce 53 N at the fingertip using a torque (from Table 7) of 228 N-cm acting at 4.25 cm from the fingertip. Since Sutter only measured a 50 N maximum force at the fingertip, this implies measurement of fingertip force did not fully challenge the PIP joint (in other words, the 53 N capability in isolation shows that the PIP joint had potential untapped by the fingertip force experiment). Obviously, fingertip force depends on the torques maintained by all three joints; the actual fingertip force will only be as strong as the weakest link in this chain.

In a similar fashion, one could conclude that a subject in An's test could exert a 62 N index fingertip force if only the DIP torque were considered. While the 3 N difference for the PIP joint may be equivocal, this is a fairly clear indication that An's experiment challenged the DIP joint more than Sutter's experiment. The arguments have shown that An's experiment more fully challenged the PIP and DIP joints than Sutter's experiment, and thus are more appropriate to use as maximum known joint torques; but they have not necessarily shown that joint torques derived from An's data represent absolute maximums for the PIP and DIP joint capabilities in isolation.

Table 10: Normal Hand Strength (Newtons) (from An et al. [1])

| | Tip Pinch | Pulp Pinch | Key Pinch | Radial Deviation | | Ulnar Deviation | |
|---|---|---|---|---|---|---|---|
| | | | | Thumb | Index | Thumb | Index |
| Male | 65 | 61 | 109 | 43 | 43 | 75 | 42 |
| Female | 45 | 43 | 76 | 25 | 31 | 43 | 28 |

**Sutter's experiment fully challenged the MCP joint, but not the PIP and DIP joints.**

Analysis of the joint torques derived from An's data showed that the index finger PIP and DIP joints can produce more than enough torque to support Sutter's observed maximum index fingertip force. Since the fingertip force results from three torques in series, the maximum will be limited by the weakest contributor (not the lowest torque, but the joint with the lowest torque-lever arm product). It follows that if the MCP joint torque limited the maximum fingertip force measurement, then the fingertip force measurement fully challenged the MCP joint and the MCP joint torque derived from Sutter's data is an authentic maximum. It also follows that if the MCP joint torque limited attainable fingertip force, that PIP and DIP torques derived from Sutter's data, while accurate for those conditions, do not reflect maximums.

Table 9 shows the maximum joint torques determined from the MCP torques in Table 8 and the PIP and DIP torques in Table 7. Tan et al. also measured fingertip forces of the index finger of two male subjects and one female subject, selectively immobilizing joints so that the fingertip forces generated by the MCP joint or the PIP joint could be determined [115]. Average maximum fingertip forces for the two male subjects were 43.9 N and 46.4 N for the MCP and PIP joints, respectively. Using the phalange dimensions given in the appendix and assuming fingertip force measurement at the middle of the distal phalange, this translates to MCP and PIP joint torques of 406 N-cm and 197 N-cm, respectively. These figures differ by only 12-14% from those presented in Table 9.

**Finger Abduction and Adduction** force capabilities have also been studied. An et al. measured maximum abduction forces between the index and middle finger of 40 N, and adduction forces of slightly over 30 N (presumably measured at the fingertip) [1]. Abduction/adduction forces between other fingers were comparable or smaller. An also measured lateral strength of the index finger and thumb (Table 10). The maximum ulnar deviation force of the index finger (towards the middle finger) of 42 N is similar to the index-middle finger adduction force measurement (lateral squeeze between the index and middle fingers), but the index finger is not in opposition to the middle finger. The 42 N figure is probably a better measurement of index finger strength, since the adduction measurement is only as strong as the weaker of the two fingers. A comparable radial deviation strength of 43 N is also given for the index finger.

**The thumb** appears to be by far the most powerful of the digits. One indication can be seen in Table 10, where the typical key pinch strength for males as 109 N. During a key pinch the subject presses the thumb against the side of the index finger. The maximum thumbtip force of 109 N is more than double Sutter's maximum of 50 N at the index fingertip. An's 75 N measurement

of thumb ulnar deviation is also much higher than any finger abduction/adduction measurements. Kroemer and Gienapp measured thumb strength of 31 male Air Force pilots [66]. The subjects produced average thumbtip forces ranging from 84 N (s.d. 18 N) for the "thumbs up" position to 99 N (s.d. 21 N) for the key pinch position with the thumb MCP joint fully flexed. The latter figure compares favorably to An's result.

## Fatigue and Force Tolerance

Little work has been done to answer the question of what percentage of the maximum human forces will be most useful for force feedback. High maximum feedback forces will contribute unnecessarily to fatique, but low maximum feedback forces will result in an inadequate range of available forces. Wiker et al. measured the effects of fatique and force levels in pulp pinches between the index finger and thumb [122]. Four male and two female subjects performed isometric pulp pinch grasps in 104 minute sessions at 5, 15, or 25% of their maximum voluntary contraction (MVC). Grasps were performed for 15 seconds, alternated with a rest period. Depending on the trial, the rest period was 15 seconds or 7.5 seconds, for a work-rest ratio of 1:1 or 2:1, respectively. The experimenters measured levels of discomfort and subjects' ability to accurately estimate forces throughout the trial.

Wiker et al. found that the level of discomfort depends on force magnitude, work-rest ratio, and the duration of effort. Subjects experienced discomfort at 25% MVC in as little as 10 minutes. Subjects tolerated 15% MVC well throughout the 104 minute trials. The work-rest ratio only had a significant effect on discomfort above 15% MVC (at 25%).

Decreased force perception sensitivity affects the subject's ability to estimate and accurately control forces. Tasks calling for low forces (5-35% MVC) will be over-forced, and tasks calling for greater forces (over 50% MVC) will be under-forced. With a work-rest ratio of 1:1 (15 seconds work and 15 seconds rest), force sensitivity remained stable, regardless of force level or discomfort. Forces equal to or greater than 15% MVC reduced force perception sensitivity at a work-rest ratio of 2:1.

Significant shifts occur in the range from 15% to 25% MVC. Subjects can operate at 15% MVC for long periods in tasks offering adequate rest. Operations at 25% MVC can also be sustained for long periods, but require greater rest and entail a higher risk of reduced force sensitivity. These results are among the best available to estimate the percentage of MVC useful in manipulation tasks, but generalization is not straightforward. It is difficult to choose a percentage of MVC appropriate for representative tasks without more information on the work-rest ratio associated with those tasks. Holding a virtual tool in a sustained grasp would result in comparatively high work-rest ratios, while intermittent manipulation would result in low work-rest ratios.

Luciani references a chart of muscle electromyograph (EMG) amplitudes, showing those amplitudes increasing as subjects who began an isometric contraction at a given percent MVC approach fatigue [68]. The chart shows no increase in EMG amplitude at the 15% MVC level, with the notation that the range less than 15% MVC is "non-fatiguing." This statement seems to support Wiker's determination that 15% MVC causes little or no fatigue. Petrofsky studied fatigue in subjects performing isometric hand grasps on a dynamometer [90]. His results show a precipitous drop in average endurance for 40% MVC trials (130 seconds) as compared to 25% MVC trials (480

seconds). The difference between the 40% MVC average endurance and the 70% MVC average endurance (60 seconds) is marked, but less drastic. The results of Luciani and Petrofsky, when considered with the work of Wiker, indicate that force levels at or below 15% MVC cause little or no fatigue, while fatigue increases rapidly for force levels between 15% and 70% MVC.

## Speed

Little information exists on maximum speeds of finger joints or representative speeds during task completion. Maximum speeds would be useful as an upper bound for no-load speeds of force-reflecting hand masters. Acceptable no-load speeds are especially important for systems that must be servo-backdriven (backdriven inertia and friction too high to be backdriven by the fingers alone), but not as important for devices that have low backdriven inertia and friction or frictional drives that can be released like clutches for free motion. Knowledge of maximum speeds can also contribute to estimates of human joint power capability in the absence of coordinated force and speed measurements. Knowledge of actual joint speeds during typical hand tasks would also be useful for determining system requirements.

Marcus, et al. at EXOS reported maximum radial joint speeds of 26 rad/s for the MCP joint and 28 rad/s for the PIP joint [33]. Discussion with the author of that information revealed a possible minor mathematical error that may have led to overestimation of maximum joint speeds [32]. This author measured maximum MCP joint speeds for four male subjects and two female subjects. Appendix B presents details of the experiment. The maximum MCP joint speed averaged across the four male subjects was about 17 rad/s. A brief investigation by EXOS engineers yielded similar results. PIP joint speed was not measured, though if the relation between EXOS' 26 rad/s and 28 rad/s estimates holds (the error was linear), maximum PIP speed might be estimated at 18 rad/s. Appendix B also contains a determination of maximum fingertip velocity.

The experimental results for the MCP joint agree well with those of Darling et al., who measured MCP and PIP joint speeds while studying the finger dynamics of four subjects [29]. A maximum-speed profile for one subject shows a peak MCP speed of 18 rad/s and a maximum PIP speed of 12 rad/s. Darling states that, in general, speeds seem to range as high as 20 rad/s [28]. Darling cites a peak PIP speed of 10 rad/s for "natural speed" movement in the PIP joint (unknown number of subjects), and a range of 3-6 rad/s for the MCP and PIP joints in "slow" motion [29].

## Power

Data from An and Sutter contribute to an estimate of maximum human joint power. The maximum MCP joint torque, calculated from Sutter's middle finger data, is 5.00 N-m. The maximum PIP joint torque, calculated from An's middle finger data, is 2.89 N-m. Linear interpolation between an MCP stall force of 5.0 N-m and an MCP no-load speed of 17 rad/s yields 2.5 N-m at 8.5 rad/s for the power calculation (assuming maximum power at 1/2 maximum angular speed and 1/2 maximum torque). The calculation for the PIP joint is similar:

$$\text{MCP joint:} \quad (8.5 \text{ rad/s})(2.5 \text{ N-m}) = 21 \text{ W}$$

$$\text{PIP joint:} \quad (9.0 \text{ rad/s})(1.44 \text{ N-m}) = 13 \text{ W}$$

The above linearly-interpolated calculation assumed maximum power at 1/2 maximum angular speed and 1/2 maximum torque. Hollerbach, et al. show that muscle does not have a linear strain/stress curve, and that maximum power occurs at 1/3 maximum speed and 1/3 maximum force [43]. This results in the following power estimates for human finger joints:

| | | | |
|---|---|---|---|
| MCP joint: | (5.67 rad/s)(1.67 N-m) | = | 9.4 W |
| PIP joint: | (6.0 rad/s)(0.96 N-m) | = | 5.8 W |

Stated simply, maximum power of a muscle in this situation would be 0.11(*maximum angular speed* × *maximum torque*).

## Human Sensing of Length, Force, and Compliance

Knowledge of human sensing capabilities can give insight into the relative significance of an increase in system capability. For example, an improvement in a performance metric that does not exceed the just-noticeable-difference (JND) for that metric will not be appreciated by the user, and will not be worth the trouble. On the other hand, a difference several times the JND will likely be appreciated, though its impact on task completion cannot be assured.

Tan et al. found that distance JND for separation of the thumbtip and index fingertip ranged from 1.0 mm with the fingers 10 mm apart, to 2.4 mm with the fingers 80 mm apart (a JND of 3-10%) [114]. Tan et al. report that the JND in human joint space is 2-2.5 degrees for the MC and PIP joints, and is relatively independent of the starting joint position [115]. Thus hand master systems should have a fingertip position resolution better than 1 mm or joint space resolution better than two degrees. (Since the joint space JND appears to be constant, this might be more useful for selecting rotational sensors.)

Pang et al. report a force JND between the thumb and forefinger of 5-10%, relatively constant over forces from 2.5 to 10 N and a finger span of 45-125 mm [87]. This information can be useful in a number of ways. For example, force interactions in a virtual environment meant to be distinguishable from each other should differ by more than 10%. Increases in maximum force of a force-reflecting system should exceed the JND or the effort will be wasted. This result should be cautiously applied to the reduction of friction forces in a system. Pang et al. note that as the force becomes small, the JND will certainly rise (and does for all other sensory modalities), due to irreducible internal noise in the sensory system.

Tan et al. report compliance JND of 5-22%, varying between subjects and experimental conditions [114]. This is particularly interesting, because compliance can be used to discriminate between objects being felt (in person, in virtual space, or through a teleoperated slave). Two pushbuttons intended to have a different "feel" in a virtual environment should have compliance differences in excess of the compliance JND. The stiffness of a force-feedback device (its ability to represent a rigid surface) is one of the most frequently cited traits of fidelity in a force-reflecting interface, so

improvement is often sought in this area. Thus, for example, an increase in computing speed to reduce system compliance by 20% would very likely be appreciated by the user.

### Human Force Control Resolution

Force control resolution should be distinguished from force JND, since force control resolution is a measure of the precision with which the subject can produce a target force. Force JND is a measure of the subject's ability to detect a difference in sensed forces. For fingertip forces from 0.25 N (0.056 lb) to 1.5 N (0.34 lb), Srinivasan and Chen found that average absolute force control error decreased from 16% to 3% [111]. Tan et al. found an average error of 2% for forces between 8.9 N (2 lbs) and 49 N (11 lbs) [115]. These results show that subjects can control larger forces with a smaller percentage error than smaller forces.

## Hand Master Requirements

Obviously, no single set of system requirements can be described, since this will depend on the tasks to be performed, the opinions of the designers, and potentially the needs of the sponsor. Furthermore, designers in this emerging technological area are hampered by a "chicken and the egg" conflict; it is difficult to determine minimum system requirements without human performance experiments that would seem to demand those very devices which we first need to design. One approach that can be taken (and has been taken with arm exoskeletons) is to overdesign the system with respect to force capability, etc., perform psychophysical and task experiments while selectively degrading the system to determine minimum requirements. Unfortunately, hand master devices are so difficult to build that the luxury of having one so good that it can still perform usefully when degraded has so far not happened. The next best approach is to analyze information from available sources, and to evaluate the successes and shortcomings of currently available force-reflecting hand masters.

### Force and Torque

Since for most actuation systems (including the human body), maximum and continuous force capabilities differ, this section discusses both of them. While data from various sources are available on **maximum** human fingertip forces and joint torques, setting design goals for hand master forces is less straightforward. *Rarely* in manipulation will people use their maximum attainable force. In a telemanipulation system with the capability of force magnification, it should *never* be necessary for the operator to exert his or her maximum force against the hand master. Such a system would be unsafe, fatiguing, and so overdesigned as to be impractical. Reflected finger forces should be within a comfortable, low-fatigue range of forces, large enough to allow the operator to feel an adequate sense of "presence" and to control the slave.

Sutter et al. conclude that good design values for maximum fingertip force in a hand master are 40 N (9.0 lb) for the index and middle fingers, and 30 N (6.7 lb) for the ring finger. Essentially, Sutter has recommended that hand masters be designed to exert 75-80% of the human's maximum force, stating that these forces can be maintained out to MCP joint excursions of 90 degrees. Sutter has recommended that the hand master be able to exert the maximum force that the operator is

consistently capable of producing. An alternate philosophy would argue against this, since most tasks can be accomplished well below maximum force, and scaled-down reflected forces may be important for fatigue prevention. In the absence of studies on distributions of forces in dexterous manipulation, existing devices may be examined for their capabilities and apparent success.

The PHANToM™ is a miniature serial link device that reflects forces to a fingertip thimble in three cartesian dimensions (x-y-z) [49, 74]. The PHANToM™ is an earth-grounded desktop system rather than a hand master, but the device resembles Oomichi's "similar shape" type hand master, with the structure positioned above the hand. The PHANToM™ has a maximum exertable force of 10 N (2.25 lbf), which is roughly 20% of Sutter's maximum index, middle, and ring finger forces (50, 50, and 40 N, respectively). This device can represent a believable virtual environment in which a conscious effort is required to drive through virtual obstacles. While greater forces may be desirable, PHANToM™serves as one example of a reasonable solution. One reason for its success with relatively low forces is its low friction and low apparent mass.

One device with arguably inadequate maximum force is an early SAFiRE prototype. The prototype had a fingertip force of 3.3 N (12 oz), and users found it relatively easy to exceed this force with their fingers to drive through virtual obstacles. The SAFiRE had maximum joint torques of 24 N-cm (34 oz-in) for the MCP joint and 11 N-cm (16 oz-in) for the PIP joint. The SAFiRE Phase I final report calls for a fingertip force increase to 22 N (5 lb) in future designs [33]. The 3.3 N performance figure represents 7-8% of Sutter's maximum fingertip forces. The 22.2 N design goal represents 44-56% of Sutter's maximum fingertip forces. Recent communication with the SAFiRE designers indicates a revised preference closer to 8.9 N (2 lb), 18-22% of the maximum.

**Continuous** force requirements will obviously be lower than maximum requirements. Wiker et al. showed that 15% of the human's maximum voluntary contraction (MVC) can be maintained for long periods [122]. This suggests that continuous force reflection more than 15% of the human maximum would be fatiguing to the operator. Wiker's experiments can be used to infer a 15% (of human maximum) ceiling on the highest useful continuous force capability, but not as proof that hand masters **require** a continuous capability that high. In fact, anecdotal experience shows that the PHANToM™ performs well as a virtual reality interface with a continuous force rating of 1.5 N (0.34 lbf), 3% of the human maximum (15% of its peak rating).

Wiker's data combined with exoskeleton design experience suggest that the range between 25% and 50% of the human maximum is an area of diminishing returns, where fatigue becomes more likely and the apparatus heavier and more cumbersome. The judicious application of peak feedback forces in this range will only be appropriate if these forces can be obtained without overencumbering the operator. Actuators with high torque-mass ratios and power densities will have a significant advantage in this area.

Based upon this discussion, the author recommends that hand master designers specify a peak force capability 20-30% of the human maximum, and a continuous force capability 3-15% of the human maximum.

## Speed

The peak angular speed of the human metacarpal-phalangeal (MCP) joint has been measured at 17 rad/s. Other investigators have found results for the proximal interphalangeal (PIP) joint to be nearly the same as that of the MCP joint [32]. Requirements for hand master speed exist in two regimes: unloaded and loaded. In order to present a transparent interface to the human, hand masters commanding unloaded slaves (not reflecting forces) should be able to move fast, perhaps approaching 100% of human capability. Because the master probably would command the slave through position control, reducing the human's ability to command quick position changes would reduce system performance. High speed would be required in rare instances, as when the slave must be commanded to catch falling objects.

Matching unloaded finger speeds is normally not a problem in DC servo motor systems with sufficiently low backdriven friction and inertia, but could be a problem for those systems that cannot be freely backdriven (e.g. piezoelectric and magnetostrictive motors if they require high preloads on the driven element for adequate traction). These motors would have to have joint-mounted force sensors and servo to zero force under no-load. This arrangement has a serious drawback: such systems are not passive and are therefore not guaranteed to be stable (a motor/transmission system that can be easily backdriven is clearly preferable). Non-backdrivable motors servoing to zero force to follow the operator's fingers would not necessarily have to match maximum human speeds: normal unloaded manipulative movements can probably take place at speeds much lower than maximum. No data on manipulative joint speeds were found, but casual observation suggests that speeds as low as one-half maximum would be useful in manipulation. Regardless of actuator and transmission capability, the inertia of a hand master will reduce the maximum joint velocity of the operator; the unencumbered human maximum speed is therefore a generous upper bound on required exoskeleton speeds. An additional caveat applies for teleoperation, where it would not be worthwhile to have a master that is faster than the slave hand; the extra speed capability would be wasted if the slave cannot match that speed.

Data for speeds of joints under load in manipulation were also not found. An, et al. tested shoulder joints at speeds from 0.52 rad/s (30 deg/s) to 5.2 rad/s (300 deg/s) and noted that even at fast speeds of 5.2 rad/s, 60-70% of maximum torque is still possible for most functions [1]. Without a figure for maximum shoulder speed, the implications for the force-speed curve are impossible to determine.

Actuators located at the finger joints of a hand master may produce linear motion. In this case, the actuators would act on a lever arm of a given radius to produce torque. An angular speed of 17 rad/s would require a no-load linear speed of between 8.5 cm/s (3.4 in/s) and 51 cm/s (20 in/s), given a lever arm of between 0.5 cm and 3 cm. These speeds are considerably faster than those attainable by the most recent magnetostrictive actuator prototypes, but may be attainable in the near future. Friction-drive actuators with a clamp mechanism that can be released to allow free

motion of the drive rod would allow high backdriven speeds while driven actuator speeds could be much lower.

## Caveat Concerning Determination of Power Requirements

This report includes a discussion of power requirements primarily for completeness, not so much as an aid for motor selection. The objective of motor selection is to match the exoskeleton motors to the relevant capabilities of the human finger joints. Exoskeletons need high torque at low speeds to simulate rigid surfaces and compressed compliant surfaces. The proper way to select a motor is to concentrate on the upper left-hand corner of the torque/speed curve, selecting a motor/reduction combination with sufficient stall torque. Figure 3a shows a representative torque/speed curve for human muscle and a linear torque/speed curve representing a conventional electric motor. Maximum power occurs at different places for motors and human muscle on the torque/speed curves in Figure 3a, so maximum power is not the way to select motors. If the reader finds this reasoning clear, he or she should skip the rest of this section.

One approach to determining the power requirement for a motor would be to linearly interpolate between the desired maximum (no-load) speed and the desired stall torque (that is, calculate the power at one-half the no-load speed and one-half the stall torque). Although this approach provides a convenient method for thinking of power requirements, it may be misleading if applied to motor selection.

First, the use of a desired no-load speed as a figure of merit is not always appropriate. It may be appropriate for direct-drive actuators that cannot be released for free motion (as with some piezoelectric and magnetostrictive designs). In this case, the motor would have to servo as fast as the operator's fingers, at nearly no-load conditions, in order to track the operator's fingers through motions that do not result in reflected forces (i.e. movements in "mid-air"). No-load speed is not as relevant for conventional electric motors. If the gear reduction is low enough, the joint may be backdriven without giving the operator noticeable difficulty (so the no-load speed is irrelevant). If the gear ratio is too high, backdriven friction and inertia will require designers to use a force sensor at the joint so that the motor can attempt to servo to zero force in order to follow the operator's movements unobtrusively. In this case, the no-load speed of the exoskeleton would need to meet the desired maximum; this speed is the maximum speed of the motor loaded with the inertia and friction of the exoskeleton and transmission, so simply looking at the motor specifications may not be useful. Successful exoskeletons with conventional motor systems seem to use gear reductions that are easily backdriven.

The interpolation method uses the desired stall torque as part of the formula for determining the desired peak power of a motor. Subsequently using this peak power rather than torque to select a motor might be considered "putting the cart before the horse." Since torque/speed curves vary, a motor selected for its power capability might or might not be able to attain the desired stall torque that was used to derive the power figure. Figure 3b shows a torque/speed curve for human muscle and a linear one for a motor with the same peak power capability. Peak power occurs at 1/3 maximum torque and 1/3 maximum speed for the muscle, and at 1/2 maximum torque and 1/2 maximum speed for the motor. One can see that the linear torque versus speed curve for the motor will result in a maximum torque only 2/3 of that required to match the muscle's maximum.

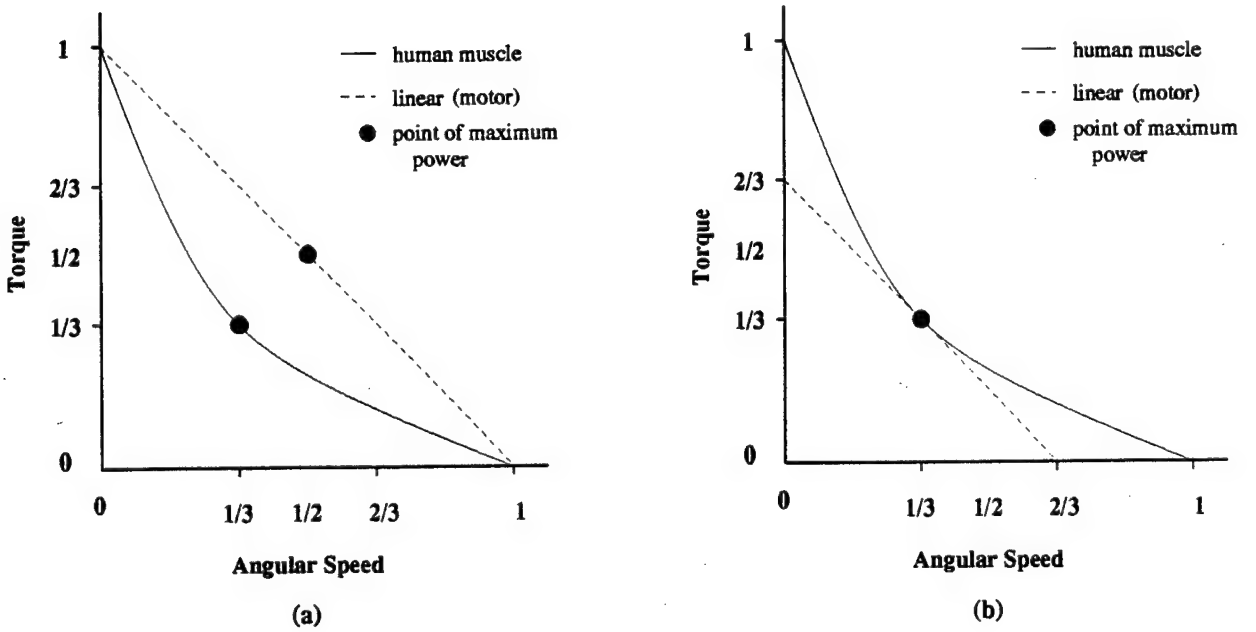


Figure 3: Linear Torque/Speed Curves Compared to Torque/Speed Curve for Human Muscle

In other words, power does not uniquely determine stall torque, and if the latter figure is the most important, then it should be the primary consideration in motor selection.

What this means for the selection of traditional electric motors is that the desired overall stall torque must first be determined, and a motor selected with a large enough stall torque that the gear ratio is low enough to enable backdriveability. In reality, the continuous and peak power requirements may not be an issue. Most tasks performed with force-reflecting dexterous masters will likely involve intermittent work, with time for the actuators to cool. Only if the user were continuously working the exoskeleton actuators or holding them at stall for extended periods would power capability become an issue. In this case, human fatigue might limit the pace of the work performed; the motor could cool while the operator rests or the feedback gain could be turned down to reduce operator fatigue and exoskeleton power consumption. Figure 3a reinforces the assertion that power in the seldom-used middle section of the speed/torque curve will not be a problem, showing a power surplus for a motor (depicted by the linear curve) selected to match the human's stall torque. For irregular intermittent tasks such as those usually encountered in teleoperation, traditional motors should be sized based on stall torque requirements.

Novel actuators that rectify vibrations to produce large displacements have advantages and disadvantages in this area with respect to traditional electric motors. On one hand, these actuators often involve periodic clamping of the drive shaft, allowing high holding forces with relatively low power consumption. On the other hand, in some designs the clamping mechanism may prevent the actuator from being freely backdriven, requiring motor speeds comparable to the desired backdriven speeds. In this case, no-load motor speed becomes as important as stall force.

## Power

Three examples will give a quick feel for the order of magnitude of the usable power needed in a force-reflecting hand master. To achieve these power output levels at the joints, actual mechanical power produced by the actuators would clearly need to be larger to account for inefficiencies in the transmission. The first example, a rough estimate of the Phase I EXOS SAFiRE joint powers, serves as a lower bound. Data on joint torques were obtained from EXOS, Inc. [32]. Linear interpolation between an imagined no-load speed of 17 rad/s for the MCP joint and a stall torque of 0.24 N-m yields 8.5 rad/s with 0.12 N-m for that joint (assuming maximum power at 1/2 maximum angular speed and 1/2 maximum torque, as in the linear example in Figure 3). The calculation is similar for the PIP joint.

$$\text{MCP joint:} \quad (8.5 \text{ rad/s})(0.12 \text{ N-m}) = 1.0 \text{ W}$$

$$\text{PIP joint:} \quad (9.0 \text{ rad/s})(0.057 \text{ N-m}) = 0.51 \text{ W}$$

The second calculation serves as an estimate of joint power that is potentially both realizable and sufficient. The joint powers calculated assume the torques required to achieve EXOS's recommended 22.2 N (5 lb) tip force have been achieved. The torques were derived from static calculations with the assumption that proximal, middle, and distal phalangeal lengths were 5, 3, and 2.5 cm, respectively. This method yields expected maximum torques of 2.2 N-m for the MCP, and 1.0 N-m for the PIP. Interpolating as above produces:

$$\text{MCP joint:} \quad (8.5 \text{ rad/s})(1.1 \text{ N-m}) = 9.4 \text{ W}$$

$$\text{PIP joint:} \quad (9.0 \text{ rad/s})(0.5 \text{ N-m}) = 4.5 \text{ W}$$

This estimate also assumes that no-load speeds of 17 rad/s and 18 rad/s can be achieved.

The third calculation was first shown in the "Human Capabilities" section of this report, and is repeated here to provide a worst-case estimate of power requirements based upon the maximum human finger joint powers. Joint torques were estimated from fingertip and mid-phalangeal force data reported by Sutter and An, respectively [1, 113]. The worst-case MCP joint torque is 5.00 N-m, and the worst-case PIP joint torque is 2.89 N-m [41]. Computing maximum power at 1/3 maximum speed and 1/3 maximum force (per Hollerbach, et al. [43]) results in the following power estimates for human finger joints:

$$\text{MCP joint:} \quad (5.67 \text{ rad/s})(1.67 \text{ N-m}) = 9.4 \text{ W}$$

$$\text{PIP joint:} \quad (6.0 \text{ rad/s})(0.96 \text{ N-m}) = 5.8 \text{ W}$$

The reader can see that these estimates span nearly one order of magnitude. While not rigorous design criteria, the calculations show a range within which future hand master systems are likely to operate.

## Power Density

Fitting an actuator having the required power into the volume available on an exoskeleton poses problems that have not yet been solved. Hand exoskeletons built to date with inductive motor drives or hydraulic actuators have had power plants or the actuators themselves mounted remotely, with a mechanical or fluid transmission.

If actuators with sufficient power densities could be developed, co-location of the actuators on the back of the finger segment just proximal to the joint to be actuated would offer several advantages. Most importantly, performance-sapping transmissions could be eliminated. Problems due to backlash, friction, and cable stretch could be reduced or eliminated. Complications such as cross-coupling caused by cable transmissions would be significantly reduced, requiring only Jacobian transformations to compute joint torques (and not even Jacobians if the master and slave are kinematically identical). The weight of the whole device would be reduced unless the actuators weigh more than the transmission-actuator combination they replace. In short, co-location is desirable for all of the traditional reasons from robotics; the chief obstacle is achieving the required power-to-volume and power-to-mass ratios.

Given an idea of the power required for a hand exoskeleton actuator, it is useful to consider the volume available to contain that actuator. For comparison, the approximate average volume of the distal, medial, and proximal finger segments have been calculated (Table 11). The calculations used the index finger data of Poznanski and Bucholz, assuming a circular cross-section for the segments [14, 15, 16, 91].

Table 11: Approximate Average Volumes for the Distal, Medial, and Proximal Finger Segments

| | length (cm) | diameter (cm) | volume ($cm^3$) |
|---|---|---|---|
| distal | 1.88 | 1.26 | 2.3 |
| medial | 2.61 | 1.50 | 4.6 |
| proximal | 4.37 | 1.72 | 10.2 |

While there is no definite volume into which on-the-finger actuators must fit, an estimate may be made in order to form a reasonable goal for actuator power density. The width of the space available on each finger of the hand exoskeleton cannot exceed the width of the finger since the adjacent fingers must be able to move freely. The length of the space would probably be limited to the length of the finger segment over which the actuator is mounted. The height of the actuator would be constrained by concerns about moment of inertia and compactness. As a design goal, one might hope for actuator packages within a rectangular volume the width, height, and length of the finger segments. These rectangular volumes for the medial and proximal finger segments would be 5.9 $cm^3$ and 12.9 $cm^3$, respectively.

Actuators will be mounted proximally to the joints which they will actuate (i.e. closer to the torso). Thus, an actuator roughly the size of the medial finger segment (5.9 $cm^3$) might be mounted above the proximal finger segment and actuate the PIP joint; since it would be smaller than the segment over which it was mounted, some room would still be left for the exoskeletal structure which must be acommodated in addition to the actuator. Likewise, an actuator roughly the size of the proximal finger segment (12.9 $cm^3$) might be mounted on the back of the hand to actuate the MCP joint. It should be pointed out that two actuators (or one 2 dof actuator) will be needed at each MCP joint for abduction/adduction as well as flexion/extension, so that the back of the hand will probably still be crowded.

For an MCP joint actuator delivering 4-7 W of usable power and occupying a volume of 12.9 $cm^3$, a power density of 0.3 - 0.5 $W/cm^3$ would be required. For a PIP joint actuator delivering 2-4 W of usable power and occupying a volume of 5.9 $cm^3$, a similar power density of 0.3 - 0.7 $W/cm^3$ would be required. This power density range includes any transmissions which may be required at the joint.

## Power-to-Mass Ratio

Based upon experience with the first SAFiRE prototype, engineers at EXOS attempted to define realistic goals for mass per degree of freedom for a hand master with actuators located on the forearm [32, 33]. They set goals of 28 grams (1 oz) per dof for the structure located on the fingers, 100 grams (3.5 oz) per dof for the structure motor and drive assembly located on the forearm, and an additional 142 grams (5 oz) per dof for additional support structures. Jau actually constructed a 16 dof hand master and slave (three fingers and a thumb with four dof each) [55]. His master glove controller also uses forearm-mounted actuators and weighs 0.9 kg (2.0 lb) on the hand, or 56 g (2.0 oz) per dof, exactly twice the EXOS goal.

The EXOS goals for mass on the hand do not include actuators on the finger joint. Attaining the goal of 28 grams (1 oz) per dof on the finger with actuators located on the finger would be truly ambitious. EXOS showed that an exoskeletal hand structure can be built with 28 grams (1 oz) per dof; Jau showed that a feasible hand master can have up to 56 g (2.0 oz) per dof on the hand.

Assuming a master glove structure could be built with about 28 grams (1 oz) per dof, and that the designer still wanted to match Jau's achievement of 56 g (2.0 oz) per dof on the hand, that would leave 28 g (1.0 oz) for the actuators, requiring a power-to-mass ratio of 70-110 W/kg in the actuators (assuming a peak power ranging from 20-30% of the human maximum MCP joint power). This power-to-mass goal is ambitious, given that human muscle has a power-to-mass ratio between 40 and 225 W/kg [25].

A MicroMo 1331 DC motor weighs 20 grams (0.71 oz). With a continuous power rating of 2 W and a peak rating of 2.7 W, the motor has a power-to-mass ratio of 100 W/kg continuous and 134 W/kg peak. Adding the 35 gram (1.23 oz) mass of a 43:1 gearhead reduces these ratios to 36 W/kg continuous and 49 W/kg peak.

The 49 W/kg power-to-mass ratio for the MicroMo 1331 motor and gear head is below the desired 70-110 W/kg range, strengthening the conclusion that DC motors are not appropriate for co-located finger joint drives. Alternative forms of actuation such as piezoelectric and magnetostrictive

motors must fill this role. Recent prototypes suggest that piezoelectric and magnetostrictive motors could attain or exceed the desired power-to-mass ratio (see the subsection on actuators for more detailed information).

Calculation of the potential power-to-mass ratio of a Terfenol-D motor supports this conclusion. The density of Terfenol D is 9.25 x $10^3$ kg/$m^3$ and its power-to-mass ratio is 20,540 W/kg. Assume from the prototype motor described by Brimhall and Hasser that a Terfenol-D linear motor has a total volume 16 times that of its Terfenol-D rods [8]. Further assume that the rest of the motor is solid steel. The density of steel is approximately 8.0 x $10^3$ kg/$m^3$. The power-to-mass ratio of the motor would be:

$$power/mass = (20540\text{W/kg})\left(\frac{9.25}{((1)9.25+(15)8.0)}\right) = (20540\text{W/kg})/14 = 1470\text{W/kg} \quad (1)$$

Since this calculation is based on a theoretical power-to-mass ratio for Terfenol-D, it does not consider inefficiencies in converting the vibrational power in the Terfenol-D to linear motive power. Even assuming a 20% efficiency and a motor/transmission structure twice as large as expected (32 times the volume of the Terfenol-D rods), the power-to-mass ratio would be 183 W/kg, within the desired range of power densities. Piezoelectric actuators have similar potential.

## Torque-to-Mass Ratio

Since adequate maximum torque or force is essential to the realistic representation of rigid surfaces, the torque-to-mass ratio of candidate actuators is an important metric. Earlier sections described target force and torque capability. The section on power-to-mass ratio, beginning on page 49, derives a target actuator mass of 28 g (1.0 oz) per degree of freedom.

A mass of 28 g and a range of possible stall torques from 20-30% (1.0-1.5 N-m) of the human MCP maximum (5.0 N-m) leads to a desired torque-to-mass ratio between 36 and 54 N-m/kg. A MicroMo 1331 DC motor and a 43:1 gearhead have a combined mass of 55 g (1.94 oz), and can produce a stall torque of .38 N-m (54 oz-in). This motor/gearhead combination has a torque-mass ratio of 6.9 N-m/kg, less than a fifth of the minimum. While further reduction in a cable transmission might effectively increase the torque-to-mass ratio (considering only the mass of the actuator package), this DC motor example is clearly less than optimal. Novel motor technologies may have an advantage in this area. For example, BSI linear motor Prototype 2 producing a stall force of 576 N and acting at a lever arm of 1 cm (so that the no-load speed of 18 cm/s equates to 18 rad/s) would produce a torque of 5.8 N-m. The resulting torque-mass ratio for this 57 g (2 oz) prototype is 100 N-m/kg, far exceeding the requirements.

## Frequency Response, Stiffness, Impedance, Dynamic Range, etc.

**Stiffness**, or compliance, greatly affects the "feel" of a force-reflecting device. Any force-reflecting device designed to represent interactions with rigid objects must be stiff. Since most objects will be rigid in any realistic scenario, the designer cannot neglect this requirement. Both the stiffness of the mechanical structure and the servo stiffness combine to contribute to the overall

system stiffness. It may be more appropriate to say that each of these factors contributes to degrade overall system stiffness, and if either factor is significantly worse than the other, its effects will dominate. Structural stiffness, the stiffness in the mechanical components, has often been easier to achieve than servo stiffness, which is limited by the finite cycle rate of the control system. Stiffness is expressed in units of force per unit length. In a stiff system, forces must be increased very rapidly as the device moves only a short distance. A slow control system will not be able to keep up with these changes and the resulting percept will be sluggish and compliant. Inadequate resolution or response delay in position sensor systems will also contribute to degradation in overall system stiffness. While servo stiffness has often been more challenging, aggressive miniaturization efforts required for lightweight hand exoskeletons may make structural stiffness more of an issue.

How stiff is stiff enough? Both structural stiffness and servo system stiffness have costs associated with them (increased weight, computational requirements, etc.), providing motivation to design systems for the minimum acceptable stiffness. One study measured 245 N/cm (140 lbs/in) as the stiffness required for a nearly-rigid cantilever beam to be indistinguishable from a "completely" rigid object when tapped by human test subjects [115]. The figure obtained in this test is not necessarily required for practical systems. As with all parameters, task functionality must serve as the ultimate justification for improving performance. The PHANToM™ has achieved subjectively convincing results with a rated stiffness of 35 N/cm (20 lbs/in) [49, 74] and in some demonstrations running as low as 17.5 N/cm (10 lbs/in) [104]. During some of those demonstrations, users can slide easily in the directions tangential to a virtual wall; this additional cue may have aided users in their "suspension of disbelief" when perceiving a rigid wall with a stiffness lower than that predicted to be necessary by Tan. Rosenberg conducted experiments with subjects' perceptions of rigid walls using virtual walls with stiffnesses ranging from 40-80 N/cm [96, 95, 97]. He added features like unidirectional dampers and bidirectional dampers to the spring wall model, or replaced the linear spring model with an exponential spring to enhance the user's perception of "wallness." He found that the wall model rated best in subject testing was a parallel combination of a linear spring with k = 45 N/cm (26 lbs/in) and a unidirectional viscous damper with heavy damping, b = 100 N/(cm/s). Becker, et al. obtained stiffnesses ranging from 1.6 N/cm (0.90 lbs/in) to 3.3 N/cm (1.9 lbs/in) for two opposing SMA springs used to actuate a prosthetic finger, underscoring the difficulties of obtaining adequate stiffness from SMA-spring-based actuation systems [2].

**Bandwidth** relates directly to servo stiffness; in many cases, increasing control system bandwidth (decreasing computation time) results in immediate and marked reductions in compliance, improving the realism of the feedback forces. Reductions in mechanism stiffness, such as that due to cable compliance, can also impact bandwidth.

How much bandwidth is enough? Presumably bandwidths exceeding those of the relevant sensory systems would not be appreciated by users of force feedback devices. Two sensory systems may contribute to the user's experience of force reflection. The most obvious is the proprioceptive/kinesthetic sense; proprioceptors sense muscle forces, while kinesthetic receptors sense the angle and velocity of joint movement. Brooks states that reliable values for kinesthetic/proprioceptive bandwidth are difficult to obtain, but estimates from 20-30 Hz have been made [12]. Srinivasan and Chen measured human performance in controlling normal forces of contact between the index finger and a glass plate and found that human force control signals above 20 Hz were lost in the noise [111]. The second possible contributor is the tactile sense, or sense of touch. A variety of

mechanoreceptors of different bandwidths and sensitivities contribute to the tactile sense. Humans can detect tactile vibrations up to 10,000 Hz, but the ability to discriminate between stimuli frequencies diminishes above 320 Hz [12]. This would indicate that frequencies above 320 Hz are not very useful, since a 320 Hz signal might be substituted for a 1000 Hz signal without appreciable change in sensation. The fact that humans can sense high frequency vibrations through the tactile mechanoreceptors certainly does not imply that the overall force feedback bandwidth must encompass these frequencies. Amplitudes for tactile stimulation range down to the micron level, so significant roll-off in the frequency response of a system can be present at tactile frequencies without eliminating the ability to stimulate the tactile sense. This suggests that systems should be designed for uniform gain only out to the frequencies useful to the proprioceptive/kinesthetic sense.

In an extensive survey, Brooks found recommendations for bandwidths from 4-20 Hz unloaded, and from 2-4 Hz loaded [12]. It is not clear whether these figures are for position control of the slave or for force control of the master. Brooks notes that master-slave systems have asymmetrical bandwidth requirements; the master force feedback requires higher bandwidth than the slave position control. This is because the slave movements must only match the lower 5-10 Hz bandwidth of human finger motions. The asymmetry works out well, since the higher bandwidth force feedback can coexist stably with the relatively low-impedance interface to the human fingers, and the lower bandwidth position control contributes to stability when interacting with high-impedance (rigid) environments.

Howe and Kontarinis examined the role of force bandwidth in performance of a close tolerance peg-in-hole insertion using a two-finger master-slave hand system with finger force feedback [45]. They found that task completion times and error rates decrease as force reflection bandwidth increases. Tests with 2-pole analog filters on the slave force sensors were conducted with filter bandwidths of 2 Hz, 8 Hz, and 32 Hz. Mean task completion times for the 2 Hz trials were only slightly better than for position control alone; operators reported that the system felt oscillatory and difficult to control, though they also reported that task completion was easier with even 2 Hz feedback. Operators performed significantly better with 8 Hz than with 2 Hz feedback, while the benefits of 32 Hz feedback over 8 Hz feedback were not statistically significant. In a separate, fragile task, Howe and Kontarinis reported failure rates of 63%, 14%, 0%, and 4% for position control, 2 Hz, 8 Hz, and 32 Hz feedback, respectively. Even with very low bandwidth feedback, errors were reduced to one-quarter the rate with position control alone.

The literature seems to suggest increasing usefulness of force-reflection bandwidths from 2-30 Hz, with diminishing gains as 30 Hz is approached and surpassed. Systems with flat responses out to 30 Hz will likely be able to represent vibrations at higher tactile frequencies with lower magnitudes sufficient for the tactile sense. Such systems will require servo rates in excess of 300 Hz for good fidelity. Slave position control will likely require bandwidths up to 10 Hz. All of these bandwidth figures are for flat response bandwidths, not sampling rates, which must be significantly higher to assure the required bandwidth. As with other metrics explored in this report, the familiar theme holds that benefits of increasing bandwidth are task specific and costs are system specific.

**Dynamic range**, the maximum attainable force divided by the backdriven friction, is one of the more important measures of hand master performance. A device that can attain a wide range of forces as untainted as possible by friction will offer the highest fidelity interface.

One device, the PHANToM™, achieved a very high dynamic range of 47.2:1 (33.5 dB). It appears to the user to be almost friction-free, with low backdriven friction at the fingertip ranging from 0.03-0.18 N (0.1-0.6 oz-in). PHANToM™has three force-reflecting cartesian degrees of freedom, and is more like a miniature manipulator than an exoskeleton. Achieving this dynamic range with an exoskeletal design, especially one with remotely-mounted actuators (e.g. on the forearm with sheathed cable transmission) would be quite challenging.

EXOS' SAFiRE device achieved a 34:1 (30.6 dB) ratio on the MCP joint and a 16:1 (24.1 dB) ratio on the PIP joint, according to the SAFiRE Phase I final report [33]. This was achieved with maximum MCP and PIP joint torques of 24 N-cm (34 oz-in) and 11.3 N-cm (16 oz-in), respectively, and friction of 0.706 N-cm (1 oz-in) for both MCP and PIP joints. The EXOS has improved the dynamic range of the Phase II SAFiRE to 146:1 (43.3 dB), with a maximum joint torque of 51 N-cm (72 oz-in) and friction less than 0.35 N-cm (0.5 oz-in).

The maximum force must be high enough to easily stop the human's finger, but friction must be low enough that obtaining the required dynamic range does not mean raising the maximum force to fatiguing levels. Every effort should be made to avoid selecting inherently high-friction mechanisms or transmissions.

### Sensing

An end-tip position resolution of 0.25 mm (0.01 in) has been recommended [33]. At four times the best finger displacement JND of 1 mm, this resolution should be sufficient. A similar goal of four times better than human resolution in joint space would require angular resolution of 0.5 degree. Technical Research Associates (TRA) and the Center for Engineering Design (CED) at the University of Utah are both developing extremely small angle sensors using proprietary technology. The TRA sensor is being developed as part of a Phase II Small Business Innovation Research exoskeleton project for the Armstrong Laboratory. Both TRA and CED are located in Salt Lake City, Utah.

The need to reliably close the force-control loop on the hand master drives the fidelity requirement for force sensors, since exceeding the human's relatively low force resolution is easy. Methods chosen have included traditional strain gauges and optical strain measurement sensors. The force-control loop should be closed through force sensors for each degree of freedom.

## Control Issues

In order to achieve adequate system performance, the control loop will have to be 10-20 times faster than the desired bandwidth [12]. Jau used a sampling rate of 2 kHz in his operationally-tested hand master and robot hand system [58]. Jau et al. describe the control system architecture for the Jau/JPL system in detail [58]. Though it is sometimes difficult with frequently evolving software in prototype systems, the gains should be adjusted when the loop time changes, as this will affect the plant. Anthropomorphic master-slave systems with joint-to-joint correspondence have an advantage because computation time for inverse kinematics and Jacobian calculations can be avoided. The disadvantage of this approach is that it restricts the form that the exoskeleton links

may take. Oomichi et al. developed a hand master with attachments only at the fingertips to avoid the difficulties in matching the form of the human fingers [86]. The control software describes the master fingertip positions with vectors that are fed to the slave, at the expense of time for inverse kinematics and Jacobian calculations.

The physical parameters of the hand master will have a significant bearing on control. Actuators, transmissions, and links should be designed from the start for high bandwidth operation, with low friction and as close to zero backlash as possible. The actuators should be sized generously enough so that the operator cannot easily overpower them; when the master force is not sufficient to encourage the operator to comply with the remote or virtual surface, the operator will appear infinitely stiff to the slave, and instability will result unless the slave bandwidth (gain) is low enough [12].

Hand master-slave systems will more likely than not have position-controlled slaves and force-controlled masters. Position-position systems can function, but with lower performance [12]. A position-controlled master with a force-controlled slave would be less useful since the force-controlled slave would have stability problems when dealing with rigid environments.

Jau controls used compliant control of the robot slave hand while operationally testing his master-slave system [58]. This greatly improved grasping capability, allowing the fingers to self-align to conform to grasped objects and creating stable multi-point contact between the fingers and those objects. Compliant control of the slave wrist allowed some self alignment of the hand orientation to the tool axis in a wrench turning task, simplifying the task by reducing the precision required. A consensus has seemed to emerge among investigators that slaves should be capable of compliant motion and that masters should be as stiff as possible. This makes intuitive sense, since the slave mimics the human body with its excellent compliance control, and the master must represent stiff environments to the human operator. The master-human and slave-environment interfaces would both involve a compliant system in contact with a stiff one, which is desirable for the sake of stability.

# CONCLUSIONS

The state of the art in force-reflecting anthropomorphic hand masters is maturing, though systems are not yet available off-the-shelf. Custom systems provide modest to impressive capabilities at great cost. Numerous parallel efforts have independently pushed the state of the art to its limits, often ignoring or relearning lessons learned previously by distant colleagues. The keys to progress in this area are development of enabling technologies such as actuators, and the preservation of a knowledge base so that new investigators can build on previous efforts with minimal duplication.

A peak human MCP joint speed of 17 rad/s has been measured. Existing data on finger forces have been interpreted to yield estimates of maximum finger joint torques. Successful force-reflecting hand master designs will be able to provide continuous forces 3-15% of the human maximum and peak forces 20-30% of the maximum capability, concentrating on a high-fidelity interface rather than a master that is as strong as the human. Moderate-force interfaces have the added advantage of reducing fatigue, though systems that are too weak could have stability problems.

In order to develop interfaces good enough so that the operator experiences the task rather than the interface, human design requirements must be considered from the start. Systems that are too heavy, laden with friction, loosely attached, have rigid transmissions between forearm and hand, do not follow finger motions, etc. will be expensive exercise weights with moving parts. The performance goals expressed in this report have recently been achieved by commercially available earth-grounded three dof systems, but success for exoskeleton systems remains at least three years away, depending on the level of funding and the progress of novel actuator technologies.

Hand masters with actuators co-located at the finger joints could provide numerous advantages, including simpler control, lighter weight, enhanced portability, and higher fidelity. Actuator co-location would considerably reduce design complexity and expense by eliminating complicated transmission systems. This breakthrough will require novel actuators with torque-to-mass ratios of 35-55 N-m/kg, power densities in the range of 0.3-0.7 $W/cm^3$ and power-to-mass ratios of 70-110 W/kg. Depending on the joint to be driven, the actuators should be capable of delivering 3-7 W peak usable power, with stall torques ranging from 35-150 N-cm. The novel actuators must be readily controllable, wear well, and not have any crippling disadvantages such as excessive noise emission or overheating. Both piezoelectric and magnetostrictive actuator technologies have the potential to meet these performance requirements.

Table 12 summarizes some recommended performance criteria for force-reflecting hand exoskeletons.

Table 12: Recommended Exoskeleton Performance Requirements

| | |
|---|---|
| peak torque | 20-30% of human isometric maximum<br>90-150 N-cm*, 45-90 N-cm† |
| continuous torque | 3-15% of human isometric maximum<br>15-75 N-cm*, 9-44 N-cm† |
| dynamic range | 33 dB |
| stiffness (at fingertip) | 35-45 N/cm |
| joint angle sensor resolution | < 2 deg |
| torque/mass ratio†† | 35-55 N-m/kg peak |
| power/mass ratio†† | 70-110 W/kg peak |
| power/volume ratio†† | 0.3 - 0.7 W/cm$^3$ peak |
| position control bandwidth | 15 Hz |
| force-reflection bandwidth | 30 Hz |

* MCP joint
† PIP joint
†† for a co-located finger joint actuator

## Future Effort

More human experimentation must be done to determine exactly what enhances task performance. Representative tasks should be performed in virtual environments and with real slaves. Sponsors should lay out careful experimental plans before systems are delivered and assure that adequate resources exist to execute those plans so that data and lessons from the new systems can expand the knowledge base and advance the state of the art.

System developers should always keep the demands of the task in mind. Portability and compactness will cost money. If desktop force reflection that is only semi-portable or semi-dexterous will meet task needs, then it should be considered. Advanced anthropomorphic force-reflecting hand masters will enable amazing capabilities for remote manipulation in specific tasks and situations where less capable systems are insufficient. As this application and its enabling technologies develop, a wider range of uses will become feasible.

# REFERENCES


[1] K. N. An, L. J. Askew, and E. Y. Chao. Biomechanics and Functional Assessment of Upper Extremities. In W. Karwowski, editor, *Trends in Ergonomics/Human Factors III*, pages 573–580. Elsevier Science Publishers B.V. (North-Holland), 1986.

[2] J. C. Becker, N. V. Thakor, and K. G. Gruben. A Study of Human Hand Tendon Kinematics with Applications to Robotic Hand Design. In *Proc. of the IEEE Int. Conf. on Robotics and Automation*, pages 1540–1545, 1986.

[3] S. Begej. Glove Controller With Force and Tactile Feedback For Dexterous Robotic Hands. NASA Phase I SBIR NAS9-18308, Begej Corp., 5 Claret Ash Rd., Littleton, CO 80127, September 1990.

[4] M. Bergamasco. Hand Force Feedback System Specification Sheet. Scuola Superiore S. Anna, Via Carducci, 40, 56127 Pisa, Italy, 1994.

[5] M. Bergamasco. Virtual Environments and Teleoperation at the ARTS Lab. Scuola Superiore S. Anna, Via Carducci, 40, 56127 Pisa, Italy, 1994.

[6] M. Bergamasco, D. M. De Micheli, G. Parrini, F. Salsedo, and S. Scattareggia Marchese. Design Considerations for Glove-like Advanced Interfaces. In *Proc. of IEEE Int. Conf. on Advanced Robotics*, pages 162–167, Pisa, Italy, June 1991.

[7] O. Brimhall and R. Goodwin. Personal Communication. Technical Research Associates, Salt Lake City UT, 1994.

[8] O. D. Brimhall and C. J. Hasser. Magnetostrictive Linear Devices for Force Reflection in Dexterous Telemanipulation. In *Proc. of the North American Conf. on Smart Structures and Materials*. SPIE, February 1994.

[9] D.L. Brock. Dynamic Model and Control of an Artificial Muscle Based on Contractile Polymers. A.I. Memo No. 1331: MIT Artificial Intelligence Lab, November 1991.

[10] D.L. Brock. Review of Artificial Muscle Based on Contractile Polymers. A.I. Memo No. 1330: MIT Artificial Intelligence Lab, November 1991.

[11] R. W. Brockett. Light Weight High Performance Manipulators. Technical Report DTIC AD-A198 647, U.S. Army Research Office, Research Triangle Park, NC, July 1988.

[12] T. L. Brooks. Telerobotic Response Requirements. In *Proc. of the IEEE Int. Conf. on Systems, Man, and Cybernetics*, pages 113–120, Los Angeles CA, 1990.

[13] P. Brown, D. Jones, S. K. Singh, and J. M. Rosen. The Exoskeleton Glove for Control of Paralyzed Hands. In *IEEE Conf. on Robotics & Automation*, pages 642–647, Atlanta, GA, 1993.

[14] B. Bucholtz and T. Armstrong. A Kinematic Model of the Human Hand to Evaluate its Prehensile Capabilities. *J. Biomechanics*, 25(2):149–162, 1992.

[15] B. Bucholtz, T. Armstrong, and T. Goldstein. Anthropometric Data for Describing the Kinematics of the Human Hand. *Ergonomics*, 35:261–273, 1992.

[16] B. Bucholtz and T. J. Armstrong. An Ellipsoidal Representation of Human Hand Anthropometry. *Human Factors*, 33(4):429–441, 1991.

[17] G. Burdea. Personal Communication. Rutgers University, Piscataway NJ, 1994.

[18] G. Burdea and P. Coiffet. *Virtual Reality Technology.* John Wiley & Sons, New York, 1994.

[19] G. Burdea and J. Zhuang. Dextrous Telerobotics With Force Feedback - An Overview. Part 1: Human Factors. *Robotica*, 9:171–178, 1991.

[20] G. Burdea and J. Zhuang. Dextrous Telerobotics With Force Feedback - An Overview. Part 2: Control and Implementation. *Robotica*, 9:291–298, 1991.

[21] G. Burdea, J. Zhuang, E. Roskos, D. Silver, and N. Langrana. A Portable Dextrous master With Force Feedback. *Presence*, 1(1):18–28, January 1992. MIT Press.

[22] G. C. Burdea. Human/Machine Interaction In Telerobotic Dexterous Feedback. In *ASME Winter Annual Meeting - Symp. on Dynamics and Control of BioMechanical Systems*, pages 65–69, December 1989.

[23] G. C. Burdea and T. H. Speeter. Portable Dextrous Force Feedback Master for Robot Telemanipulation (PDMFF). In *Proc. of NASA Conf. on Space Telerobotics*, pages 153–161, January 1989.

[24] D. G. Caldwell. Pseudomuscular Actuator for Use in Dexterous Manipulation. *Med. and Biol. Engrg. and Computing*, 28:595–600, 1990.

[25] D. G. Caldwell. Polymeric Gels: Pseudo Muscular Actuators and Variable Compliance Tendons. In *Proc. of the IEEE/RSJ Int. Conf. on Intelligent Robots and Sys. (IROS)*, pages 950–957, July 1992.

[26] S. Chang, H. Tan, B. Eberman, and B. Marcus. Sensing, Perception, and Feedback for VR. In *VR Systems '93*, New York NY, October 1993. SIG-Advanced Applications.

[27] Bridgestone Corp. Rubbertuators and Applications for Robots, Technical Information No. 1. Corporate literature, ACFAS Group, 3-1-1, Ogawahigashi-Machi, Kodaira-shi, Tokyo 187, Japan, FAX (0423) 41-3807.

[28] W. G. Darling. Personal Communication. University of Iowa, Iowa City IA, 1995.

[29] W. G. Darling and K. J. Cole. Muscle Activation Patterns and Kinetics of Human Index Finger Movements. *J. Neurophysiology*, 63(5):1098–1108, May 1990.

[30] T. W. Duerig and K. N. Melton. Designing With the Shape Memory Effect. In *Proc. of the 1989 Materials Research Society Int. Meeting on Advanced Materials*, pages 581–597, 1989.

[31] K. Escher and E. Hornbogen. Shape Memory Alloys for Robot Grippers and Mechanical Hands. In *Fourth European Space Mechanisms and Tribology Symp.*, 1989.

[32] EXOS. SAFiRE Phase II Quarterly Report. SBIR Contract for NASA, October-December 1993.

[33] EXOS, Inc. Development of a Force Feedback Anthropomorphic Teleoperation Input Device for Control of Robot Hands. NASA Phase I SBIR NAS8-38910, EXOS Inc., 8 Blanchard Rd., Burlington, MA 01803, August 1991.

[34] R. C. Goertz. Philosophy and Development of Manipulators. In H. L. Martin and D. P. Kuban, editors, *Teleoperated Robotics in Hostile Environments*, pages 257–262. Robotics Int. of the Soc. of Manufacturing Engineers, 1951. Original figures are not included.

[35] R. C. Goertz, W. M. Thompson, and R. H. Olsen. Electronic Master Slave Manipulator . U.S. Patent #2,846,084, August 1958.

[36] D. Gomez, G. Burdea, and N. A. Langrana. The Second-Generation Rutgers Master SGRM. In *VR Systems '93*, New York NY, October 1993. SIG-Advanced Applications.

[37] A. Grahn. Personal Communication. Bonneville Scientific Inc., Salt Lake City UT, 1994.

[38] A. R. Grahn. Piezoelectric Motor in Robot Finger Joint. *NASA Tech Briefs*, 18(1):57–58, January 1994.

[39] B. Hannaford, L. Wood, D. McAffee, and H. Zak. Performance Evaluation of a Six-axis Generalized Force-Reflecting Teleoperator. *IEEE Trans. on Systems, Man, and Cybernetics*, 21(3):620–633, 1991.

[40] Y. L. Harvill, T. G. Zimmerman, and J. G. Grimaud. Motion Sensor Which Produces an Asymmetrical Signal in Response to Symmetrical Movement. U.S. Patent #5,097,252, March 1992.

[41] C. J. Hasser. Manipulating Molecular Models in "Inner Space" Using a Force-Reflecting Control Arm. Presentation to the Wright Laboratory Symp. on Computational Materials Sci., Wright-Patterson AFB OH, July 1992.

[42] S. Hirose, K. Ikuta, and Y. Umetani. A New Design Method of Servo-actuators Based on the Shape Memory Effect. In *Proc. of the 5th CISM-IFTOMM Symp. on Theory and Practice of Robots and Manipulators*, pages 339–349, 1984.

[43] J. M. Hollerbach, I. W. Hunter, and J. Ballantyne. A Comparative Analysis of Actuator Technologies for Robotics. In M. Rahimi and W. Karwowski, editors, *The Robotics Review 2*. MIT Press, 1991.

[44] J. Hong and X. Tan. Calibrating a VPL DataGlove for Teleoperating the Utah/MIT Hand. In *Proc. of the IEEE Int. Conf. on Robotics and Automation*, pages 1752–1757, 1989.

[45] R. D. Howe and D. A. Kontarinis. Task performance with a dextrous teleoperated hand system. In *Telemanipulator Technology '92*, Boston, November 1992. SPIE.

[46] I. W. Hunter, S. Lafontaine, J. M. Hollerbach, and P. J. Hunter. Fast Reversible NiTi Fibers for Use in Microrobotics. In *Proc. IEEE Workshop on Micro Electro Mechanical Systems*, pages 166–170, Nara, Japan, 1991.

[47] K. Ikuta. Micro/Miniature Shape Memory Alloy Actuator. In *Proc. of the IEEE Int. Conf. on Robotics and Automation*, pages 2156–2161, 1990.

[48] Micro Mo Electronics Inc. Micro Mo Miniature Drive Systems. corporate literature, 742 Second Avenue S., St. Petersburg FL, 1992.

[49] SensAble Devices Inc. The PHANToM Force-Reflecting Interface. corporate literature, 225 Court Street, Vanceburg KY, 1993.

[50] H. Iwata. Artificial Reality with Force-feedback: Development of Desktop Virtual Space with Compact Master Manipulator. *Computer Graphics*, 24(4):165–170, August 1990. (ACM SIGGRAPH '90 Proceedings).

[51] S. C. Jacobsen, E. K. Iversen, C. C. Davis, D. M. Potter, and T. W. McLain. Design of a Multiple Degree of Freedom, Force Reflective Hand Master/Slave with a High Mobility Wrist. In *Third Topical Meeting on Robotics and Remote Systems*, Charleston, South Carolina, March 13-16 1989. Sponsored by ANS, IEEE and SME.

[52] S. C. Jacobsen, E. K. Iversen, D. F. Knutti, R. T. Johnson, and K. B. Biggers. Design of a Multiple Degree-of-Freedom, Force-Reflective Hand Master/Slave with a High-Mobility Wrist. In *Proc. of 3rd Topical Meeting on Robotics and Remote Systems*, 1989.

[53] S. C. Jacobsen, F. M. Smith, E. K. Iverson, and D. K. Backman. High Performance, High Dexterity, Force Reflective Teleoperator. In *Proc. 38th Conf. on Remote Sys. Tech.*, pages 180–185. American Nuclear Society, November 1990.

[54] S. C. Jacobsen, F. M. Smith, E. K. Iverson, and D. K. Backman. High Performance, High Dexterity, Force Reflective Teleoperator. In *American Nuclear Soc. Winter Meeting.* American Nuclear Society, 1990.

[55] B. M. Jau. Anthropomorphic Four Fingered Robot Hand and Its Glove. In *Int. Conf. of the IEEE Engineering in Medicine and Biology Soc.*, pages 1940–1941, 1990.

[56] B. M. Jau. A Mobile, Dexterous Dual-Arm Telemanipulation System for Hazardous Environments. In *ANS 4th Topical Meeting on Robotics and Remote Sys.* American Nuclear Society, February 1991. Albuquerque, NM.

[57] B. M. Jau. Man-Equivalent Telepresence Through Four Fingered Human-Like Hand System. In *Proc. of the IEEE Int. Conf. on Robotics and Automation*, pages 843–848, May 1992.

[58] B. M. Jau, M. A. Lewis, and A. K. Bejczy. Anthropomorphic Telemanipulation System in Terminus Control Mode. In *Proc. of RoManSy '94: The Tenth CISM-IFToMM Symp. on Theory and Practice of Robots and Manipulators*, 1994.

[59] E. G. Johnsen and W. R. Corliss. *Teleoperators and Human Augmentation.* NASA SP-5047, 1967.

[60] L. Jones and J. L. Thousand. Servo Controlled Manipulator Device. U.S. Patent #3,263,824, August 1966.

[61] K. Kaczmarek and P. Bach y Rita. Tactile Displays. In W. Barfield and T. Furness, editors, *Advanced Interface Design and Virtual Environments.* Oxford University Press, 1993.

[62] L. Kiesewetter. The Application of Terfenol in Linear Motors. In *2nd Intl. Conf. on Giant Magnetostrictive and Amorphous Alloys for Sensors and Applications*, pages 1–18, 1988.

[63] D. A. Kontarinis, J. S. Son, W. J. Peine, and R. D. Howe. A Tactile Shape Sensing and Display System for Teleoperated Manipulation. In *IEEE Conf. on Robotics & Automation*, 1995.

[64] J. Kramer. Force Feedback and Texture Simulating Interface Device. U.S. Patent #5,184,319, February 1993.

[65] J. Kramer and L. Liefer. The talking glove: An expressive and receptive "Verbal" communication aid for the deaf, deaf-blind, and nonvocal. In *Proc. Annual Conf. Computer Tech/Spec Ed/Rehab*, pages 335–340, Northridge CA, 1987. Cal State Univ.

[66] K. H. E. Kroemer and E. M. Gienapp. Hand-Held Device to Measure Finger (Thumb) Strength. *J. Appl. Physiol.*, 29(4):526–527, 1970.

[67] L. Li. Personal Communication. NASA Johnson Space Center, Houston TX, 1994.

[68] R. J. Luciani. Quantification of neck muscle fatigue due to lateral acceleration by surface electromyographic analysis. Master's thesis, Wright State University, Dayton OH, 1982.

[69] Y. Maeda. Development of an Anthropomorphic Robot Arm (Mark-2). In *IEEE Int. Workshop on Intelligent Motion Control*, pages 389–394, August 1990.

[70] T. Maeno, T. Tsukimoto, and A. Miyake. The Contact Mechanism of an Ultrasonic Motor . In *Proc. of IEEE Conf. on Ultrasonics and Ferroelectrics*, pages 535–538, 1991.

[71] B. A. Marcus, B. An, and B. Eberman. EXOS Research on Master Controllers for Robotic Devices. In *Fifth Annual Workshop on Space Operations Applications and Research (SOAR '91)*, pages 238–245. NASA, USAF, July 1991.

[72] B. A. Marcus, B. An, and B. Eberman. Making VR Feel Real. In *Virtual Worlds Conf. Proc.* SRI International, June 1991.

[73] B. A. Marcus and D. J. Sturman. Exotic Input Devices. In *Proc. NCGA Conf.*, pages 293–299, 1991.

[74] T. H. Massie and J. K. Salisbury. Probing Virtual Objects With the PHANToM Haptic Interface. In *ASME Winter Annual Meeting–Session on Haptic Interfaces for Virtual Environment and Teleoperator Systems*, Chicago, November 1994.

[75] M. Massimino and T. B. Sheridan. Variable Force and Visual Feedback Effects On Teleoperator Man-machine Performance. In *NASA Conference on Space Telerobotics*, Pasadena CA, 31 January - 2 February 1989.

[76] J. E. Miesner and J. P. Teter. Piezoelectric/Magnetostrictive Resonant Inchworm Motor. In Nesbitt W. Hagood, editor, *1994 North American Conf. on Smart Structures and Materials,* Proceedings Vol. 2190: Smart Structures and Intelligent Systems. SPIE, Orlando FL, February 1994.

[77] A. H. Mishkin and B. M. Jau. Space-Based Multifunctional End Effector Systems: Functional Requirements and Proposed Designs. Technical Report 88-16, NASA JPL, Pasedena, California, April 1988.

[78] R. S. Mosher. Industrial Manipulators. *Scientific American*, 211(4):88–96, 1964.

[79] R. S. Mosher and B. Wendel. Force-Reflecting Electrohydraulic Servomanipulator. *Electro-Technology*, 66:88–96, December 1960.

[80] Y. Nakano, Y. Hosada, and M. Fujie. Hitachi's Robot Hand. *Robotics Age*, 6(7):18–20, July 1984.

[81] D. V. Newton, E. Garcia, and G. C. Horner. Development of a Linear Piezoelectric Motor. In N. W. Hagood, editor, *1994 North American Conf. on Smart Structures and Materials,* Proceedings Vol. 2190: Smart Structures and Intelligent Systems. SPIE, Orlando FL, February 1994.

[82] K. Ohnishi. A Novel Ultrasonic Linear Actuator. In *Proc. of IEEE Conf. on Ultrasonics and Ferroelectrics*, pages 206–212, 1991.

[83] T. Oomichi, M. Higuchi, A. Okino, N. Kawauchi, Y. Shimizu, A. Maekawa, K. Ohnishi, and T. Hayashi. Intelligent Control of Four Fingered Manipulator System. In *Proc. of the Int. Symp. on Advanced Robot Tech. (ISART)*, page 589. Japan Industrial Robot Association (JIRA) and Advanced Robot Technology Reasearch Association (ARTRA), March 1991.

[84] T. Oomichi, A. Maekawa, and T. Hayashi. Multiple Sensory Bilateral Control of A Manipulator With Dexterous Hand. In *The Second Workshop on Manipulators, Sensors and Steps Towards Mobility*, pages 10.1–10.7. University of Salford, England, October 1988.

[85] T. Oomichi, T. Miyatake, A. Maekawa, and T. Hayashi. Mechanics and Multiple Sensory Bilateral Control of a Fingered Manipulator. In *Robotics Research: The Fourth Int. Symp.*, pages 145–153, Cambridge, MA, 1988. MIT Press.

[86] T. Oomichi, A. Okino, M. Higuchi, A. Maekawa, and K. Ohnishi. Development of Working Multifinger Hand Manipulatior. In *Proc. of the IEEE Int. Workshop on Intelligent Robots and Systems*, pages 873–880, 1990.

[87] X. D. Pang, H. Z. Tan, and N. I. Durlach. Manual Discrimination of Force Using Active Finger Motion. *Perception & Psychophysics*, 49(6):531–540, 1991.

[88] B. V. Park. The Edge: Medicine Meets VR. *Workstation News*, page 16, August 1992.

[89] N. J. M. Patrick, T. B. Sheridan, M. J. Massimino, and B. A. Marcus. Design and Testing of a Non-reactive, Fingertip Tactile Display for Interaction with Remote Environments. Source: Beth Marcus at EXOS, 1991.

[90] J. S. Petrofsky. Quantification Through the Surface EMG of Muscle Fatigue and Recovery During Successive Isometric Contractions. *Aviation, Space, and Environmental Medicine*, 52(9):545–550, September 1981.

[91] A. Poznanski. *The Hand in Radiologic Diagnosis.* W. B. Saunders Co., Philadelphia, 2nd edition, 1993. pp 35-40.

[92] P. Richard, G. Burdea, G. Birebent, D. Gomez, N. Langrana, and Philippe Coiffet. Human Factors Tests for Virtual Environments: Visual Tracking and Haptic Feedback. submitted to Presence – Teleoperation and Virtual Environments, MIT Press, October 1994.

[93] P. Richard, G. Burdea, and P. Coiffet. Human Performance in Tasks Involving Virtual Objects with Force Feedback. In *Proc. of Interface to Real and Virtual Worlds Conference*, pages 229–238, Montpellier, France, 1993. In French.

[94] P. Richard, G. Burdea, D. Gomez, and P. Coiffet. A Comparison of Haptic, Visual and Auditive Force Feedback for Deformable Virtual Objects. In *The Fourth International Conference on Artificial Reality and Tele-Existence (ICAT '94)*, Tokyo, Japan, July 1994.

[95] L. B. Rosenberg. Perceptual Design of a Virtual Rigid Surface Contact. Technical Report AL/CF-TR-1994-0029, USAF Armstrong Laboratory, Wright-Patterson AFB OH, 1992.

[96] L. B. Rosenberg. Perceptual Design of Virtual Haptic Sensations. In *VR Systems '93*, New York NY, October 1993. SIG-Advanced Applications.

[97] L. B. Rosenberg. *Virtual Fixtures: Perceptual Overlays Enhance Operator Performance in Telepresence Tasks.* PhD thesis, Stanford Univ., June 1994. Mech. Eng. Dept.

[98] M. E. Rosheim. Compact Telerobot Hand. *NASA Tech Briefs*, pages 84–85, December 1993.

[99] A. Rovetta and X. Wen. Telemanipulation Control of a Robotic Hand with Cooperating Fingers by Means of Telepresence with a Hybrid Virtual-Real Structure. In *Proc. of the 1992 IEEE/RSJ Int. Conf. on Intelligent Robots and Sys. (IROS)*, pages 1125–1129, July 1992.

[100] J. K. Salisbury. *Kinematic and Force Analysis of Articulated Hands.* PhD thesis, Stanford University, May 1982. Dept. of Mech. Eng.

[101] J. K. Salisbury. Teleoperator Hand Design Issues. In *Proc. of the IEEE Int. Conf. on Robotics and Automation*, pages 1355–1360, 1986.

[102] G. Schadebrodt and B. Salomon. The Piezo Traveling Wave Motor, a New Element in Actuation. *PCIM*, pages 46–50, July 1990.

[103] J. S. Schoenwald, P. M. Beckham, R. A. Rattner, B. Vanderlip, and B. E. Shi. End Effector Actuation with a Solid State Motor. In *Proc. of the IEEE Int. Conf. on Robotics and Automation*, pages 108–113, April 1988.

[104] SensAble Devices, Inc. Personal Communication. 225 Court Street, Vanceburg KY, 1993.

[105] M. Shahinpoor. Design and modeling of a Novel Fibrous SMA Actuator. In V. K. Varadan, editor, *1994 North American Conf. on Smart Structures and Materials*, Proceedings Vol. 2189: Smart Materials. SPIE, Orlando FL, February 1994.

[106] M. Shahinpoor. Design and Modeling of a Novel Spring-Loaded Ionic Polymeric Gel Actuator. In V. K. Varadan, editor, *1994 North American Conf. on Smart Structures and Materials*, Proceedings Vol. 2189: Smart Materials. SPIE, Orlando FL, February 1994.

[107] M. Shahinpoor. Microelectromechanics of Ionic Polymeric Gels as Synthetic Robotic Muscles. In V. K. Varadan, editor, *1994 North American Conf. on Smart Structures and Materials*, Proceedings Vol. 2189: Smart Materials. SPIE, Orlando FL, February 1994.

[108] B. L. Shields, S. W. Peterson, A. M. Strauss, and J. A. Main. Design and Control of a Hand Exoskeleton for Use in Extravehicular Activity. In *44th International Astronautical Congress, Smart Materials and Adaptable Structures Symposium*, Graz, Austria, October 1993.

[109] K. B. Shimoga. Force and Touch Feedback Devices for Dexterous Telemanipulation. In *NASA-CIRSSE Conf. on Intelligent Robotics for Space Exploration*, pages 158–176, Sept/Oct 1992.

[110] K. B. Shimoga. Perceptual Feedback Issues in Dexterous Telemanipulation. Technical Report RAL/KBS-2-92, Univ. of Toronto, Robotics & Automation Lab, 1992.

[111] M. A. Srinivasan and J. Chen. Human Performance in Controlling Normal Forces of Contact with Rigid Objects. In *ASME Winter Annual Meeting–Session on Haptic Interfaces for Virtual Environment and Teleoperator Systems*, New Orleans, November 1993.

[112] Staff. New Ideas in Motion. *PCIM*, pages 37–38, April 1987.

[113] P. H. Sutter, J. C. Iatridis, and N. V. Thakor. Response to Reflected-Force Feedback to Fingers in Teleoperations. In *Proc. of the NASA Conf. on Space Telerobotics*, pages 65–74. NASA JPL, January 1989.

[114] H. Z. Tan, X. D. Pang, and N. I. Durlach. Manual Resolution of Length, Force, and Compliance. In *Proceedings of ASME Winter Conference*, November 1992.

[115] H. Z. Tan, M. A. Srinivasan, B. Eberman, and B. Cheng. Human Factors for the Design of Force-Reflecting Haptic Interfaces. In *ASME Winter Annual Meeting–Session on Haptic Interfaces for Virtual Environment and Teleoperator Systems*, Chicago, November 1994.

[116] J. P. Teter and A. E. Clark. Magnetostrictive Linear Motor. U.S. Patent #5,039,894, August 1991.

[117] Y. Tomikawa, K. Adachi, M. Aoyagi, T. Sagae, and T. Takano. A Rod Type Ultrasonic Motors using Longitudinal and Torsional Vibration Modes. In *Proc. of IEEE Conf. on Ultrasonics and Ferroelectrics*, pages 229–231, 1991.

[118] W. Townsend and L. Tarricone. Design of a High Performance Miniature (Knuckle-Sized) Joint Drive for Exoskeleton Hand Teleoperators. Air Force Phase I SBIR AL-TR-1992-0186, Barrett Technology, Inc., Cambridge, MA, April 1992.

[119] K. Uchino. Piezoelectric and Electrostrictive Actuators. In *Proc. of IEEE Conf. on Ultrasonics and Ferroelectrics*, pages 610–618, 1986.

[120] Y. Wang. Mission Accomplished: Teleoperated Laparoscope. *NASA Tech Briefs*, 18(1):16–17, January 1994.

[121] G. Westling and R. S. Johansson. Factors Influencing the Force Control During Precision Grip. *Experimental Brain Research*, 53:227–284, 1984.

[122] S. F. Wiker, E. Hershkowitz, and J. Zik. Teleoperator Comfort and Psychometric Stability: Criteria for Limiting Master-Controller Forces of Operation and Feedback During Telemanipulation. In *Proc. NASA Conf. on Space Telerobotics*, pages 99–107, Pasadena CA, 1989.

[123] A. Zarudiansky. Remote Handling Devices. U.S. Patent #4,302,138, November 1981.

# APPENDIX A: CALCULATIONS OF FINGER JOINT TORQUES FROM FORCES NORMAL TO PHALANGES

This appendix details the derivation of finger joint torques given a set of three forces, each acting on the middle of a phalanx (finger bone). Certain finger parameters, such as phalange (link) length and joint angle must also be given or assumed. Table 13 shows the assumed link lengths. The link dimensions were obtained from the author's hand, since none of the sources cited has all the necessary dimensions. To roughly gauge the average nature of the author's hand, his crotch-to-tip finger lengths of 5.4, 7.2, 8.4, 7.7, and 6.2 cm can be compared to the average lengths 5.9, 7.5, 8.6, 8.0, and 6.1 given in the first column of Table 22 (crotch-to-tip length should not be confused with total length from the MCP joint). In addition, the author's first phalanx on finger III (middle finger) of his right hand measures 6.8 cm, almost exactly the average given in Table 21.

Table 13: Link (Phalangeal) Lengths Used in Torque Calculations (cm)

| | Proximal | Middle | Distal |
|---|---|---|---|
| Index | 5 | 3 | 2.5 |
| Middle | 5.5 | 3.25 | 2.5 |
| Ring | 5 | 3 | 2.5 |
| Little | 3.75 | 2.75 | 2.5 |

Table 14 shows the assumed joint angles, where the joint angle is defined as the difference between the current position and the fully extended position. All joint angles are zero when the finger is fully extended along a straight line through the forearm and hand. A rough approximation of a cylindrical grasp by the author (using the right hand represented by the measurements in Table 13) generated the joint angles in Table 14.

Table 14: Joint Angles Used in Torque Calculations (Degrees)

| | MP | PIP | DIP |
|---|---|---|---|
| Index | 53 | 61 | 51 |
| Middle | 53 | 61 | 51 |
| Ring | 53 | 61 | 51 |
| Little | 53 | 61 | 51 |

Figure 4 shows a vector diagram for the torque computation. The diagram denotes link length vectors, mid-phalangeal force vectors, joint angles, and joint torques.

The cross product of the radius vector and the force vector yields the contribution of each force to a given joint torque. Each radius vector describes the location of the point of application of a force with respect to the point about which torque is being calculated. The radius and force vectors were calculated as follows, where $\phi$ is the joint angle:

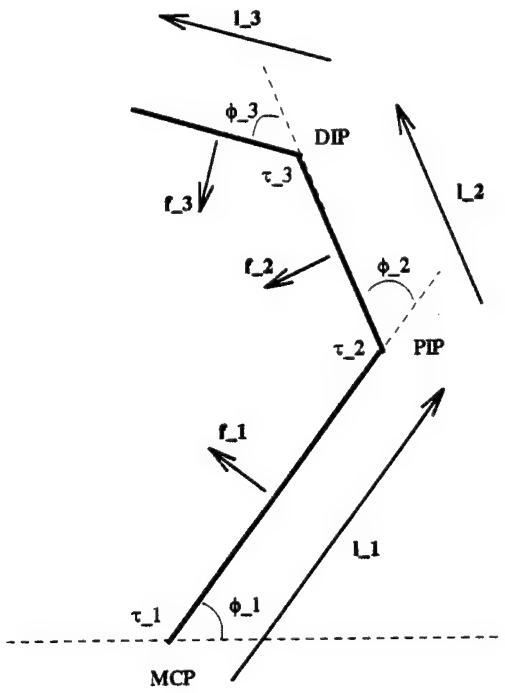


Figure 4: Vector Diagram for Finger with Mid-Phalangeal Forces

$$\mathbf{l}_i = l_i \cos\left(\sum_{j=1}^{i} \phi_j\right)\mathbf{i} + l_i \sin\left(\sum_{j=1}^{i} \phi_j\right)\mathbf{j} \tag{2}$$

$$\mathbf{f}_i = f_i \cos\left(90^\circ + \sum_{j=1}^{i} \phi_j\right)\mathbf{i} + f_i \sin\left(90^\circ + \sum_{j=1}^{i} \phi_j\right)\mathbf{j} \tag{3}$$

The joint torques can then be calculated:

$$\tau_1 = 0.5\mathbf{l}_1 \times \mathbf{f}_1 + (\mathbf{l}_1 + 0.5\mathbf{l}_2) \times \mathbf{f}_2 + (\mathbf{l}_1 + \mathbf{l}_2 + 0.5\mathbf{l}_3) \times \mathbf{f}_3 \tag{4}$$

$$\tau_2 = 0.5\mathbf{l}_2 \times \mathbf{f}_2 + (\mathbf{l}_2 + 0.5\mathbf{l}_3) \times \mathbf{f}_3 \tag{5}$$

$$\tau_3 = 0.5\mathbf{l}_3 \times \mathbf{f}_3 \tag{6}$$

# APPENDIX B: MEASUREMENT OF MAXIMUM JOINT AND FINGERTIP SPEEDS

Three simple experiments were performed by the author with a small sample of subjects to gauge the peak human MCP joint speed and peak index fingertip velocity when the subject flexes the index finger at the MCP joint. In the first experiment, subjects were asked to rapidly cycle all of the fingers of their dominant hand from full flexion of all joints to full extension for 15 seconds. The number of cycles completed was measured, and the peak angular joint speed for the MCP joint was calculated based on assumptions of sinusoidal motion.

The latter two experiments were performed to roughly gauge the average speed of the dominant index fingertip as the subject oscillated the MCP joint. In both experiments, subjects were instructed to hold their MCP joint axis as stationary as possible, while rapidly flexing and extending the MCP joint so the fingertip cycled between two points. The number of cycles between the two points was counted for about 20 seconds, and from that the average fingertip speed for the trial was determined. For the relatively small MCP angular movement, the movement of the fingertip was approximated as a line, rather than an arc.

## Experiment One: MCP Joint Velocity

Subjects were asked to hold their dominant hands in a lightly clenched fist, and then to extend their fingers as fast as possible to make a flat hand, and then flex back to a fist. Angular displacement for the MCP joint was approximately 90 degrees. Subjects cycled from flat hand to fist as many times as possible in 15 seconds. Subjects were instructed to move their hand through the full range of motion every cycle, and were observed for compliance, but joint angles were not measured during the actual trials. Table 15 and Table 16 show results for male and female subjects, respectively.

Table 15: MCP Joint Cycles and Angular Speed (cm/s) for Male Subjects in 15 Second Trial

| | CJH | BOH | RES | MLC | mean | s.d. |
|---|---|---|---|---|---|---|
| cycles | 54 | 54 | 49 | 45 | 50.5 | 4.4 |
| peak speed (rad/s) | 17.8 | 17.8 | 16.1 | 14.8 | 16.6 | 1.4 |

Table 16: MCP Joint Cycles and Angular Speed (cm/s) for Female Subjects in 15 Second Trial

| | ALZ | ARM | mean | s.d. |
|---|---|---|---|---|
| cycles | 43 | 43 | 43 | 0 |
| peak speed (rad/s) | 14.1 | 14.1 | 14.1 | 0 |

Peak angular speeds were calculated by assuming the joint motion was sinusoidal and taking the amplitude of the velocity derivative. Equation (7) is the equation of motion for the joint angle, where $A$ is the amplitude of the motion. Equation (8) describes the angular velocity of the joint, and Equation (9) takes the magnitude of that sinusoidal signal to obtain the maximum angular joint speed for an amplitude of $\pi/4$ (half of the peak-to-peak amplitude of $\pi/2$, or 90 degrees).

$$\theta(t) = A \sin 2\pi(\frac{cycles}{duration})t \tag{7}$$

$$\dot{\theta}(t) = A2\pi(\frac{cycles}{duration}) \cos 2\pi(\frac{cycles}{duration})t \tag{8}$$

$$\omega_{max} = A2\pi(\frac{cycles}{duration}) = \frac{\pi}{4}2\pi(\frac{cycles}{duration}) \tag{9}$$

## Experiment Two: Fingertip Speed with MCP Joint Centered Between Two Targets

Subjects held their dominant hands on a table, thumb up, with the index finger pointing outward and the rest of the fingers curled under the hand. The rotational axis of the MCP joint intersected the table at about 45 degrees, as the index finger pointed down towards the table. At rest, the extended index finger fell halfway between two target points. For male subjects, the points were 10 cm apart; for females, they were 7.5 cm apart. When viewed from above, the two target points and the MCP joint formed an isosceles triangle. Starting with the index finger at one of the target points, the subject cycled between the points as fast as he or she was able for 19 seconds. Table 17 and Table 18 show results for male and female subjects, respectively. Average speeds for male subjects were obtained with Equation (10), with similar calculations for females. Peak speeds were obtained by using Equation (9) with $A = 5$ cm and $A = 3.75$ cm.

$$v_{avg} = (\frac{20cm}{cycle})(\frac{cycles}{duration}) \tag{10}$$

Table 17: Fingertip Cycles and Speed (cm/s) for Male Subjects with Targets 10 cm Apart

| | CJH | BOH | BD | ME | PVW | mean | s.d. |
|---|---|---|---|---|---|---|---|
| cycles | 60 | 56 | 59 | 56 | 62 | 59 | 2.6 |
| avg. speed (cm/s) | 63.0 | 58.8 | 62.1 | 58.8 | 65.1 | 62 | 2.7 |
| max. speed (cm/s) | 99.2 | 92.6 | 97.6 | 92.6 | 102.5 | 96.9 | 4.3 |

Table 18: Fingertip Cycles and Speed (cm/s) for Female Subjects with Targets 7.5 cm Apart

| | DW | MS | ALZ | ARM | mean | s.d. |
|---|---|---|---|---|---|---|
| cycles | 53 | 49 | 37 | 53 | 48 | 7.6 |
| avg. speed (cm/s) | 41.8 | 38.7 | 29.2 | 41.8 | 37.9 | 6.0 |
| max. speed (cm/s) | 65.7 | 60.8 | 45.9 | 65.7 | 59.5 | 9.4 |

## Experiment Three: Fingertip Speed with MCP Joint In Front of One of Two Targets

Subjects held their dominant hands at the edge of a table, thumb up, with a pointed index finger held parallel over the surface of the table. Fingers were curled below the table surface, against the table edge. Two target points were drawn on a piece of paper placed on the table under the index finger. In this second fingertip speed experiment, the location of the pivot point (MCP joint) with respect to the two targets was varied for comparison with earlier results. Instead of aligning the MCP joint equidistant from both targets, the MCP joint was moved in front of one target, at the top end point of an "L," with the targets forming the corner and opposite point of the "L." Targets were moved closer together for this experiment to accomodate the new arrangement.

The hand posture with the fingers curled next to the table edge allowed the subjects to hold their fingers parallel to the table surface instead of awkwardly pointing down at the table with unused curled fingers resting on top of the table. This posture change was an uncontrolled deviation from the first fingertip speed experiment, but was judged to be less cumbersome for the subjects. The first experiment could be reperformed at the edge of a table if desired.

Subjects cycled their fingers between targets for 19 seconds. Targets for the male subjects were 8.5 cm apart and targets for females were 6.5 cm apart. Average speeds for this experiment were obtained with calculations similar to Equation (10). Peak speeds were obtained by using Equation (9) with $A = 4.25$ cm and $A = 3.25$ cm. Table 19 and Table 20 show results for male and female subjects, respectively.

Table 19: Fingertip Cycles and Speed (cm/s) for Male Subjects with Targets 8.5 cm Apart

| | CJH | BOH | BD | ME | PVW | mean | s.d. |
|---|---|---|---|---|---|---|---|
| cycles | 75 | 80 | 70 | 80 | 70 | 75 | 5 |
| avg. speed (cm/s) | 67.1 | 71.6 | 62.6 | 71.6 | 62.6 | 67.1 | 4.5 |
| max. speed (cm/s) | 105.4 | 112.4 | 98.4 | 112.4 | 98.4 | 105.4 | 7.02 |

Table 20: Fingertip Cycles and Speed (cm/s) for Female Subjects with Targets 6.5 cm Apart

| | MS | ALZ | ARM | mean | s.d. |
|---|---|---|---|---|---|
| cycles | 91 | 67 | 77 | 78.3 | 12.0 |
| avg. speed (cm/s) | 62.3 | 45.8 | 52.7 | 53.6 | 8.2 |
| max. speed (cm/s) | 97.8 | 72.0 | 82.8 | 84.2 | 13.0 |

# APPENDIX C: HAND MECHANICS AND ANTHROPOMETRY

To adequately design a hand master, a designer must have a knowledge of hand mechanics and anthropometry that is beyond the scope of this appendix. Some of the most important results are presented here, but the reader is encouraged to explore further. In particular, this author highly recommends that the reader directly consult a book chapter by Dubousset [5]. While this appendix cites some of Dubousset's work, important results such as those describing kinematic angular offsets of the joints and joint ranges of motion have not been discussed here. Another book chapter by Hollister and Giurintano does an excellent job of describing finger joint motion and should also be consulted directly [10].

## Joint Rotation

Designing exoskeleton joints to track finger joints rotating about some anatomically buried area of rotation poses enough difficulties without considering any complex motions that take place inside the finger joint. Modelling the finger joints with fixed centers of rotation simplifies the design so much that designers will probably do it regardless of whether or not the simplification is verified! Fortunately, Bucholtz, et al. have confirmed that the DIP and PIP joints of the four fingers can be modeled with fixed centers of rotation [3]. This conclusion agrees with Dubousset's observation that the PIP joint rotates in a single plane, with no lateral movement whatsoever, around a single flexion/extension axis that passes across the head of the proximal phalanx [5]. Dubousset states that the DIP joint behaves similarly. He does describe some axial rotation of the medial phalanx with PIP flexion/extension, but states that it is much less significant than at the MCP joint.

Some investigators have presented similar opinions for the MCP joint, but others have contended that the motion at the MCP joint is more complex. Dubousset describes this complex motion [5]:

> Because of the asymmetry of the metacarpal head in the sagittal plane, flexion-extension movements of the proximal phalanx do not occur in one axis only. As with the knee, these movements take place about a series of axes, *the geometric pivot of which lies on a spiraling arc that becomes more and more palmar as flexion increases* [emphasis by Dubousset].

Dubousset also notes that asymmetry of the collateral metacarpal ligaments produces passive axial rotation, changing from pronation to supination as the flexed MCP joint is extended [5]. The significance of this axial rotation for hand master design is not clear. Unless the hand master has rings around the fingers with pins anchored directly in bone (unlikely!), at least some rotational compliance will exist between the hand and hand master, possibly keeping the axial rotation from producing discomfort.

Bucholtz, et al. confirmed that the finger joint centers of rotation may be estimated with reasonable accuracy either by using the geometric method of Reuleaux (which detects the mean

instantaneous centers of curvature of planar joints) or by determining the center of curvature of the head of the phalange proximal to the given joint (using an x-ray image). Reuleaux's method can be described briefly [3]:

> A local coordinate system is attached to the fixed segment, while two points on the moving segment are tracked. A perpendicular is erected from the midpoint of the line segment connecting one of the moving points at one joint rotation angle with the same point at a second angle. This is done for both of the points that are tracked. Where these two perpendiculars intersect is defined as the mean instantaneous center of rotation for the given rotation.

## Phalanx Length and Adjustability Requirements

Knowledge of the statistical distribution of hand dimensions in the population and how those dimensions are related to each other can aid the hand master designer in a number of different ways. Obviously, the range of hand dimensions will determine the range of adjustment necessary for the hand master. It may be the case for some dimensions that the range is small enough that no adjustment is necessary. The ultimate goal is to fit as much of the population as possible with as few adjustments as possible. The discussion in this section concentrates on the fingers and finger joints. For any hand master that will be integrated with an arm or wrist master, anthropometric and kinematic information relative to the wrist must also be considered. Work cited in this section, particularly that of Bucholtz, deals with this information.

Goodwin has determined in work performed for the Armstrong Laboratory that a hand master should have adjustable proximal phalange and metacarpal lengths, but that fixed segment lengths would be sufficient for the medial and distal phalanges [1]:

> If the rigid mechanism is centered over the middle phalanges, then the variation over 90% of the population (+/- 2 mm for digit II) will be distributed across two joints, and allow a fixed center of rotation to fall within a millimeter of its actual location. Adjustability of this segment, therefore, would be on the order of one or two millimeters, and is not necessarily required. Variability of hand size is more a function of the proximal phalanges (+/- 4 mm) as well as the metacarpals (+/- 7 mm), and adjustability will be a key design feature at those locations. These two segments alone account for over 70% of hand size, and must be accommodated to achieve an accurate and effective fit. The remaining variation in hand size is accounted for by the distal phalanges, which may not need to be accounted for, providing an open-tip exoskeleton is designed.

Bucholtz, et al. collected anthropometric data describing hand kinematics and modeled this anthropometry as a function of external hand measurements using tables of coefficients [3]. These models were able to very accurately predict bone segment length and distances between joint center points based upon finger segment length. The models were able to predict joint segment length

and lateral MCP knuckle position based upon hand length and breadth measurements, but with less accuracy. The models also predict segment breadth and depth [4]. Such models would allow adjustment of link lengths and offsets in a virtual slave hand to match that of the user with just a few simple hand measurements.

## The Thumb

The thumb adds tremendous capability to the human hand, but complicates the task of the hand master designer. The thumb has one less phalanx than the fingers, with a two-degree of freedom joint buried deep in the hand at the carpal-metacarpal (CMC) joint. The MCP joint of the thumb, at the edge of the palm, also has two degrees of freedom: flexion/extension and abduction/adduction, the same as in the CMC joint [10]. The interphalangeal (IP) joint of the thumb (the knuckle just below the fingernail) provides the most distal degree of freedom. With two dofs in the CMC joint, two in the MCP joint, and one in the IP joint, the thumb might be regarded as having five degrees of freedom. In fact, the abduction/adduction motion of the MCP joint is coupled strongly to the abduction/adduction motion of the CMC joint; these two joint motions effectively provide only one degree of freedom of actuation, with the resulting motion a bit more complex than in the single joint case [10]. Consequently, only four degrees of freedom should be required to actuate the thumb.

The thumb can function usefully without the IP joint, but this joint is vital for bringing the thumb into opposition with any part of the hand except for the fingertips, so significant reason exists for designing a telerobotic hand system with a 4 dof thumb, where the fingers might only have 3 dof (with DIP joints omitted). At least one force-reflecting hand master was designed with 4 dof for the thumb, "one degree of freedom (DOF) to bring the thumb from a position opposing the fingers into a lateral or salute position and one DOF in each of the three distal joints [11]."

Bucholtz and Armstrong constructed a model of the human hand to predict joint angles in various grasps [2]. While they do not give results indicating whether or not the joints of the thumb can be modeled with fixed centers of rotation, they do describe the motion of the CMC joint. Bucholtz and Armstrong note that even though the thumb CMC joint can be viewed as a saddle joint with two degrees of freedom, the first metacarpal (in the palm) experiences significant rotation due to incongruity between the trapezium and the metacarpal base and laxity of the ligaments in the area. Presumably this rotation of the first metacarpal results in a rotation of the entire thumb distal to the CMC joint. While there are only two legitimate degrees of freedom at the CMC joint, they are not around orthogonal Cartesian axes as with the motions of the finger MCP joints. Hollister et al. agree, stating that while the axes of rotation are fixed, they are not perpendicular to each other or to the bones, and they to not intersect [9]. Bucholz and Armstrong dealt with this by adding a third degree of freedom to the CMC joint in their model. Adding a third degree of freedom to a hardware system would be cumbersome and expensive, so it would be desirable to design an exoskeleton that can track the complex motions of the CMC joint with only two actuated degrees of freedom, perhaps following a parametric path. Hollister and Giurintano's description of thumb CMC joint motion might be helpful here [10, 9]. Tracking the motions of the CMC joint is also difficult because the ideal point to affix the exoskeleton, just distal to the CMC joint, is buried in the palm. The most proximal place to have an exoskeleton attachment would be just distal of

the thumb MCP joint. With this arrangement, a single attachment point must be used to track and reflect forces to 3 dof on the thumb.

## Condensed Anthropometry Data

The Air Force has conducted at least three hand anthropometry studies, documented in technical reports available from the Defense Technical Information Center (DTIC) [6, 7, 8]. While these technical reports are the definitive references for the studies, the results relevant to hand master design can be condensed into a few short pages. The condensed information appears in the sections below.

### Hertzberg, et al.

In 1950, Hertzberg, et al. completed an anthropometry study of over 4,000 male USAF flying personnel [8]. Of the many measurements taken, the few that are relevant to hands are defined below:

**hand length** Subject's right hand is extended, palm up. With the bar of the sliding caliper lying along his palm, measure the distance from the proximal edge of the navicular bone at the wrist (near the wrist crease) to the tip of the middle finger.

**hand breadth at metacarpale** Subject's right hand is extended, palm up. With the bar of the sliding caliper lying across his palm, measure the maximum breadth across the distal ends of the metacarpal bones (knuckles).

**hand breadth at thumb** Subject's right hand is extended, palm up, with the thumb lying along the side and in the plane of the palm. With the bar of the sliding caliper resting on the palm and the caliper's fixed arm at the knuckle (the joint of the metacarpal bone and the first phalanx) of the thumb, measure the breadth at right angles to the long axis of the hand.

**thickness at metacarpale III** Subject's right hand is held with the fingers extended. Using the sliding caliper, measure the thickness of the knuckle (the joint of the metacarpal bone and the first phalanx) of the middle finger.

**palm length** Subject's right hand is extended, palm up. With the bar of the sliding caliper resting on the palm, measure from the proximal edge of the navicular bone at the wrist (wrist crease) to the skin crease formed where the middle finger folds upon the palm.

**first phalanx III length** Subject's right hand is held in a fist. Using the sliding caliper, measure the length of the first segment of the middle finger across the surfaces of the third metacarpal and the second phalanx.

**finger diameter III** Subject's right middle finger is inserted into a series of graduated holes. Record the diameter of the hole which most closely approximates the maximum diameter of the finger.

Table 21 contains means, standard deviations, fifth percentile, and ninety-fifth percentile values for the relevant measurements from Hertzberg, et al.

Table 21: Various Hand Dimensions of Male USAF Personnel (cm)

| *joint* | *mean* | *s.d.* | *5%<* | *95%<* |
|---|---|---|---|---|
| Hand length | 19.02 | 0.86 | 17.59 | 20.44 |
| Hand breadth MC | 8.83 | 0.41 | 8.18 | 9.51 |
| Hand breadth thumb | 10.35 | 0.53 | 9.47 | 11.22 |
| Hand thickness MC III | 2.97 | 0.18 | 2.67 | 3.25 |
| Palm length | 10.77 | 0.54 | 9.89 | 11.69 |
| First phalanx III length | 6.78 | 0.30 | 6.32 | 7.25 |
| Finger diameter III | 2.18 | 0.12 | 2.00 | 2.36 |
| Wrist circumference | 17.39 | 1.00 | 15.9 | 19.0 |

## Garrett

In 1970, Garrett published two companion reports on the anthropometry of Air Force male and female hands [6, 7]. The studies included total hand length, total finger lengths, knuckle widths and breadths, as well as most dimensions of the palm. Individual phalangeal dimensions were not included.

The studies were conducted in the summer of 1968 on 148 Air Force men and 211 Air Force women. The mean hand breadth and hand circumference measurements for the male sample pool were identical to those for a larger pool of 2420 men measured a year previously. The mean hand breadth and hand circumference measurements for the female sample pool compare to within 2% to those for a pool of 1905 women measured as part of a larger study that ran concurrently. The various measurements taken are defined below:

**wrist crease baseline** An imaginary line extending along the skin crease at the base of the hand (palm side), and outward to either side.

**hand length** Subject's right hand is extended, palm up. With the bar of the sliding caliper parallel to the long axis of the hand, measure the distance from the wrist crease baseline to the tip of the longest finger.

**hand breadth** Subject's right hand is extended, palm down, thumb held away from the fingers. With the bar of the sliding caliper lying across the back of the hand, measure the breadth of the hand between metacarpal-phalangeal joints II and V.

**hand circumference** Subject's right hand is extended, palm down, thumb held away from the fingers. With the tape passing over metacarpal-phalangeal joints II and V, measure the circumference of the hand.

**hand thickness** Subject's right hand is extended. With the sliding caliper, measure the maximum thickness of the metacarpal-phalangeal joint of digit III.

**hand depth** Subject's right hand is extended with the thumb lying adjacent to the volar surface (palm side) of digit II (index finger). With the sliding caliper, measure the maximum depth from the volar side of the thenar pad (base of thumb) to the dorsal surface of the hand.

**wrist breadth** Subject's right hand and wrist lie on the measuring board. With the sliding caliper, measure the breadth of the wrist at the level of the wrist crease baseline.

**knuckle dimensions** Subject's right hand is extended. With the sliding caliper, measure the maximum breadth and maximum depth of the relevant joint. Using the elliptical approximation $C = \sqrt{\frac{a^2+b^2}{2}}$, calculate the circumference of the joint.

**crotch height** The perpendicular distance from the wrist crease baseline to the webbed crotch between two fingers.

**finger length (crotch to tip)** The distance along the axis of the digit from the midpoint of its tip to the level of the same numbered crotch (the crotch to the right on the right hand). Note: fingertip to crotch is not the same as fingertip to the center of the MP joint.

**finger length (wrist crease to tip)** The distance along the axis of the digit from the midpoint of its tip to the wrist crease baseline.

Table 22 and Table 23 describe finger lengths and palm dimensions measured for males and females, respectively. Likewise, Table 24 and Table 25 describe knuckle depths, breadths, and circumferences. Table 26 and Table 27 describe various hand dimensions, including length, breadth and thickness. The tables contain mean, standard deviation, fifth percentile, and ninety-fifth percentile values for each measurement.

Table 22: Finger Lengths and Palm Dimensions of USAF Male Flying Personnel (cm)

| | Finger length: crotch to tip | | | | Finger length: wrist crease to tip | | | | Crotch height | | | |
|---|---|---|---|---|---|---|---|---|---|---|---|---|
| | *mean* | *s.d.* | *5%<* | *95%<* | *mean* | *s.d.* | *5%<* | *95%<* | *mean* | *s.d.* | *5%<* | *95%<* |
| Thumb (I) | 5.87 | 0.45 | 5.07 | 6.57 | 12.70 | 1.13 | 11.05 | 14.68 | | | | |
| Crotch I | | | | | | | | | 6.81 | 0.60 | 5.85 | 7.78 |
| Index (II) | 7.53 | 0.46 | 6.83 | 8.19 | 18.52 | 0.88 | 17.33 | 20.06 | | | | |
| Crotch II | | | | | | | | | 11.05 | 0.60 | 10.17 | 12.08 |
| Middle (III) | 8.57 | 0.51 | 7.82 | 9.47 | 19.52 | 0.92 | 18.10 | 21.04 | | | | |
| Crotch III | | | | | | | | | 10.87 | 0.58 | 10.09 | 11.86 |
| Ring (IV) | 8.05 | 0.47 | 7.44 | 8.93 | 18.72 | 0.91 | 17.52 | 20.28 | | | | |
| Crotch IV | | | | | | | | | 9.72 | 0.51 | 8.98 | 10.53 |
| Little (V) | 6.14 | 0.47 | 5.44 | 6.99 | 16.61 | 0.91 | 15.11 | 18.10 | | | | |

Table 23: Finger Lengths and Palm Dimensions of Female USAF Personnel (cm)

| | Finger length: crotch to tip | | | | Finger length: wrist crease to tip | | | | Crotch height | | | |
|---|---|---|---|---|---|---|---|---|---|---|---|---|
| | *mean* | *s.d.* | *5%<* | *95%<* | *mean* | *s.d.* | *5%<* | *95%<* | *mean* | *s.d.* | *5%<* | *95%<* |
| Thumb (I) | 5.37 | 0.44 | 4.68 | 6.12 | 11.05 | 1.00 | 9.51 | 12.83 | | | | |
| Crotch I | | | | | | | | | 5.72 | 0.56 | 4.85 | 6.69 |
| Index (II) | 6.90 | 0.52 | 6.10 | 7.80 | 16.67 | 0.89 | 15.21 | 18.14 | | | | |
| Crotch II | | | | | | | | | 9.86 | 0.60 | 8.87 | 10.85 |
| Middle (III) | 7.79 | 0.51 | 7.01 | 8.68 | 17.65 | 0.87 | 16.22 | 19.05 | | | | |
| Crotch III | | | | | | | | | 9.81 | 0.59 | 8.86 | 10.78 |
| Ring (IV) | 7.31 | 0.52 | 6.52 | 8.22 | 16.76 | 8.94 | 15.28 | 18.20 | | | | |
| Crotch IV | | | | | | | | | 8.72 | 0.60 | 7.67 | 9.67 |
| Little (V) | 5.46 | 0.44 | 4.80 | 6.24 | 14.64 | 0.92 | 13.11 | 16.12 | | | | |

Table 24: Dimensions of Knuckle Joints of USAF Male Flying Personnel (cm)

| | Breadth | | | | Depth | | | | Circumference | | | |
|---|---|---|---|---|---|---|---|---|---|---|---|---|
| *joint* | *mean* | *s.d.* | *5%<* | *95%<* | *mean* | *s.d.* | *5%<* | *95%<* | *mean* | *s.d.* | *5%<* | *95%<* |
| Thumb (I) DIP | 2.29 | 0.13 | 2.07 | 2.51 | 2.02 | 0.15 | 1.78 | 2.25 | 6.79 | 0.38 | 6.12 | 7.41 |
| Index (II) PIP | 2.15 | 0.13 | 1.96 | 2.37 | 1.94 | 0.12 | 1.75 | 2.16 | 6.43 | 0.36 | 5.84 | 7.10 |
| Index (II) DIP | 1.84 | 0.12 | 1.65 | 2.04 | 1.55 | 0.13 | 1.36 | 1.75 | 5.34 | 0.33 | 4.85 | 5.81 |
| Middle (III) PIP | 2.18 | 0.14 | 1.97 | 2.41 | 2.01 | 0.14 | 1.79 | 2.26 | 6.60 | 0.39 | 6.02 | 7.20 |
| Middle (III) DIP | 1.84 | 0.12 | 1.65 | 2.04 | 1.60 | 0.13 | 1.38 | 1.81 | 5.41 | 0.34 | 4.87 | 5.98 |
| Ring (IV) PIP | 2.02 | 0.13 | 1.80 | 2.23 | 1.89 | 0.13 | 1.67 | 2.12 | 6.14 | 0.37 | 5.54 | 6.79 |
| Ring (IV) DIP | 1.72 | 0.11 | 1.55 | 1.92 | 1.51 | 0.13 | 1.30 | 1.73 | 5.08 | 0.31 | 4.59 | 5.67 |
| Little (V) PIP | 1.77 | 0.14 | 1.55 | 2.01 | 1.67 | 0.12 | 1.47 | 1.89 | 5.40 | 0.36 | 4.88 | 6.00 |
| Little (V) DIP | 1.57 | 0.12 | 1.37 | 1.76 | 1.37 | 0.13 | 1.17 | 1.55 | 4.64 | 0.32 | 4.11 | 5.20 |

Table 25: Dimensions of Knuckle Joints of Female USAF Personnel (cm)

| | Breadth | | | | Depth | | | | Circumference | | | |
|---|---|---|---|---|---|---|---|---|---|---|---|---|
| *joint* | *mean* | *s.d.* | *5%<* | *95%<* | *mean* | *s.d.* | *5%<* | *95%<* | *mean* | *s.d.* | *5%<* | *95%<* |
| Thumb (I) DIP | 1.90 | 0.12 | 1.71 | 2.11 | 1.66 | 0.12 | 1.49 | 1.87 | 5.61 | 0.33 | 5.07 | 6.18 |
| Index (II) PIP | 1.82 | 0.10 | 1.65 | 2.00 | 1.62 | 0.10 | 1.45 | 1.79 | 5.40 | 0.29 | 4.96 | 5.88 |
| Index (II) DIP | 1.54 | 0.10 | 1.38 | 1.71 | 1.28 | 0.09 | 1.15 | 1.45 | 4.46 | 0.26 | 4.08 | 4.94 |
| Middle (III) PIP | 1.83 | 0.10 | 1.68 | 2.01 | 1.67 | 0.11 | 1.49 | 1.86 | 5.50 | 0.28 | 5.05 | 6.00 |
| Middle (III) DIP | 1.53 | 0.09 | 1.38 | 1.70 | 1.31 | 0.09 | 1.16 | 1.48 | 4.48 | 0.26 | 4.10 | 4.93 |
| Ring (IV) PIP | 1.69 | 0.10 | 1.51 | 1.85 | 1.57 | 0.11 | 1.39 | 1.76 | 5.12 | 0.27 | 4.69 | 5.59 |
| Ring (IV) DIP | 1.43 | 0.09 | 1.30 | 1.60 | 1.25 | 0.09 | 1.10 | 1.40 | 4.22 | 0.24 | 3.86 | 4.64 |
| Little (V) PIP | 1.46 | 0.09 | 1.32 | 1.64 | 1.39 | 0.09 | 1.27 | 1.56 | 4.48 | 0.25 | 4.13 | 4.94 |
| Little (V) DIP | 1.31 | 0.09 | 1.17 | 1.47 | 1.13 | 0.09 | 0.99 | 1.29 | 3.86 | 0.24 | 3.51 | 4.24 |

Table 26: Various Hand Dimensions of USAF Male Flying Personnel (cm)

| *joint* | *mean* | *s.d.* | *5%<* | *95%<* |
|---|---|---|---|---|
| Hand length | 19.72 | 0.93 | 18.32 | 21.15 |
| Hand breadth | 8.96 | 0.40 | 8.32 | 9.71 |
| Hand circumference | 21.59 | 0.90 | 20.02 | 23.08 |
| Hand thickness | 3.29 | 0.20 | 2.98 | 3.61 |
| Hand depth | 6.19 | 0.45 | 5.50 | 7.02 |
| Wrist breadth | 6.78 | 0.37 | 6.26 | 7.33 |
| Wrist circumference | page missing from report | | | |

Table 27: Various Hand Dimensions of Female USAF Personnel (cm)

| *joint* | *mean* | *s.d.* | *5%<* | *95%<* |
|---|---|---|---|---|
| Hand length | 17.93 | 0.86 | 16.53 | 19.29 |
| Hand breadth | 7.71 | 0.38 | 7.06 | 8.32 |
| Hand circumference | 18.71 | 0.83 | 17.45 | 20.15 |
| Hand thickness | 2.76 | 0.18 | 2.46 | 3.05 |
| Hand depth | 5.17 | 0.39 | 4.53 | 5.82 |
| Wrist breadth | 5.83 | 0.33 | 5.36 | 6.44 |
| Wrist circumference | 14.98 | 0.71 | 13.85 | 16.21 |

# Appendix C References


[1] O. Brimhall and R. Goodwin. Personal Communication. Technical Research Associates, Salt Lake City UT, 1994.

[2] B. Bucholtz and T. Armstrong. A Kinematic Model of the Human Hand to Evaluate its Prehensile Capabilities. *J. Biomechanics*, 25(2):149–162, 1992.

[3] B. Bucholtz, T. Armstrong, and T. Goldstein. Anthropometric Data for Describing the Kinematics of the Human Hand. *Ergonomics*, 35:261–273, 1992.

[4] B. Bucholtz and T. J. Armstrong. An Ellipsoidal Representation of Human Hand Anthropometry. *Human Factors*, 33(4):429–441, 1991.

[5] J. F. Dubousset. The Digital Joints. In R. Tubiana, editor, *The Hand*, chapter 16. W. B. Saunders, 1981.

[6] J. W. Garrett. Anthropometry of the Hands of Female Air Force Flight Personnel. Technical Report AMRL-TR-69-26, USAF Aerospace Medical Research Laboratory, Wright-Patterson AFB OH, 1970.

[7] J. W. Garrett. Anthropometry of the Hands of Male Air Force Flight Personnel. Technical Report AMRL-TR-69-42, USAF Aerospace Medical Research Laboratory, Wright-Patterson AFB OH, 1970.

[8] H. T. E. Hertzberg, G. S. Daniels, and E. Churchill. Anthropometry of Flying Personnel. WADC Technical Report 52-321, DTIC AD 047953, USAF Wright Air Development Center, Wright-Patterson AFB OH, 1953.

[9] A. Hollister, W. L. Buford, L. M. Myers, D. J. Giurintano, and A. Novick. The Axes of Rotation of the Thumb Carpometacarpal Joint. *J. of Orthopaedic Research*, 10:454–460, 1992.

[10] A. M. Hollister and D. J. Giurintano. How Joints Move. In P. W. Brand and A. M. Hollister, editors, *Clinical Mechanics of the Hand*, chapter 4. Mosby, St Louis, 1993.

[11] S. C. Jacobsen, E. K. Iversen, D. F. Knutti, R. T. Johnson, and K. B. Biggers. Design of a Multiple Degree-of-Freedom, Force-Reflective Hand Master/Slave with a High-Mobility Wrist. In *Proc. of 3rd Topical Meeting on Robotics and Remote Systems*, 1989.

# APPENDIX D: UNIT CONVERSIONS

Table 28: Unit Conversions for Frequently Cited Units

| | | | | |
|---|---|---|---|---|
| 1 | lb | = | 4.45 | N |
| 1 | in-lb | = | 11.30 | N-cm |
| 1 | oz-in | = | 0.706 | N-cm |
| 1 | lb/in | = | 1.75 | N/cm |
| 1 | g/mm | = | 0.0981 | N/cm |
| 1 | Kgf | = | 9.81 | N |

# APPENDIX E: PHOTOGRAPHS


Figure 5: VPL Dataglove

This page intentionally left blank.

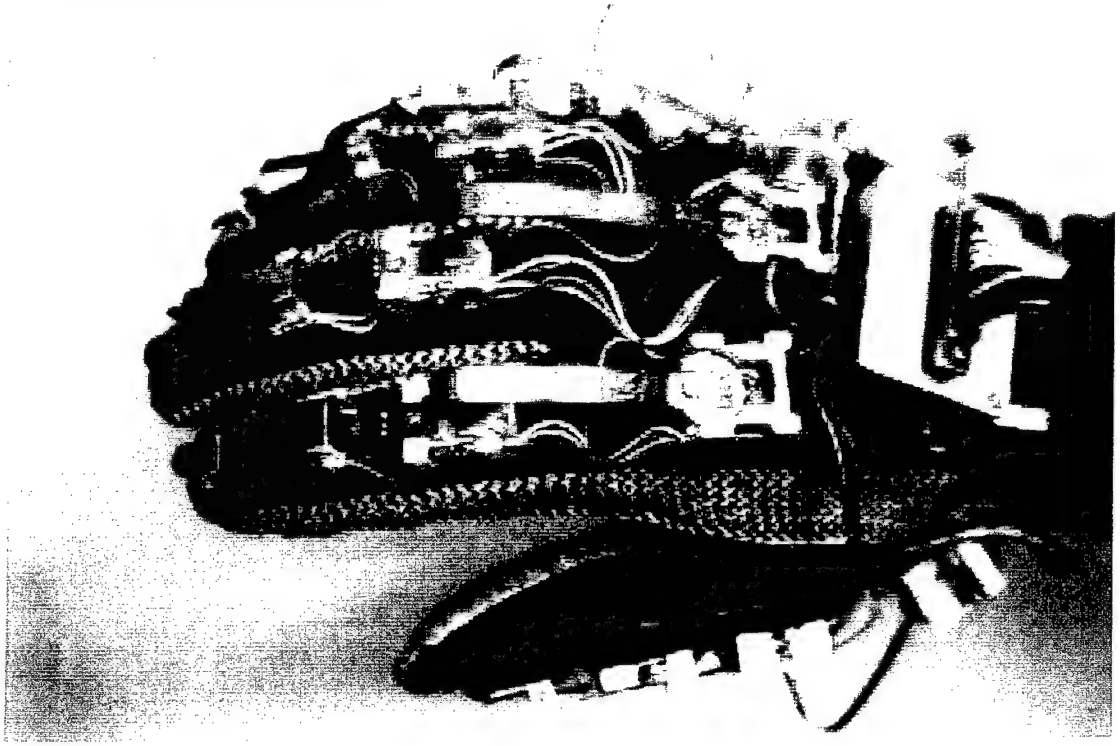

Figure 6: PERCRO Position-Sensing and Tactile Feedback Hand Master (Bergamasco et al.)

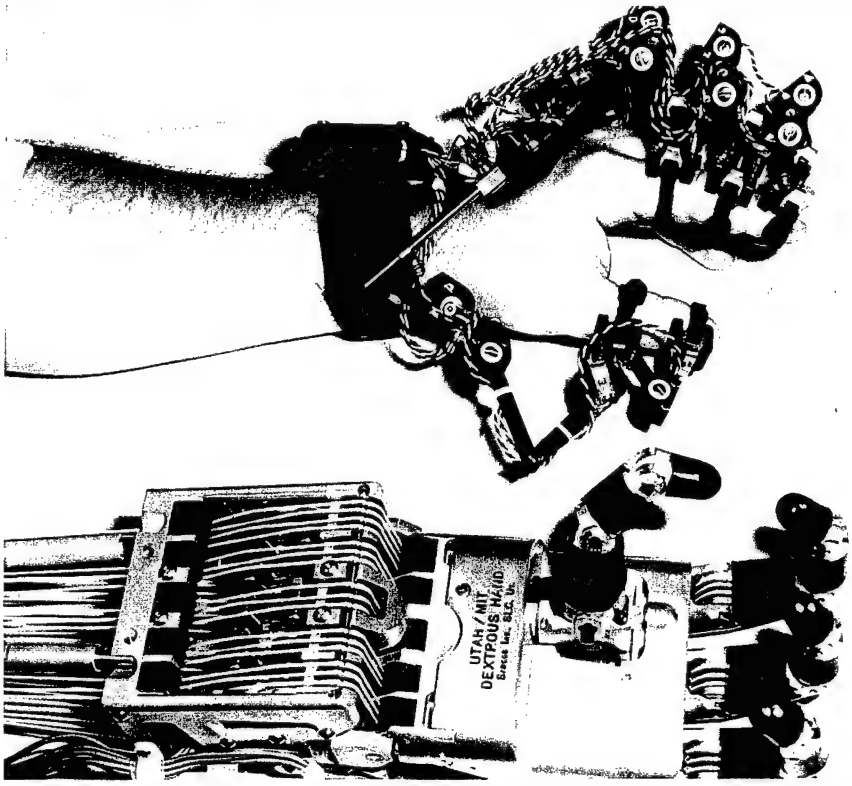


Figure 7: A. D. Little/EXOS Hand Master with Utah-MIT Dexterous Hand

This page intentionally left blank.

Figure 8: PERCRO Force-Reflecting Hand Master by Bergamasco et al. (Side View)

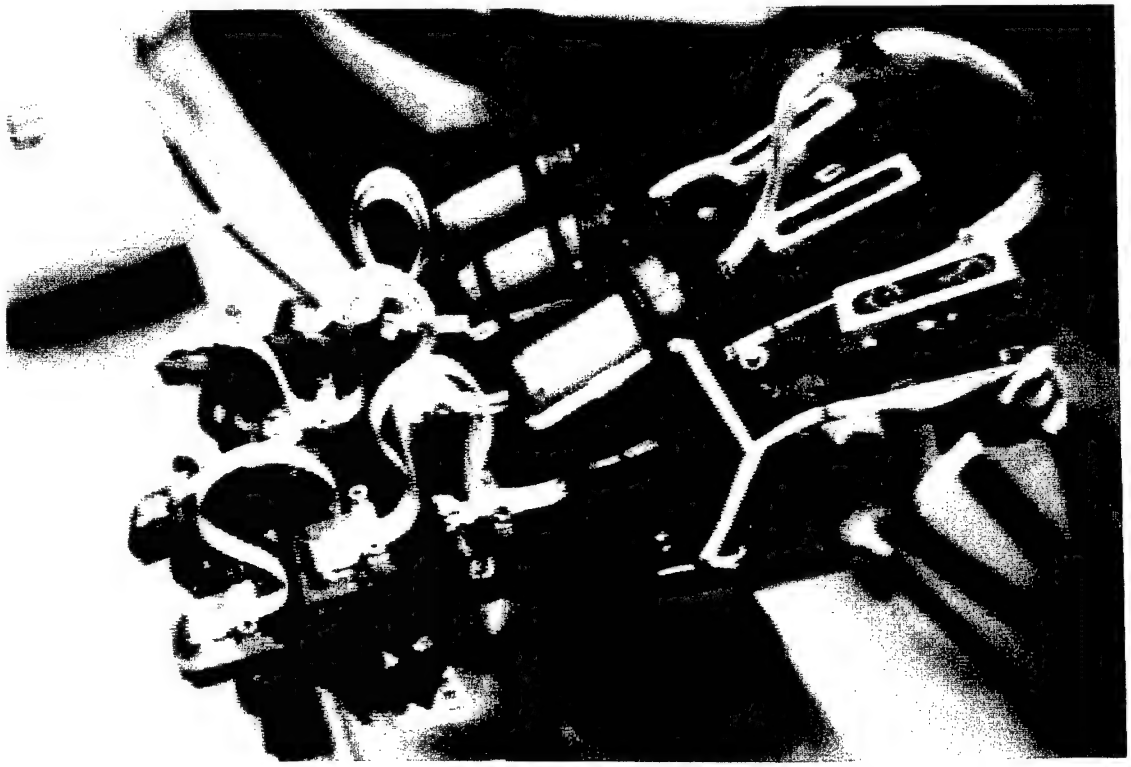

Figure 9: PERCRO Force-Reflecting Hand Master by Bergamasco et al. (Top View)

This page intentionally left blank.

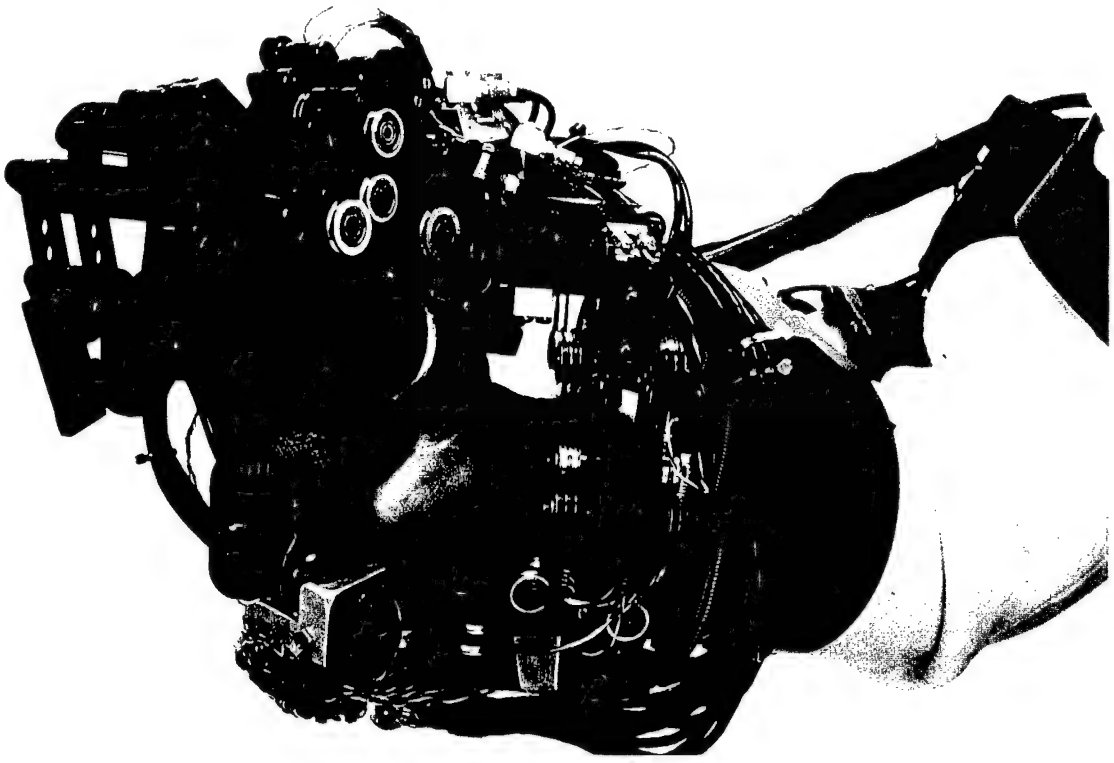

Figure 10: Sarcos TOPS Force-Reflecting Hand Master

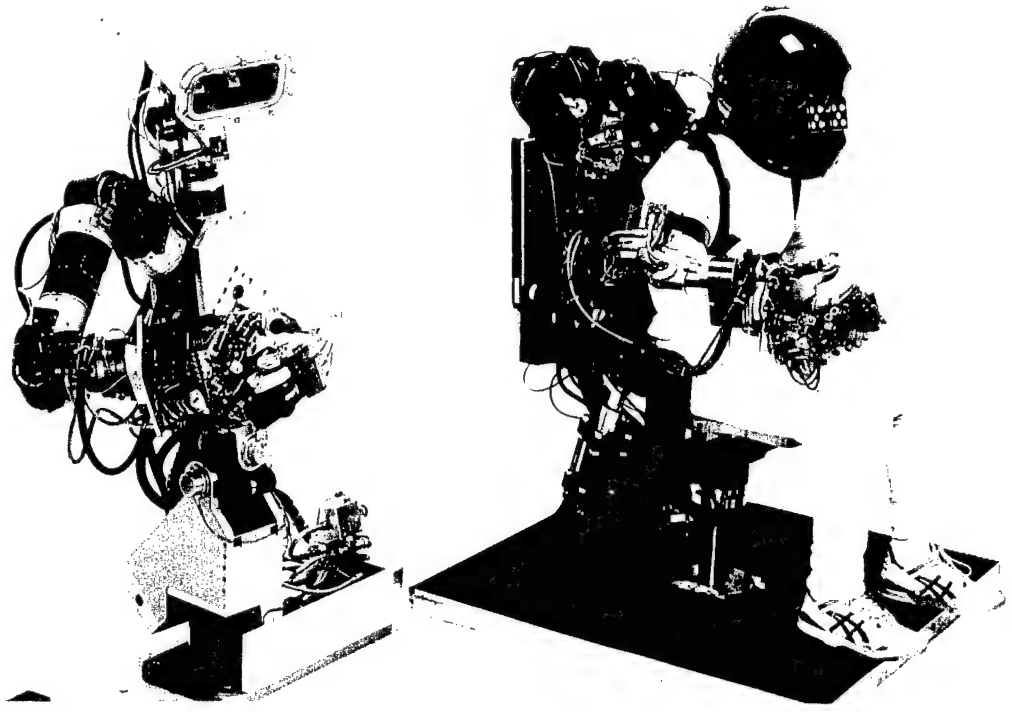

Figure 11: Sarcos TOPS Force-Reflecting Master and Slave System

This page intentionally left blank.


Figure 12: Sarcos Dexterous Arm Master (Hand Detail)


Figure 13: Sarcos Dexterous Arm Master

This page intentionally left blank.

Figure 14: Force-Reflecting Hand Master Built by Oomichi et al.

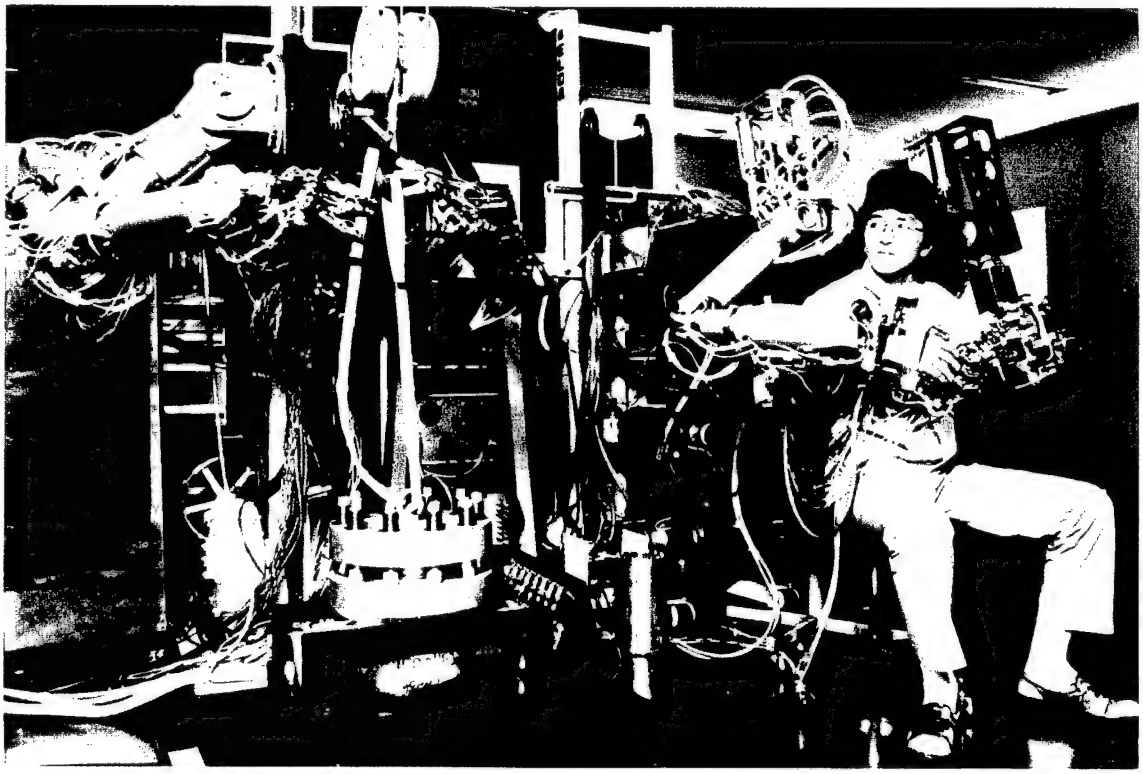

Figure 15: Force-Reflecting Master and Slave System by Oomichi et al.

This page intentionally left blank.

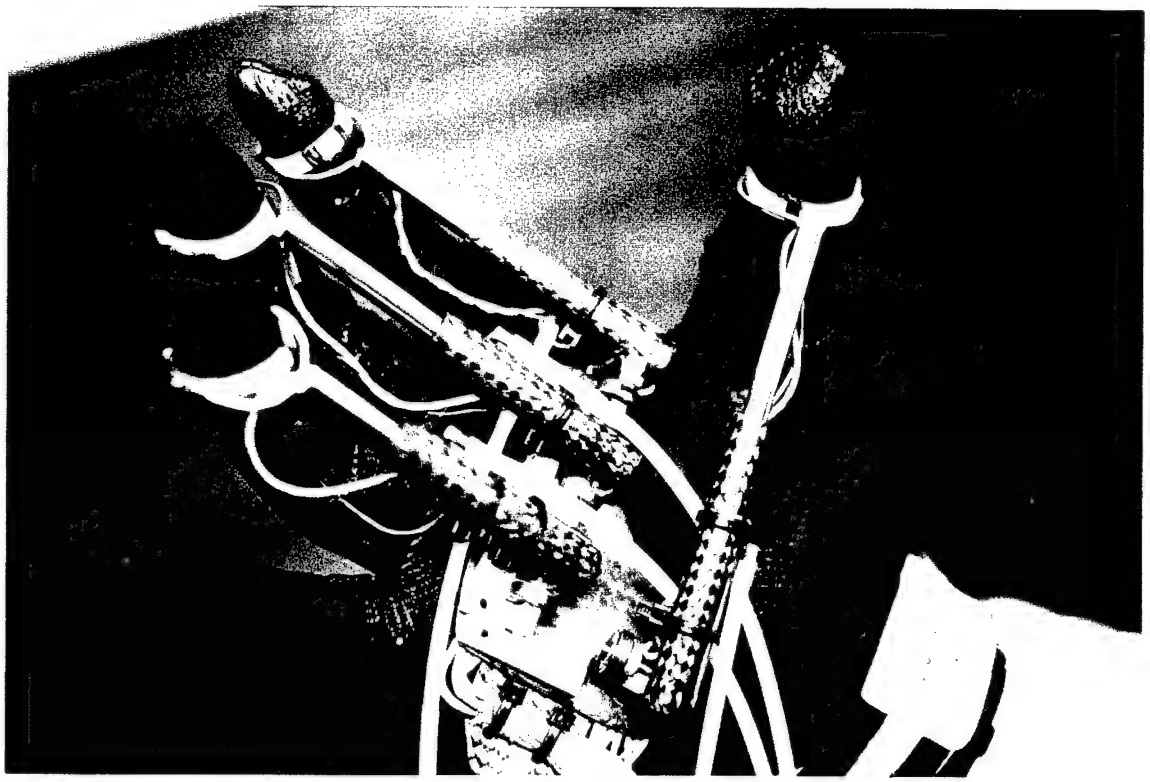

Figure 16: Burdea's Rutgers Master II with Pneumatic Cylinders in Palm

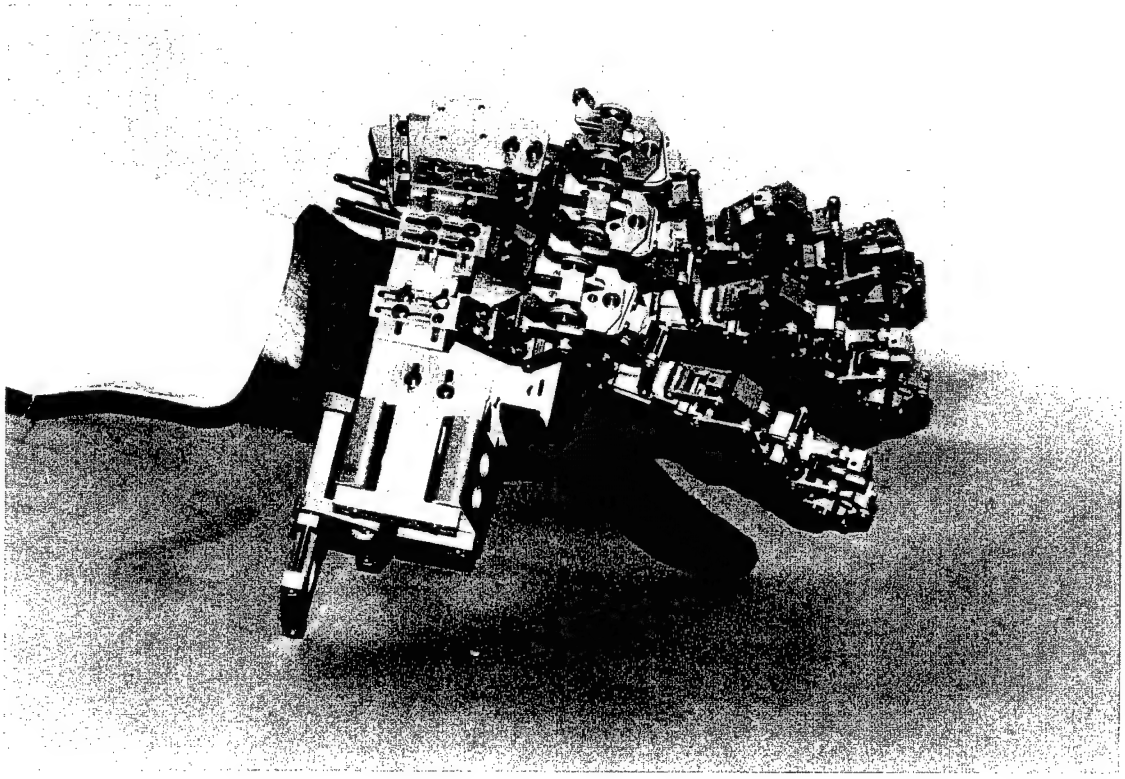

Figure 17: Jau's Force-Reflecting Hand Master; Part of a Hand and Arm Master-Slave System

This page intentionally left blank.

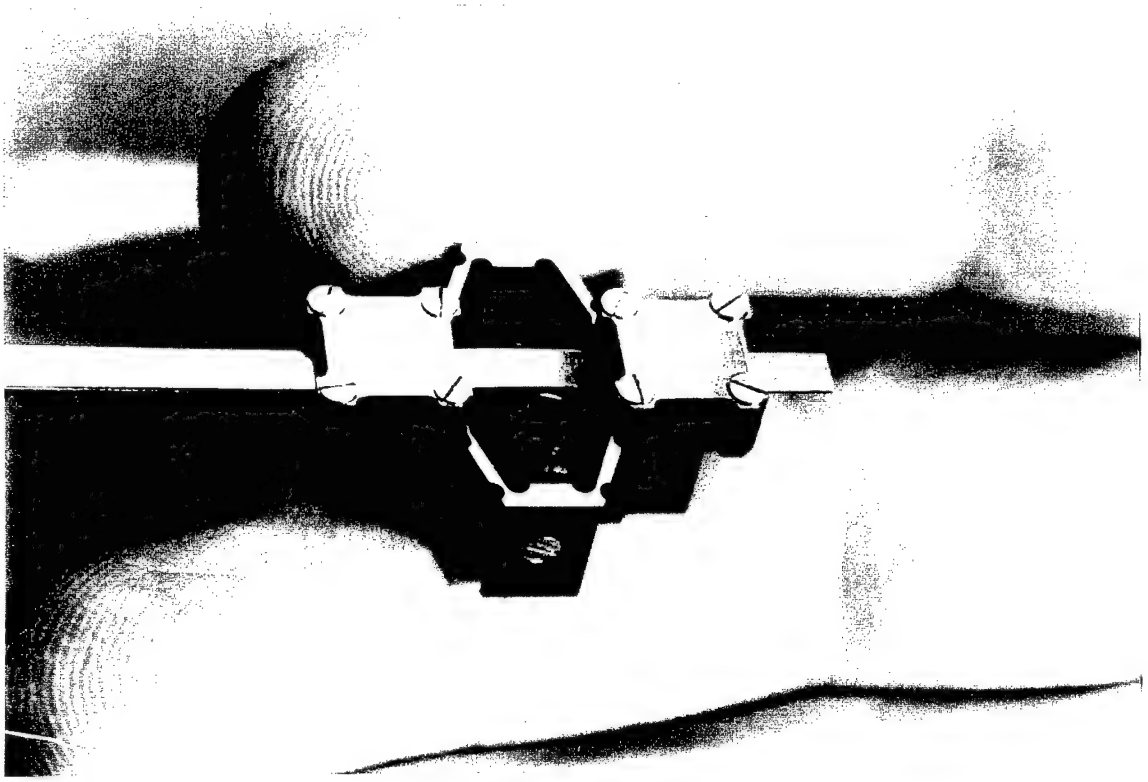

Figure 18: Magnetostrictive Linear Exoskeleton Motor (Technical Research Associates)

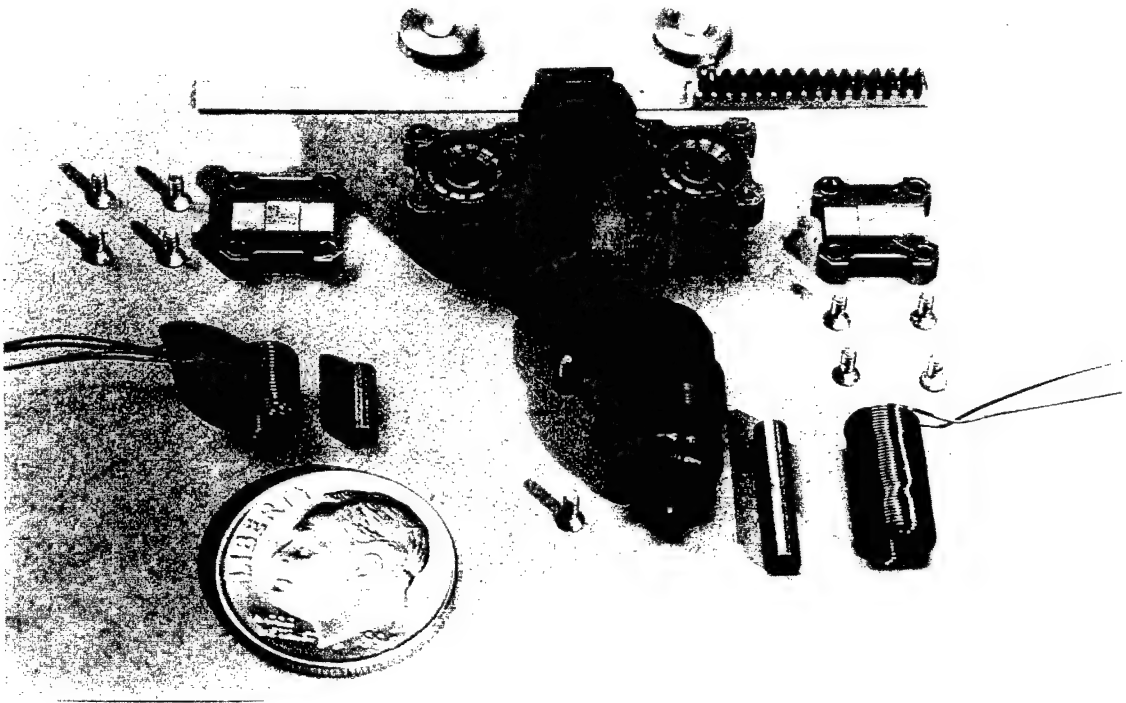

Figure 19: Breakout View of TRA Motor, with Terfenol-D Cylinders Visible

This page intentionally left blank.

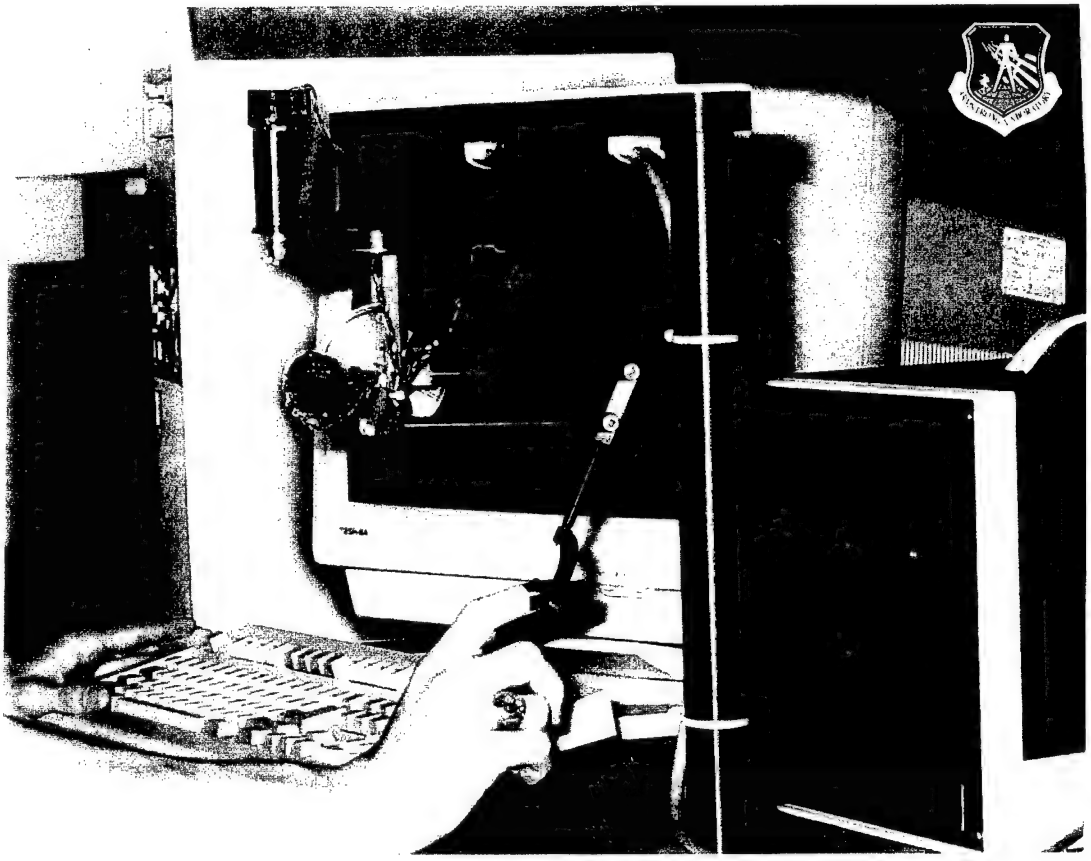

Figure 20: The PHANToM™ Force-Reflecting Haptic Interface (SensAble Devices)

This page intentionally left blank.

# APPENDIX F: HAND MASTER DATA SHEETS

This page intentionally left blank.

# Force-Reflecting Hand Master Data Sheet: Begej

**Description:** Three dof per finger (spherical MP, and PIP). System is intended to have two fingers and a thumb.

**Actuator/Transmission:** DC motor w/worm gear and semicircular virtual joint. Motor for most or all joints is MicroMo 1319, with variable gearheads. PIP joint gearhead is 6.3:1, MP joint gearhead is 22:1, different ratio for abduction/adduction of MP joint. Worm gear in series with gearheads, ratio 36:1. Additional ratio in series due to action of worm gear on semicircular virtual joint with a given radius (possibly 52 mm for MP joint).

**Sensing:** absolute, single turn Begej analog "optical encoder" for position. Martech MTRS-9080 optical force sensor measures cantilever displacement.

**Specifications:** 20 N force at tip of finger. 62 deg angular motion range, 1 deg play in hinge (lateral?).

**Limitations:** Exo joints don't fit all human joints – especially the thumb. Currently developing thumb design that will splint PIP joint and use DIP joint and spherical base joint. With large gear ratios, joints are not backdriveable (especially MP joint).

**Comments:** Begej progressed through three different joint designs.

**Status of Effort:** As of 24 Mar 94, 24-month Phase II SBIR effort has been extended, in part due to difficulties with thumb design, and other workload at company.

**Contact(s):** Stefan Begej
Begej Corporation
5 Claret Ash Rd
Littleton CO 80127-3536
(303) 932-2186

Larry Li (tech monitor)
NASA Johnson Space Center
Automation Robotics Division
Mail Code EC5
Houston TX 77058
(713) 483-9160
Email: li@ctsd2.jsc.nasa.gov

## References

[1] Begej S. Glove Controller With Force and Tactile Feedback For Dexterous Robotic Hands. NASA Phase I SBIR NAS9-18308, Begej Corp., 5 Claret Ash Rd., Littleton, CO 80127, September 1990.

This page intentionally left blank.

## Force-Reflecting Hand Master Data Sheet: Bergamasco

**Description:** Reflects flexion/extension forces to 3 dof in the first three fingers (little finger excluded) and the thumb. No force reflection to abduction/adduction motions.

**Actuator/Transmission:** DC servo motors, mounted on the back of the hand, transmit forces through a tension tendon transmission system.

**Sensing:** All dofs (including abduction/adduction) have rotation sensors.

**Specifications:**

| | |
|---|---|
| **Angular ranges** | |
| abduction/adduction: | $-15° \leq \theta_a \leq 15°$ |
| proximal flexion/extension: | $0° \leq \theta_f \leq 90°$ |
| medial flexion/extension: | $0° \leq \theta_f \leq 90°$ |
| distal flexion/extension: | $0° \leq \theta_f \leq 80°$ |
| **Force Ranges (Normal to Phalanx)** | |
| interaction force on proximal phalanx: | $0 \leq F_p \leq 1$N |
| interaction force on medial phalanx: | $0 \leq F_p \leq 1$N |
| interaction force on distal phalanx: | $0 \leq F_p \leq 1$N |
| **Resolution** | |
| angular position resolution (all dof's): | $R_\theta = 0.1°$ |
| interaction force resolution (all dof's): | $R_F = 0.05$N |

**Hand Attachments, Human Factors Design:** "The exoskeletons are supported by a metacarpal plate connected to a forearm exoskeleton integrating two sensorized and actuated joints at the wrist level." Forces are applied at the center of each phalanx.

**Limitations:** Device appears to be quite bulky.

**Status of Effort:** Active. As of July 1995, Dr. Bergamasco's World Wide Web page states that the device is being assembled.

**Contact(s):** Massimo Bergamasco
Scuola Superiore S. Anna
Via Carducci, 40, 56127 Pisa, Italy
PHN: +39-50-883287
FAX: +39-50-883215
E-mail: bergamasco@sssup1.sssup.it
WWW page: http://roy.sssup.it/

## References

[1] M. Bergamasco. Haptic Interfaces: the Study of Force and Tactile Feedback Systems. In *Proc. of the Fourth IEEE Int. Workshop on Robot and Human Communication*, pages 15–20, Waseda University, Tokyo, July 1995.

This page intentionally left blank.

# Force-Reflecting Hand Master Data Sheet: Cybernet

**Description:** The Cybernet PER-Force Finger Forcer mounts on the 6 dof Cybernet PER-Force Hand Controller in place of the joystick terminus that comes as standard equipment with the hand controller. It has 11 dof for position sensing (two for each of four fingers and three for the thumb) and 5 dof force reflection (one for each finger and the thumb).

**Actuator/Transmission:** Five DC brushless servo motors actuate the device. An early gearbox transmission design was discarded due to lack of backdrivability, and larger motors now drive the hand master through synchronous (toothed) belt transmissions.

**Sensing:** HP optical encoders on the motors, combined with conductive plastic linear potentiometers on sliders and cermet rotational potentiometers, are used to calculate fingertip location. The system has no force sensors; force commands are executed open-loop.

**Specifications:** See attached sheet from Cybernet. Only a crude prototype has been built; specifications are estimates.

**Hand Attachments, Human Factors Design:** The user's hand rests in a U-shaped stirrup that embraces the palm and back of the hand. The thumb is at the open end of the "U." The user inserts his or her fingertips into thimbles.

**Limitations:** With only fingertip interfaces, the device cannot simulate contact forces at more proximal phalanges. The addition of tactile feedback to the inner sides of the fingers might give the location-of-contact cues that Jau has found important in manipulation.

**Comments:** This is a unique design, and it will be interesting to see how well it works.

**Status of Effort:** This active Phase II SBIR contract had been underway for about 14 months in July 1995. The completion date for this 24-month contract may slide.

**Contact(s):**

Heidi Jacobus
Cybernet Systems Corp.
1919 Green Rd. Ste. B-101
Ann Arbor MI 48105
PHN: 313-668-2567
FAX: 313-668-8780
Email: heidi@cybernet.com

CYBERNET Systems Corporation
1919 Green Road, Suite B-101
Ann Arbor, Michigan 48105
(313) 668-2567
*FAX: (313)668-8780*

# PER-Force™ Finger Forcer Option

*Adds Direct Force Feedback and Finger Motion Monitoring to PER-Force - You Can "feel' Objects*

Simulating a "sense of touch" by "force-reflection" at your finger tips integrating 5 axis force reflection and 11 axis position sensing of the fingers.

The PER-Finger Forcer option is attached on top of Cybernet's proven 6 degree-of-freedom handcontroller unit. This attachment provides tactile force feedback for

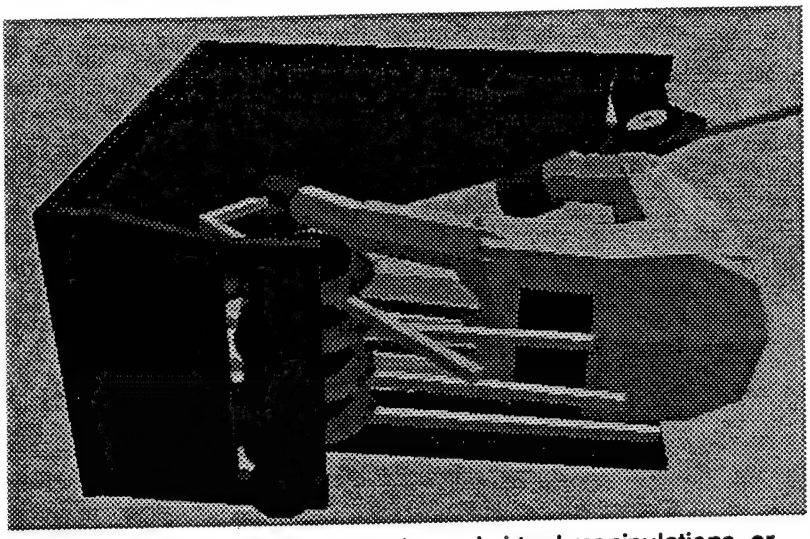

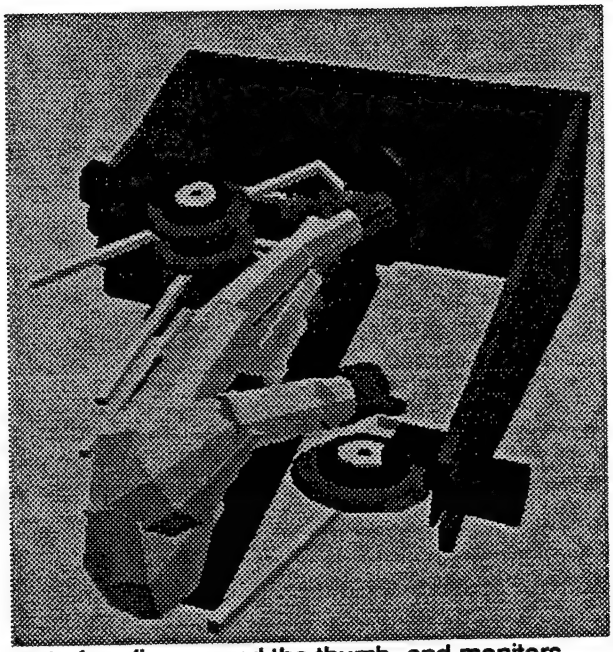

up to four fingers and the thumb, and monitors finger/thumb motion in 11 degrees of freedom (two for each finger and three for the thumb). Actuation in performed through five miniature brushless DC servo mechanisms to minimize weight and maximize forces generated.

The user's hand is grasped around the palm, leaving each finger and the thumb free to be inserted into small stirrups at the ends of the actuation arm mechanisms. This hand-insertion method allows the user to quickly and easily insert his/her hand or remove it.

An operator can use these motorized finger interfaces to precisely position dexterous robot hands, train/replay/record virtual manipulations, or manipulate graphically displayed virtual objects .

This new device is especially well suited for teleoperation in environments where direct viewing or manipulation is limited. Examples include murky underwater environments with reduced light and obstructions such as underground excavation applications.

Similarly, visualization and control of multiple dimensions on a 2 dimensional CRT screen is difficult. Remote teleoperation or computer generated haptic (touch) input/output is required to manipulate a robot when it is unsafe, impossible, or impractical for humans to touch a worksite directly. Force-reflection provides intuitive feedback to an operator for these tasks.

### PER-Force Features and Benefits

- The PER-Force, with Finger Forcer option, is the only 6 axis force-reflecting joystick commercially available with an integral finger force-reflective tactile interface as well. This design originated from our proven 6 axis product and, is compact enough to easily accommodates restricted envelope applications.
- Cost-effective device due to construction from readily available production components using a simplified design.
- Provides a general purpose computer controller interface. This allows you to control dissimilar slave robots and dexterous manipulators, or to construct "virtual" force feel interfaces through Cybernet supplied control software libraries.
- Provides a complete MS-DOS/Unix C development environment for easy control system modification, reconfiguration, and interfacing.

## Specifications

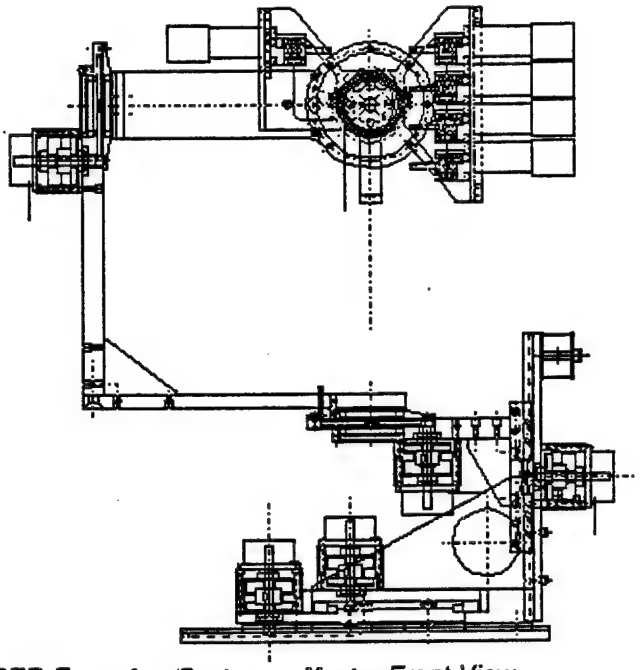

*PER-Force **Arm/Dexterous Master** Front View*

The PER-Force Finger Forcer option is driven by a serial port from any MS-DOS, VME, Unix, or Macintosh type computer system. The device can be flexibly programmed to control either slave robots or graphical display systems. It provides position, rate, or force feedback to the operator.

| **Control Modes** | **User Selected** |
|---|---|
| Force-Position | Scaling |
| Position-Position | Position Lock |
| Rate-Position | Orientation Lock |
| User Programmed | Axis Lock |

**Dimensions** TBD

**Power Supply/Computer Unit**
3" H x 7" W x 6"D (Table Top Mount)

**Weight**

| | |
|---|---|
| Joystick | TBD |
| Power/Computer Unit | 2 1/4 lbs. |

**Power Requirements**
120 VAC/60 Hz @ 3.8 amps (estimated)

**Interconnect Options**
RS-232/422
Ethernet (Optional)
Parallel I/O
Analog-Digital/Digital-Analog
Custom

**Position Resolution**
11 Revolute Axes TBD

**Range of Travel**
Full Fnger Motion Range

**Force Feedback Sensitivity (per axis)**

| | |
|---|---|
| Maximum Force Output | 2 lbs. (peak) |
| Long Duration Force Output | 0.3 lbs. |
| Minimum Force Output | <1 oz. |

**Motors**
5 Brushless DC Type

**Motor Controller Software**
C Library
- Parameter Setting
- Calibration
- Servo Control
- Position-Force Based Constraint Servos
- Virtual Forcing "Feels"
- Source code/libraries available

MS-DOS/OS-9/VxWorks/MacOS/Unix Compatible

**Computer Features**
Standard Interfaces
- PC-Compatible
- RS-232/422 Ports
- Parallel Port
- Ethernet (Optional)



We will build custom units to your specifications. Available for mounting on devices other than the PER-Force Handcontroller. Contact us for prices and delivery times.

CYBERNET Systems Corporation

1919 Green Road, Suite B-101
Ann Arbor, MI 48105-2554
Telephone: (313)668-2567 Fax:(313)668-8780
e-mail: heidi@cybernet.com
APPLELINK:H.Jacobus

This page intentionally left blank.

# Force-Reflecting Hand Master Data Sheet: Dartmouth Exoskeleton

**Description:** A thumb and forefinger exoskeleton designed for the hands of paralyzed patients. The thumb has three actuated degrees of freedom; one for flexion/extension of the last two joints together (MCP, IP), one for flexion/extension of the CMC joint, and one for abduction/adduction. The forefinger has two degrees of freedom: one for flexion/extension of the MCP joint, and another for flexion/extension of the PIP and DIP joints together.

**Actuator/Transmission:** DC electric motors actuate cable tendons on the palmar aspect of the fingers to produce flexion, while return springs on the dorsal aspect of the fingers generate flexion forces.

**Sensing:** Potentiometers manufactured by Clarostat are attached over each phalanx using four-bar linkages. Angle measurements and errors in the paper referenced below are given in volts, without mention of the potentiometer range of motion or driving voltage.

**Specifications:** None given.

**Hand Attachments, Human Factors Design:** The finger attachment has some similarities to the EXOS Dexterous Hand Master, with spring-loaded aluminum V-blocks. These V-blocks are attached to a Lycra glove, with leather sewn into certain areas for reinforcement and stability.

**Limitations:** Cannot produce finger abduction/adduction forces. No force sensing capability has been reported.

**Comments:** The single reference describing this work lacks information on joint and fingertip forces produced.

**Status of Effort:** Funding not continued; the project was shelved after completion of the first prototype.

**Contact(s):** Sunil K. Singh
Thayer School of Engineering
Dartmouth College
Hanover NH 03755-8000

sunil@northstar.dartmouth.edu

## References

[1] P. Brown, D. Jones, S. K. Singh, and J. M. Rosen. The Exoskeleton Glove for Control of Paralyzed Hands. In *IEEE Conf. on Robotics & Automation*, pages 642–647, Atlanta, GA, 1993.

This page intentionally left blank.

# Force-Reflecting Hand Master Data Sheet: EXOS

**Description:** The Sensing and Force Reflecting Exoskeleton (SAFiRE) applies forces to the thumb, index finger, and wrist. The Phase II SAFiRE device has eight active degrees of freedom: three on the thumb, three on the index finger, and two on the wrist. After investigation to determine a suitable mechanical system, linkages grounded to the forearm that apply 3D Cartesian forces to the fingertip were chosen. The endpoints of the exoskeleton digits for the thumb and index finger are attached at the fingertips, and include passive freedoms that are intended to allow for comfortable finger motion.

The basic electronics and control hardware consist of two DSP processors connected to an SGI graphics workstation. One DSP handles dynamics simulation software and communications while the kinematics software resides on the other DSP. The VR display graphics and user interface module is implemented with the Sense8 package on the SGI and communicates with the DSPs via parallel I/O on a SCSI bus. The dynamics simulation environment contains a number of objects that can be manipulated with the SAFiRE. The kinematics code contains kinematic models of the SAFiRE device and the human hand and is responsible for transforming joint angles and position information into Cartesian space for the dynamics and graphics modules, as well as converting Cartesian forces to motor torques.

**Actuator/Transmission:** The SAFiRE device is actuated by DC motors, which are remotized and connected to the device joints with a cable and gear transmission.

**Sensing:** Incremental optical encoders attached to motors for measuring motor position. An Ascension Bird™ is attached to the forearm to sense forearm position and orientation.

**Specifications:** Total weight – <1.8 kg (<4 lbs)
Mechanical stiffness – 245 N/cm (140 lb/in) typically
Max. torque – 51 N-cm (72 oz-in) typically
Friction – <0.35 N-cm (<0.5 oz-in) for all joints
Max. force at tip – 4.4 N (1 lb) at fingertips and 8.9 N (2 lb) at palm

**Hand Attachments, Human Factors Design:** Actuator packages are grounded to the forearm; tips of the manipulator are attached to the fingertips and to the palm via a cuff.

**Limitations:** Maximum force reflection capability still allowed human finger to drive through virtual obstacle. The weight of the device causes fatique.

**Results of personal trial of early prototype:** Significant position-dependent friction in the sheathed cable transmission, chatter upon contact with a virtual surface, and hand attachment. The joints were simple hinges, and the device did not follow finger movements well. EXOS indicates that these problems are not an issue in the final device delivered to NASA Marshall.

**Comments:** EXOS reports that when the forearm is fixed in position, virtual walls feel reasonably stiff when tapped with fingertips. Impact forces arising from collisions with objects are reportedly crisp and distinct.

**Results of personal trial:** The maximum force was great enough that it easily gave the illusion of a hard surface; the user has to make a conscious effort to push past it.

**Status of Effort:** Phase II SBIR completed and delivered to NASA Marshall.

**Contact(s):** Beth Marcus
EXOS, Inc.
2A Gill St.
Woburn MA 01801
PHN: 617-933-0022
FAX: 617-933-0303
Email:
bam@media-lab.media.mit.edu

Joseph P. Hale *(technical monitor)*
NASA Marshall Space Flight Center
EO 23
MSFC AL 35812
PHN: 205-544-2193
FAX: 205-544-5551
Email: joe.hale@msfc.nasa.gov

## References

[1] S. Chang, H. Tan, B. Eberman, and B. Marcus. Sensing, Perception, and Feedback for VR. In *VR Systems '93*, New York NY, October 1993. SIG-Advanced Applications.

[2] EXOS, Inc. Development of a Force Feedback Anthropomorphic Teleoperation Input Device for Control of Robot Hands. NASA Phase I SBIR NAS8-38910, EXOS Inc., 8 Blanchard Rd., Burlington, MA 01803, August 1991.

[3] B. A. Marcus, B. An, and B. Eberman. EXOS Research on Master Controllers for Robotic Devices. In *Fifth Annual Workshop on Space Operations Applications and Research (SOAR '91)*, pages 238–245. NASA, USAF, July 1991.

[4] B. A. Marcus, B. An, and B. Eberman. Making VR Feel Real. In *Virtual Worlds Conf. Proc.* SRI International, June 1991.

# Force-Reflecting Hand Master Data Sheet: Iwata

**Description:** A desktop force-reflecting hand interface for virtual reality. The index finger and thumb each have one force-reflecting degree of freedom, and the remaining three fingers are joined together for a third flexion/extension degree of freedom (Iwata has published a good photograph of this device [1]). The user's palm rests in a bracket that is actuated by a six dof parallel stage.

**Actuator/Transmission:** Electric motors

**Sensing:** The reference includes no information on force or position sensing.

**Specifications:** Max torque at each joint is given as 3 Kg*cm [sic] He probably meant 3 Kgf where 1Kgf = 9.81N, so 3 Kgf*cm = 29.43 N*cm (41.68 oz*in)

**Limitations:** Limited to pinch-type grasps because of the single dof plates for the fingers.

**Comments:** Designed as computer input device, not necessarily for telerobotic control.

**Status of Effort:** This effort is believed to be inactive.

**Contact(s):**

Hiroo Iwata
Institute of Engineering Mechanics
University of Tsukuba
Tsukuba, Ibaraki, 305 Japan

## References

[1] H. Iwata. Artificial Reality with Force-feedback: Development of Desktop Virtual Space with Compact Master Manipulator. *Computer Graphics*, 24(4):165–170, August 1990. (ACM SIGGRAPH '90 Proceedings).

This page intentionally left blank.

# Force-Reflecting Hand Master Data Sheet: Jau/JPL

**Description:** 16-dof hand master exoskeleton, part of an overall master-slave arm and hand system with 23-dof each on the master and slave arms, as well as seven extra compliance-control dofs on slave arm and fingers that greatly improve grasping capability. The master and slave are kinematically identical. The hand has three fingers and an anthropomorphic thumb mounted at the side of the palm.

**Actuator/Transmission:** All actuators are backdrivable dc servomotor. Actuators for the hand master are mounted on the forearm, near the elbow. Transmission between the actuator package and hand master is by flex cable. Some sort of variable gearing exists on some finger dofs. Four-bar mechanisms and pulleys backdrive the human finger joints. The driven pulleys are located above the finger joints and four-bar mechanisms link the pulleys with finger linkages. (Finger rotates at same rate as pulley.)

**Sensing:** Strain-gauge force sensors are embedded at every joint of the master glove, and potentiometers placed in each of the drive packages sense position (16 force and 16 position sensors).

**Specifications:** 0.83 N (3 oz) force-reflection threshold. Can lift 30 lbs (in which grasp?)

**Hand Attachments, Human Factors Design:** An off-the-shelf glove secures the hand master to the operator's hand. Metal parts of the hand master are woven to the glove. The hand master is adjustable for size. A base plate on the back of the hand transmits force to the operator to reflect the wrist dofs. The control glove weighs 1.1 kg (2.43 lbs), including an attachment bracket for attaching the glove to the wrist. The actual mass on the back of the hand and fingers is 0.9 kg (2.0 lbs).

**Comments:** Fiber optic cables carry communications between system components.

**Questions:** Specs of 5 lb/7.5 lb at fingertip/thumbtip are for slave; what about master?
Which finger dofs have variable gearing? Master or slave?
Is 0.83 N force-reflection threshold at fingertip?

**Status of Effort:** Master hand has been completed, as well as master arm and slave hand. As of 29 Apr 92, slave arm was being finished. Latest paper will be presented at IEEE conference in Nice, France. As of May 1995, this project has been suspended due to lack of funding at NASA. Suspension occurred just after the system became operational, before many operational tests could be performed.

**Contact(s):**

Dr. Bruno Jau
Bldg 23
Jet Propulsion Laboratory
4800 Oak Grove Dr
Pasadena CA 91109
(818) 354-1875

Dr. Tony Becjzy
Bldg 23
Jet Propulsion Laboratory
4800 Oak Grove Dr
Pasadena CA 91109
(818) 354-4568

Dr. Becjzy is the head of the effort. Dr. Jau is the project leader.

## References


[1] B. M. Jau. Anthropomorphic Four Fingered Robot Hand and Its Glove. In *Int. Conf. of the IEEE Engineering in Medicine and Biology Soc.*, pages 1940–1941, 1990.

[2] B. M. Jau. A Mobile, Dexterous Dual-Arm Telemanipulation System for Hazardous Environments. In *ANS 4th Topical Meeting on Robotics and Remote Sys.* American Nuclear Society, February 1991. Albuquerque, NM.

[3] B. M. Jau. Man-Equivalent Telepresence Through Four Fingered Human-Like Hand System. In *Proc. of the IEEE Int. Conf. on Robotics and Automation*, pages 843–848, May 1992.

[4] B. M. Jau, M. A. Lewis, and A. K. Bejczy. Anthropomorphic Telemanipulation System in Terminus Control Mode. In *Proc. of RoManSy '94: The Tenth CISM-IFToMM Symp. on Theory and Practice of Robots and Manipulators*, 1994.

## Force-Reflecting Hand Master Data Sheet: LRP Hand Master

**Description:** This hand master is being developed at the Laboratoire de Robotique de Paris (LRP). The exoskeletal structure affixes to the dorsal aspect of the fingers. According to Burdea et al., the LRP Hand Master attaches to all five fingers, providing force reflection to three flexion dofs on each finger and two flexion dofs on the thumb, for a total of 14 dofs.

**Actuator/Transmission:** DC "disc" motors with a torque capability of 1.07 N-m (continuous) and 11.48 N-m (peak) drive 0.45 mm diameter microcable tendons to produce flexion forces.

**Sensing:** "The motion of the cables is measured by potentiometers mounted on each motor shaft to a resolution of one degree" (this author believes the statement to mean one degree of joint motion, but it is unclear) [2]. "Miniature force sensors with an overload limit of 100 N are placed on the back of the palm in order to monitor cable strain" [2].

**Hand Attachments, Human Factors Design:** Appears to have a common V-block and circumferential band finger attachment, with additional straps around the palm. "The exoskeleton is comprised of 3 pairs of parallel link mechanisms spanning the length of each finger and attached to an immobile base on the back of the hand..." [3].

**Limitations:** None of the references reviewed mentioned sensing of or force-reflection to the abduction/adduction dofs.

**Status of Effort:** This effort is believed to be active, though investigators did not supply any information dated later than 1992.

**Contact(s):** M. Bouzit
e-mail: bouzit@robot.uvsq.fr

R. Chellald
e-mail: ryad@robot.uvsq.fr

Dr. Philippe Coiffet
Laboratoire de Robotique de Paris
University of Paris
10-12 Avenue de L'Europe
78140 Velizy, France
PHN: 011-33-1-39-25-49-65
FAX: 011-33-1-39-25-49-67

## References

[1] M. Bouzit, P. Richard, and P. Coiffet. LRP Dextrous Hand Master Control System. Technical report, Laboratoire de Robotique de Paris, Paris, France, 1992.

[2] G. Burdea and P. Coiffet. *Virtual Reality Technology.* John Wiley & Sons, New York, 1994.

[3] L. Turki and P. Coiffet. On Grasp Synthesis and Planning of Multifingered Robot Hands for a Telemanipulation Task. In *Proc. of the Fourth IEEE Int. Workshop on Robot and Human Communication*, pages 141–146, Waseda University, Tokyo, July 1995.

This page intentionally left blank.

# Force-Reflecting Hand Master Data Sheet: Mitsubishi Heavy Industries

**Description:** Project initiated in 1983 by the Ministry of International Trade and Industry (MITI). This is a dual arm master-slave system. Master and slave arms both have 7 dof. The left hand is 14 dof, while the right hand is 13 dof [4]. The hands have fingers, with 3 dof each (one abduction/adduction and two flexion/extension dofs per finger). The 13th dof in the slave is provided by a bending joint at the palm–the master may or may not have a corresponding sensor. The 14th dof in the left hand is provided by a rotating "swing joint," with an offset, at the base of the thumb. The slave fingers also have a number of tactile sensors. These tactile sensors provide feedback to actuated pads that push on the operator's fingers to provide a tactile feeling of the contact state on the fingers.

**Actuator/Transmission:** The fingers on the slave hand are motor driven with a unique low friction water cylinder transmission that has cable attachments at the motor and joint ends. The 7 arm dofs on the slave arms are driven with a motor/harmonic drive combination. All dofs on the master arms are pneumatically actuated. [1]. "The master finger manipulator is driven directly by wire rope" [2].

**Sensing:** Master and slave fingers have position-sensing potentiometers about 5 mm in diameter. Slave has two-axis force sensor with 0.1N threshold, located in finger. The master has force sensors in the center of each link in the finger sections.

**Specifications:** Finger joint torque 2-5 N-m
0.5 N (0.11 lb) "relative resolution of feedback for force"
0.4 N (0.09 lb) tactile feedback resolution (may be improved to 0.1 N (0.022 lb) with improved S/N ratio on tactile sensor)
maximum speed of slave fingers is about 1 Hz

**Hand Attachments, Human Factors Design:** Thimble-like attachments on fingertips, similar to NOSC/TOPS system by Sarcos. Thimbles appear to cover distal interphalangeal (DIP) joint, which is not free to move. "To reduce the restriction due to the change of distance between joints resulting from the bend and stretch of the finger, attention is made only to the position of finger tips for the positional relation between master and slave." The hand passes through a band that surrounds the palm and the back of the hand—other than this band and the finger thimbles, the rest of the back of the operator's hand is left bare.

**Limitations:** The master arms are bulky and awkward. Authors cited limitations on force-reflection fidelity of master fingers, in part because the master finger sections and the operator's fingers all function as manipulators in a very constricted workspace.

**Comments:** This is a complete two-arm bilateral force-reflecting system. John Bares believes that it may have more complete hand sensing and feedback than any other two-arm system.

The system has demonstrated various tasks typical of nuclear plant maintenance, such as the disassembly of a large valve. An earlier, one-arm version of the system enabled an operator to turn a nut on a bolt without being able to see the workpieces.

Operator fatigue is a problem, due to the large number of dofs and physical burden of the master arms. To help alleviate this problem, MHI conducted research regarding teaching various routines (e.g., pick and place) in an object-oriented language. While these methods helped somewhat to reduce operator burden, operation of the two-arm system is still very demanding.

Due to the large number of motors, sensors, and related components, initialization of the system is a slow process, and system reliability is a problem.

The system uses a Sun4 for task planning. MHI has used both an IRIS 210 (on the right arm and hand) and a MASSCOMP (on the left arm and hand) for motion contol. Positions of the slave fingers are controlled by a vector scheme that servos on the relative positions of the master fingertips, rather than using joint angles as direct inputs.

**Status of Effort:** As of 20 Oct 92, Mitsubishi was improving the dual arm system with the intention of evolving it into a salable product.

**Contact(s):** Takeo Oomichi (Manager)
Naoto Kawauchi (Research Engineer)
Machinery Laboratory
Takasago Research and Development Center
Mitsubishi Heavy Industries, LTD.
2-1-1 Shinhama, Arai-cho,
Takasago, Hyogo Prefecture, 676 Japan
PHN: 0794-45-6743
FAX: 0794-45-6924 (or x6962)

John Bares is a Carnegie-Mellon University researcher who was at MHI Takasago until 31 Oct 92. Much of the information and references for this profile were provided by him.

## References

[1] T. Oomichi, M. Higuchi, A. Okino, N. Kawauchi, Y. Shimizu, A. Maekawa, K. Ohnishi, and T. Hayashi. Intelligent Control of Four Fingered Manipulator System. In *Proc. of the Int. Symp. on Advanced Robot Tech. (ISART)*, page 589. Japan Industrial Robot Association (JIRA) and Advanced Robot Technology Reasearch Association (ARTRA), March 1991.

[2] T. Oomichi, A. Maekawa, and T. Hayashi. Multiple Sensory Bilateral Control of A Manipulator With Dexterous Hand. In *The Second Workshop on Manipulators, Sensors and Steps Towards Mobility*, pages 10.1–10.7. University of Salford, England, October 1988.

[3] T. Oomichi, T. Miyatake, A. Maekawa, and T. Hayashi. Mechanics and Multiple Sensory Bilateral Control of a Fingered Manipulator. In *Robotics Research: The Fourth Int. Symp.*, pages 145–153, Cambridge, MA, 1988. MIT Press.

[4] T. Oomichi, A. Okino, M. Higuchi, A. Maekawa, and K. Ohnishi. Development of Working Multifinger Hand Manipulatior. In *Proc. of the IEEE Int. Workshop on Intelligent Robots and Systems*, pages 873–880, 1990.

# Force-Reflecting Hand Master Data Sheet: NOSC/Sarcos

**Description:** 9 dof hand with 3 dof wrist–includes 4 dof thumb with force reflection (FR) at every dof, 3 dof index finger includes 2 dofs with flexion/extension FR, and one lateral dof w/o FR. Middle finger has two FR flexion/extension dofs. Part of TOPS arm and hand teleoperator system built by Sarcos for the Naval Ocean Systems Center (NOSC).

**Actuator/Transmission:** Hydraulic. Small amount of leakage reported in first prototype; Sarcos has developed redundant sealing. Six dofs have antagonist cable tendon pairs routed from hydraulic acuators over backs of fingers. Three other dofs are direct hydraulic drive.

**Sensing:** Position–small Rotational Variable Differential Transformers (RVDTs) designed and built by Sarcos
Force–strain gauges mounted on link plates (dorsal aspects of fingers)

**Specifications:** The system has undergone functional testing (including underwater), but no quantitative characterization.

**Hand Attachments, Human Factors Design:** The exoskeleton has four-bar linkage type mechanisms with a virtual pivot point located at the human knuckle's pivot point. Uses thimbles for attachment to fingers. Thumb folds in from side to match human kinematics (unlike Utah-MIT hand). Attachment is like "open-palm glove"–slide fingers through rings, insert fingers into thimbles. Operator fatigue not bad–operators could do simple tasks for up to 1.5 hours.

**Limitations:** Very bulky. Large hydraulic power plant.

**Comments:** Gravity compensation down to wrist of TOPS master, does not include hand.

**Status of Effort:** This project died when NOSC moved from Hawaii to San Diego. The next version would likely have had only four dofs with trigger pull. The Sarcos Dexterous Arm Master is a commercial descendant of this system.

**Contact(s):**

Dr. Frasier Smith
Sarcos Research Corp.
360 Wakara Way
Salt Lake City UT 84108
PHN: 801-581-0155
FAX: 801-581-1151
Email: f.smith@sarcos.com

**Note on References:** Due to project uncertainty and funding irregularity, this project was not well documented. AL/CFBA has NOSC videotape of functional testing. References [2] and [3] are alternate designations for the same conference paper.

## References


[1] S. C. Jacobsen, E. K. Iversen, D. F. Knutti, R. T. Johnson, and K. B. Biggers. Design of a Multiple Degree-of-Freedom, Force-Reflective Hand Master/Slave with a High-Mobility Wrist. In *Proc. of 3rd Topical Meeting on Robotics and Remote Systems*, 1989.

[2] S. C. Jacobsen, F. M. Smith, E. K. Iverson, and D. K. Backman. High Performance, High Dexterity, Force Reflective Teleoperator. In *Proc. 38th Conf. on Remote Sys. Tech.*, pages 180–185. American Nuclear Society, November 1990.

[3] S. C. Jacobsen, F. M. Smith, E. K. Iverson, and D. K. Backman. High Performance, High Dexterity, Force Reflective Teleoperator. In *American Nuclear Soc. Winter Meeting*. American Nuclear Society, 1990.

# Force-Reflecting Hand Master Data Sheet: Rutgers Master

**Description:** Hand master for three fingers and a thumb. Pneumatic cylinders are placed in the palm–there is only one actuator per finger, with connections between the fingertip and a base in the palm. Workspace is limited, but users apparently report good feel; the system is also lightweight and relatively inexpensive.

**Actuator/Transmission:** Pneumatic cylinders between fingertips and palm. Forms a "direct drive" force-reflection system.

**Sensing:** Linear Variable Differential Transformers on early versions, then a VPL Dataglove was integrated with three-finger system for position sensing. Force sensing is unknown, but force application is believed to be open-loop. Second-generation system, the Rutgers Master II (RM II) has linear sensors on custom pneumatic pistons and Hall-effect sensors on pivoting base of pneumatic pistons to eliminate the need for a sensing glove.

**Specifications:** For second-generation device, the maximum piston forces at various pressures are:

| pressure | force |
|---|---|
| 6.9 kPa (1 psi) | 0.16 N |
| 414 kPa (60 psi) | 9.83 N |
| 552 kPa (80 psi) | 13.11 N |
| 690 kPa (100 psi) | 16.38 N |

Due to static friction, the force measurement resolution is smaller than that indicated by the 12-bit A/D conversion (0.0024 N at 60 psi). Actual force resolution for the RMII is 5 g (0.05 N). Assuming an operating pressure of 690 kPa (100 psi), the device has a dynamic range of 330:1 (16.4/0.05 = 330).

**Limitations:** Can only simulate grasp forces between the palm and the fingertips. Contact of the fingers with objects supported externally cannot be simulated. As with other hand masters, cannot simulate weight of objects unless connected to an earth-grounded or perhaps torso-grounded force-reflection system.

**Status of Effort:** Second-generation system has been constructed. Human subject tests have been performed with the first-generation device. This effort is active.

**Contact(s):**

Dr. Grigore Burdea
Core Bldg. CAIP Center
Rutgers University
P.O. Box 1390
Frelinghuysen Rd
Piscataway, NJ 08855-1390

## References

[1] G. Burdea and P. Coiffet. *Virtual Reality Technology.* John Wiley & Sons, New York, 1994.

[2] G. Burdea and J. Zhuang. Dextrous Telerobotics With Force Feedback - An Overview. Part 1: Human Factors. *Robotica*, 9:171–178, 1991.

[3] G. Burdea and J. Zhuang. Dextrous Telerobotics With Force Feedback - An Overview. Part 2: Control and Implementation. *Robotica*, 9:291–298, 1991.

[4] G. Burdea, J. Zhuang, E. Roskos, D. Silver, and N. Langrana. A Portable Dextrous master With Force Feedback. *Presence*, 1(1):18–28, January 1992. MIT Press.

[5] G. C. Burdea and T. H. Speeter. Portable Dextrous Force Feedback Master for Robot Telemanipulation (PDMFF). In *Proc. of NASA Conf. on Space Telerobotics*, pages 153–161, January 1989.

[6] D. Gomez, G. Burdea, and N. Langrana. The Second Generation Rutgers Master "RM-II". In *AUTOMATION '94, The Third Int. Conf. on Automation Tech.*, Taipei, Taiwan, July 6-9 1994.

[7] D. Gomez, G. Burdea, and N. A. Langrana. The Second-Generation Rutgers Master SGRM. In *VR Systems '93*, New York NY, October 1993. SIG-Advanced Applications.

## Force-Reflecting Hand Master Data Sheet: Virtex

**Description:** This is a force-reflecting version of the Virtex Cyberglove. In addition to force feedback, it also has nine-pin binary (not proportional) tactile array feedback on the very ends of the fingertips (near the fingernail, distal to the fingerprint sworl).

**Actuator/Transmission:** Electromagnetic motors provide forces which are transmitted to the joints by plastic cables in low-friction guides. The on/off tactile feedback pins use solenoid actuators and also use cable transmission to the fingertip.

**Sensing:** Tachometers on the motors give velocity information. This glove is believed to be a modification of the Cyberglove, which uses strain sensors to sense position.

**Specifications:** None available.

**Hand Attachments, Human Factors Design:** The device is a glove that the user wears.

**Limitations:** Nine sheathed tactile feedback cables on each fingertip may be a difficult encumbrance to the operator.

**Status of Effort:** Active. Virtex plans to make the device available as a product in 1995.

**Contact(s):** Jim Kramer
Virtual Technologies
2175 Park Blvd.
Palo Alto CA 94306
PHN: (415) 321-4900
FAX: (415) 321-4912
E-mail: info@virtex.com

## References

[1] J. Kramer. Force Feedback and Texture Simulating Interface Device. U.S. Patent #5,184,319, February 1993.



☆ U.S. GOVERNMENT PRINTING OFFICE: 1996-751-326